1-1-2016

Investigating Coastal Erosion Variability and Framework Geology Influence Along the Grand Strand, South Carolina

Aundrea Marie Dolan
Coastal Carolina University

Investigating coastal erosion variability and framework geology influence along the Grand Strand, South Carolina

By

Aundrea Marie Dolan

Submitted in Partial Fulfillment of the

Requirements for the Degree of Master of Science in

Coastal and Marine Systems Science in the

School of Coastal and Marine Systems Science

Coastal Carolina University

2016

Dr. Paul Gayes Major Professor	Dr. Till Hanebuth Committee Member
Dr. Jenna Hill Committee Member	Dr. Jennifer Miselis Committee Member
Dr. Michael Roberts Dean, College of Science	Dr. Paul Gayes Director of SCMSS

Dedication

This accomplishment would not be possible without the unwavering support of my family and friends. Their optimism, advice, listening ear, and love have allowed me to get to where I am today. I truly consider myself lucky to have such dedicated and trusting people surrounding me every day. I would like to especially thank my parents for instilling a curiosity and affection for the outdoors; combined these qualities have forged my love for the natural sciences. I am comforted by the knowledge that they will always support me and for that I am forever grateful.

Acknowledgements

I would like to express my deepest appreciation to my graduate advisor, Dr. Paul Gayes, who has consistently infused a sense of curiosity and adventure in regards to research. Without his guidance and suggestions, this thesis would not have been possible. I would additionally like to thank my dedicated and insightful committee members, Dr. Till Hanebuth, Dr. Jenna Hill, and Dr. Jennifer Miselis. Their knowledge and persistence in answering my many questions and concerns have been monumental in this process. Further, this research would not have come together without the assistance of my dedicated and talented colleagues, fellow graduate and undergraduate cohorts. I would namely like to thank Thomas Mullikin, Pamela Martin, Shinobu Okano, Robert Sheehan, Brian Johnson, Jamie Phillips, Preston O'Brien-Gayes, Quaye Trimble, and Michael Slattery for their technical support along the way. Many of you provided hours of your time to entertaining my many questions and assisting in data collection with patience and persistence. An additional thanks to Julie Quinn, Karen Fuss, Lisa Prendergast Swanger, and Jim Whitfield for being both functional and emotional support along the way. My undergraduate assistant, Taylor Determan, also deserves special thanks for her support in data processing, which improved efficiency and progress. Finally, I would like to extend a large thank you to AJ Kammerer, Mary Lee King, Karsen Schottleutner, Brittany Stockmaster, Matt Kestner, Samantha Ladewig, Amanda Roach, Samantha Corley, Alison Bojarski, Nathan Lentini, Todd Rhodes, Patrick Mears, Josh Humbertson, and Jon-Erik Taylor for being enormous supports. Their constant belief in my abilities, insight into data, and hilarious, optimistic attitudes created an environment of high morale and motivation on long days. I wish the best for you all and hope to cross paths in the future.

Abstract

Increasing erosional pressures along coastal systems require a better understanding of the mechanisms of natural and human-induced alterations. This is especially important in sediment-starved coastal systems where the effects from geologic framework may exert a disproportionate influence on shoreline behavior. Existing studies into geologic framework and shoreline variability are comprehensive and well documented; yet analysis into the spatial relationships between shoreline variability, lower shoreface morphodynamics, and framework in South Carolina is limited.

The Grand Strand region of South Carolina has an extensive set of geophysical data, such as CHIRP seismic, sidescan sonar, borehole logs, and inner shelf cores. In addition, there is a rich suite of RTK-DGPS surveys of a shoreline contour (MHW; 0.625 m) collected monthly since 2007 to consider shoreline variability over 52 km of coastline. Calculation of various statistical parameters using the USGS Digital Shoreline Analysis System v4.2 software, including end point rate (EPR), linear regression rate (LRR) and shoreline change envelope (SCE), provides quantitative assessment of shoreline behavior. Spectral analysis is utilized to define patterns in spatial variability. In effort to target the sediment-limited lower shoreface, a multibeam survey of the region was acquired and identified sections of low relief, low backscatter cuspate-like linear scour depression features in close proximity to the depth of closure. The 6-meter contour wad digitized onto backscatter imagery and intensity values were extracted and correlated to shoreline (MHW) change throughout the study area. Chi-square analysis and correlations between geologic and physical metrics (e.g. paleochannel presence, shoreface slope, backscatter intensity) were computed to identify spatial relationships.

Analyses indicate a relationship between shoreline change and backscatter intensity where deep paleochannels were present. Furthermore, power spectral density of the rate-of-change statistics show dominant spatial frequencies consistent between shoreline change and backscatter variability. Findings suggest interplay between shoreface morphology and the spatial variability of the shoreline with framework geology. Further, an intriguing relationship between Cretaceous boundary outcrops along the lower shoreface and offshore cusps suggest a connection between the bathymetric features and framework. The offshore cusps further align with inner shelf linear scour depressions located further offshore and appear to reflect the transition from beach processes into shelf processes, propagating into the self-sustaining linear scour depressions further offshore.

Table of Contents

List of Tables

List of Figures

Figure 9: Seasonal wind direction and magnitudes as measured from Buoy 41004 offshore of Charleston, SC. Measured wind speeds are from 2007-2009, showing predominantly N-S directions.

Figure 10: Recorded storm events, graphed in prevailing wind direction in degrees from North, along the Grand Strand from October 2006 through January 2009, encompassing the period before the renourishment projects. Recorded wind speed is depicted in the size of the icons.

Figure 11: Schematic image of ATV-mounted GPS measurement of the mean high water line based on positional surveys. An accurate MHW line is interpolated from the 0.46 and 0.76-meter elevations, in addition to the berm and dune lines.

Figure 12: Mean high water shoreline positions from 2006-2009 are seen in green. A user-defined baseline is seen in white; DSAS transects are cast at 50m increments. The intersection of the transects and shorelines are the point at which shoreline rate of change statistics are calculated. Multibeam backscatter is imaged offshore, with meter contours in yellow. Backscatter values are extracted at the intersection of the 6m contour and DSAS transects.

Figure 13: Borehole 'Hor-05' in Central Myrtle Beach. The orange point represents the location of the borehole, the cyan the location of the CHIRP, while the remaining purple points represent various other CHIRP shotpoints. For a description of the borehole log, see Figure 16.

Figure 14: Borehole 'Hor-07' located in Myrtle Beach. The orange point represents the location of the borehole, the cyan the location of the CHIRP, while the remaining purple points represent various other CHIRP shotpoints. For a description of the borehole log, see Figure 17.

Figure 15: Borehole 'Hor-12' loacted in North Myrtle Beach. The orange point represents the location of the borehole, the cyan the location of the CHIRP, while the remaining purple points represent various other CHIRP shotpoints. For a description of the borehole log, see Figure 18.

Figure 16: Borehole log for Hor-05 as accounted by Putney and other (2002).

Figure 17: Borehole log for Hor-07 as accounted by Putney and other (2002).

Figure 18: Borehole log for Hor-09 as accounted by Putney and other (2002).

Figure 19: A typical BERM beach profile, located in Surfside Beach, used to define characteristics of the shoreface. The decrease in standard deviation is used to identify ‘closure’, while the change in slope into a relatively flat rise is used to define the depth of the shoreface.

Figure 20: A schematic of multibeam sonar seen as adapted from The United States Navy.

Figure 21: One-meter backscatter pixels are seen in the varied grey scale squares. The intersection of DSAS transects and the 6m contour is represented by the red dot. A one-meter contour is created on all sides of the point of intersection and the average of the extracted backscatter values is calculated to assess variability.

Figure 22: Spatial features along the Grand Strand, including inlets, barrier islands and spits, paleochannels, groins, offshore cusps, and nourishment projects.

Figure 23: Shoreline change envelope (m; blue) and linear regression rate (m/y; red) for the Grand Strand, south to north. Inlets are highlighted in gray and characteristically experience high levels of shoreline change and variability than the rest of the shoreline. A gap in data collection occurred in northern Surfside Beach, into southern Myrtle Beach around the Myrtle Beach State Park shoreline. Recorded offshore cusps and highlighted alongshore in the purple.

Figure 24: Power spectral density graphs on a log-log scale for Garden City. Significant frequencies are reported in Table 5.

Figure 25: Power spectral density graphs on a log-log scale for Surfside Beach. Significant frequencies are reported in Table 5.

Figure 26: Power spectral density graphs on a log-log scale for Myrtle Beach. Significant frequencies are reported in Table 5.

Figure 27: Power spectral density graphs on a log-log scale for Arcadian Shores. Significant frequencies are reported in Table 5.

Figure 28: Power spectral density graphs on a log-log scale for North Myrtle Beach. Significant frequencies are reported in Table 5.

Figure 29: An example of offshore cusps imaged in multibeam bathymetry with draped backscatter, located in Surfside Beach. Locations consisting of offshore cusps have similar geometries, although length and depth of cusps vary.

Figure 30: Offshore cusps imaged alongside a shoreline borehole log. The yellow arrow indicates cusp location, green indicating the Cretaceous unit, while the orange arrow indicates the Pleistocene unit. The crest of the cusps aligns with the top of the Cretaceous boundary documented in the log (green unit). The Cretaceous unit consists of calcareous sandstone overlain by the shelly sand Pleistocene deposits.

Figure 31: Nearshore multibeam imagining overlain onto sidescan sonar imagery taken in 2003. Visual inspection reveals a strong relationship between the offshore cusps and linear scour depressions seen in backscatter extending offshore.

Figure 32: Spatial relationship between where the Cretaceous boundary is outcopping on the shoreface along the Grand Strand- limited by locations where CHIRP seismic profiles have been imaged along the inner shoreface. Where outcropping, offshore cusps reflect similar distributions.

Figure 33: A side scan sonar image of backscatter draped on bathymetric data showing offshore shoal and linear scour depression systems in Myrtle Beach and North Myrtle Beach. Yellow and red points in the top image represent where instruments were deployed to collect bottom samples. These were used to ground truth backscatter, and analysis confirmed low backscatter regions contain fine sands and troughs contain coarse sands and gravel. The bottom image implies the direction of flow across the sediment beds, from north to south. Adapted from Barnhardt, 2009.

Figure 34. A cross section, taken from the Surfside Beach cross section seen in *Figure 29,* indicating the inferred direction of flow from north to south, as similar to research documented in Barnhardt (2009) and seen in *Figure 32*.

Figure 35: A simulated beach profile showcasing shoreface steepening. The red profile indicates the shoreface before base erosion, and the blue profile showcases the effect of bottom shoreface erosion without upper shoreface erosion.

Figure 36. A cross section of multibeam backscatter and bathymetry over the offshore cusp features, just offshore of the onshore cusps seen in the above image. The similar length in wavelengths of offshore and onshore cusps indicate a possible connection.

Figure 37: The presence of offshore cusps corresponding to the volume of nearshore bars alongshore. The presence of offshore cusps appear to be spatially related to areas of relatively higher bar volume.

Figure 38. Schematic identifying the location of the offshore cusps in relation to stratigraphic boundaries along a typical Grand Strand beach profile. Temporal scales of change along each beach region are indicated at the top portion of the image. The offshore cusps are most often located below the depth of closure, however larger scale events may transport some of cusp sediments into the active beach.

1. Introduction

Coastal systems are dynamic areas, undergoing change constantly driven by a range of physical and geologic factors including, but not limited to, longshore and cross shore currents induced by wind and waves, sediment fluxes, storm events, and, interaction with societal infrastructure. Under conditions of low to moderate sediment supply, it is these physical processes and features that can lead to erosional pressures causing landward migration of the shoreline with rising sea levels. Recession and accretion rates vary both temporally and spatially on many different scales due to regional fluctuations in physical and geologic settings along with local hydrodynamic conditions. With an increasingly massive and static footprint of societal infrastructure located along a dynamic shoreline, there is a strong interest in better understanding, characterizing influences on and potential future behavior of shoreline movement into the future.

Historically, the behavior of the coastline has often been characterized by a shoreline or a two-dimensional line based on various criteria (e.g top of the primary dune crest (SC OCRM, 1988) or a specific vertical elevation contour (List et al., 2006; Thieler et al., 2009; Nelson and Hapke, 2015) as a means to track behavior of beaches in space and time. This is partially an outgrowth of long-term data sets (dating back >100 years) available to consider coastal change. Such long-term shoreline datasets, however, were infrequently surveyed; often separated by decades between surveys (Morton and Miller, 2005). Analysis of change over decadal scales shows the long-term trends of coastal change but the small number of samples and potential of biasing of the trends by shorelines being measured shortly after major storm events complicates the interpretation of change (Douglas and Crowell, 2000). Nevertheless, these datasets do document change on decade to century time scales and serve as a bridge between relatively long-term interests in societal applications and long-term evidence of shoreline migration.

Surveys of shorelines over shorter periods of days to months such as classic work of List et al., 2006; Riggs et al., 1995; Thieler and Danforth, 1994 and the remarkable time series established by the Corps of Engineers at the Field Research Facility at Duck, North Carolina (Army Corps of Engineers Field Research Facility, 2016) provide insight into shorter term variability of the beach system responding to individual storm effects, seasonal change in wind, and wave climate. In the case of the unusually detailed time series at Duck-FRF, effects of interannual drivers such as ENSO on the behavior of the shoreline can be resolved (Hanson, 2015). Similarly the higher frequency surveys of shorelines such as studies by List et al. (2006) demonstrate the diverse response of the shoreline along long sections of the coast such as the Outer Banks of North Carolina and the relative magnitudes of erosion and recovery associated with storm events.

Shorelines remain an important measure of coastal behavior as efforts to address the spatial variability and redistribution of sediment within the overall active beach system (dunes, subaerial beach, intertidal and surf zone and shoreface) are challenged by costs and logistics of integrating technologies suitable to provide more definitive and integrated characterization across the entire beach system (e.g. LIDAR, SHOALS, multibeam, and increasing X-Band Radar/LIDAR systems such as FRF's CLARIS system). Scientists have additionally identified the complex influence that framework geology has on regional bathymetry and, therefore, coastal morphology (Schwab et al., 2000; Riggs et al., 1999; Pilkey et al., 1993; Schupp et al., 2006; Belknap and Kraft, 1985; McNinch, 2004). In areas where sediment input is low, as found along much of the mid-Atlantic margin, framework geology contributes a dominant influence on coastline behavior (Riggs et al., 1995; Miselis and McNinch, 2006). Given the immediate proximity to societal infrastructure, quantitatively correlating framework geology influence to shoreline behavior and characterizing the mechanisms causing the erosional variabilities is very important.

Potential impacts to coastal communities from dynamic change in coastal morphology require thoughtful actions from local governments and private entities. Morphology is controlled by mechanisms affecting both subaerial and submarine portions of the beach; therefore management efforts should consider the dynamic coupling between the two. For this reason, unique regional settings and factors demand careful implementation of hard and soft coastal protection in the densely developed regions. These actions can fundamentally conflict with their stated purpose of shoreline preservation. An improperly designed hardened structure, such as jetties and groins, can cause sediment starvation of adjacent beaches. The lifetime of nourishment projects, designed to temporarily address long term negative sediment budgets for the beach system, is limited and can provide a false sense of security to chronic erosion issues, and places heavy demand on financial resources (Komar, 1976). Quantifying a local sediment budget, modeling cross-shore and long-shore transport processes, and analyzing shoreline mobility over various temporal and spatial scales supports informed decision-making for the best shoreline protection practices.

Studies have shown that the variable framework geology throughout the littoral zone often leads to disparate rates of erosion alongshore and can complicate prediction of coastal erosion patterns and rates (Schwab et al., 2000; Riggs et al., 1999; Pilkey et al., 1993; Schupp et al., 2006; Belknap and Kraft, 1985; Miselis and McNinch, 2006; Schwab et al., 2014). Numerical models are often used in engineering applications to assess and predict natural and anthropogenic (impacts from hard and soft shoreline protection) shoreline changes over yearly time scales (Kriebel and Dean, 1985; Thieler et al., 2000). Geologic models, however, are aimed to illustrate the changes that occur along longer time scales, assessing upwards of decades worth of variability. For these reasons, quantifying the impact of various shoreline features and mechanisms into a comprehensive assessment has proved difficult for scientists and engineers alike. Regional factors and aspects of the various models should be incorporated when aiming to provide educated management and mitigation decisions.

1.1 Nearshore Morphodynamics

Physical morphology and erosional patterns occurring along a coastline vary both temporally and spatially. Reasons for the variance and, consequently disparate rates of erosion alongshore are a result of differing rates of sediment input, variability in underlying geologic framework, local geography (e.g. proximity to inlets, orientation of the coast), and a continually fluctuating wave, wind, and current climate. The slope of the surf zone profile has a strong influence on physical processes driving sediment movement and in turn beach morphology. Low sloping beaches dissipate wave energy over larger areas and contain a wider surf zone, whereas steep profiles typically contribute to smaller energy losses until interaction with the beach face (Short and Wright, 1983). This zone extends across the exposed beach to a depth where sediment is no longer active, or transported, throughout the system, herein noted by the depth of closure (DoC) (Figure 1) (Hallermeier, 1981). Along a shoreface, the depth of closure is the yearly limit of profile change considering effective wave height, or that which wave height only exceeds 12 hours per year (Hallermeier, 1981). Questions arise in the concept of a separation between the shoreface and continental shelf; as researches have well documented, there is exchange of sediments between the two zones (Park et al. 2009; Schwab et al., 2013; Pilkey et al., 1993). Yet, the importance of utilizing quantifiable measures for assessment of processes and responses occurring in the active littoral zone remains and the DoC continues to be used despite its simplification of sediment transport.

Wave energy input into the littoral zone is responsible for the creation of nearshore currents, sediment transport dynamics, and, as mentioned, beach morphology and associated variability or temporal trends of accretion or erosion. Understanding the interplay that wave action and beach morphology have on each other, Short and Wright (1983) detail a morphodynamic classification of surf zones dealing with transformation of wave energy across the littoral zone. Beaches with low-sloping profiles are considered dissipative beaches and tend to support offshore wave breaking, resulting in minimal incident-wave energy reaching the shore (Short and Wright, 1983). Opposite of a dissipative profile are reflective beaches where diminished surf zones create an environment for formation of incident wave energy, leading to dissipation closer to shore (Short and Wright, 1983). More complexly, intermediate beaches contain various morphologies existing between entirely reflective and dissipative beaches. Slovinsky (2001) defined South Carolina mean beach profiles and morphologies using empirical orthogonal functions and found that inlet proximity was the most influential factor in controlling profile variability. Applicable to management efforts, the depth of closure along South Carolina, averaging -5 meters along the Grand Strand, was also determined to further provide insight into profile variability and sediment transport (Slovinsky, 2001; Park et al., 2009).

1.2 Framework Geology and Modeling the Coastal Zone

Many studies have identified the influence framework geology on sediment transport, and consequently shoreline variability, in the coastal zone (Schwab et al., 2000; Riggs et al., 1999; Pilkey et al., 1993; Schupp et al., 2006; Belknap and Kraft, 1985; Miselis and McNinch, 2006). Outcropping strata creates variable topography, therefore generating anomalous wave radiation along the shore, and differential sedimentary environments causing contrasting vulnerabilities to erosion. The Grand Strand region, a 100-kilometer stretch of shoreline along the northern coast of South Carolina, has recently been studied to discern the geologic units underying the area (Barnhardt et al., 2009). The unique framework situated beneath the Grand Strand has been shown to play a large role in the shoreline variability seen along the coast (Barnhardt, 2009). Well-documented paleodrainage systems have previously been connected to areas of erosional hotspots (Park et al., 2009). Sediment coverage in the area is highly inconsistent, with thin lenses characterizing both the shoreface and the offshore regions. Nearshore, this sediment availability is highly reliant on the external source of sediment from longshore transport. Sediment budget and transport along the Grand Strand has been the focus of various research efforts, highlighting the regional sediment deficit (Barnhardt, 2009; Park et al., 2009, Gayes et al., 2003; Patchineelam et al., 1999).

An accurate account of the elements impacting coastal evolution should be established along the Grand Strand to further aid shore and long-term management needs. Unfortunately, modeling of longshore transport and wave motions are limited by quantitatively accounting for accurate sediment budgets, access to complete temporal and spatial observations of processes, and associated observations. In order to develop a better understanding of the complex aspects of shoreline change occurring along the Grand Strand, antecedent geology has been the focus of recent investigation. As exemplified in studies done by Barnhardt (2009) and Park et al. (2009), sediment availability in the Grand Strand region is highly limited. Many locations of outcropping framework components make up much of the coastal zone and largely in the offshore region. These features have the potential to influence shoreline behavior due to the limit of sediment in the coastal system and that these older deposits may be an important source of sediment to this sediment starved system (Barnhardt, et al., 2009; Kana, et al., 2013).

Advancement of data collection methods in recent decades has allowed for progress to be made in characterization of the mechanisms leading to fluctuating erosional pressures. Still, localized linkage of underlying geological framework to shoreline variability in the Grand Strand region of South Carolina needs improvement. These increasing pressures of rapid growth, combined with increasing rates of erosion due to continued sea level rise, demand the need to recognize the interactions between these portions of the system (Leatherman et al., 2000). Annual to decadal predictions of shoreline change are important to city managers that must determine the balance and priorities between social and economic services. Additionally, the Federal Emergency Management Agency (FEMA) and other managers are concerned with decadal scales that reflect vulnerability of public infrastructure and utilities affecting coastal economies. Horry County is the second fastest growing region in the United States and the rapidly increasing growth puts larger populations at risk during extreme weather events and the resulting land loss and flooding (UN Atlas of the Ocean). Given the increasing economic and human activity along the Horry County coastlines, understanding the factors influencing coastline behavior will enhance future predictions in shoreline position and erosion, which will prove essential for hazard mitigation and recovery.

Here, a method for analyzing shoreline behavior in connection to geologic framework variability is presented. In 2006 the South Carolina Coastal Erosion Study, a joint effort between federal, state, and academic entities, characterized the geologic framework of the Grand Strand. The findings of the study supported the notion that framework does provide a dominant control of shoreline behavior, namely in areas of known paleodrainage systems. Further, it added to a large supply of geophysical and quantitative shoreline data, which is supplemented in this study. The goal of the presented research is not to predict coastal variability and erosion, rather to enhance the assessment of geologic framework in unexplained regions of shoreline variability. In doing so, a deeper understanding of the lower shoreface and beach system is established to move toward a more predictive capacity.

2. Study Area

The survey areas depicted in this study are located throughout the littoral zone along Long Bay, South Carolina, as part of the greater Grand Strand region (Figure 2). The Grand Strand is a 100 km long arcuate segment of coast stretching from the mouth of Winyah Bay at Murrells Inlet in the south to the northern border of South Carolina. Shore-attached beaches are dominant in the northern portion with areas of Surfside Beach and Garden City characterized by established barrier island systems to the south. The coastline is a part of the greater megacusp shoreline extending from Cape Fear, North Carolina to as far south as Cape Romain, South Carolina, known as Long Bay. Shoreline orientation is generally SW-NE, though variations in exact position largely influence direction of longshore transport and sediment mobility (Slovinsky, 2001) (Figure 3).

2.1 Geologic Setting

The Grand Strand is part of a margin-scale structural high referred to as the Carolina Platform (Figure 4). Situated on the apex midsection of the platform, the Grand Strand is in a considerably more stable geologic setting when compared to areas along the dipping portions of the platform (Slovinsky, 2001). A result of millions of years of shelf reworking and sea level fluctuations, the basement rock in the region is ancient sedimentary framework. It is overlain by a thin veneer of unconsolidated sediments, thinning with a great degree of disparity along shoreface and offshore regions. At times exposed, the Carolina platform was often incised by river and deltaic systems throughout the Pleistocene (Barnhardt, 2009). Today, these paleorivers are well-documented along the Grand Strand (Figure 5), with major paleochannels extending offshore of northern Surfside Beach, central Myrtle Beach, and the northern section of North Myrtle Beach nearing Hog Inlet. The resulting topographic variations have incised into the otherwise low-relief shelf and have been correlated to shoreline variability (Barnhardt, 2009, Park et al., 2009). Everts et al. (1987) speculated subaerial paleoriver systems enhance the ability for shore perpendicular flows to form, acting as a low relief area for transport of sediments offshore and exert a control on shoreline change variability along the coast.

Drainage in the region is influenced by the Grand Strands' location atop of the mid-Carolina Platform high and governs the input of sediments into the coastal region. Studies have highlighted the lack of sediment input from modern river systems due to the diversion of large volumes of sediments off the platform high, reflected in the patchy distribution of unconsolidated sediments offshore (Baldwin, et al., 2006;Riggs and Belknap, 1998; Patchineelam et al., 1999) (Figure 6). Chirp seismic imaging collected as part of the 2009 South Carolina Coastal Erosion Study showcases the disparity in distribution as thin 'lenses' of sediment a top of a reflective ravinement surface (Figure 7), which is often found outcropping on the inner shoreface. The varied distribution of thin sediments supports the notion that the Grand Strand region is a sediment-starved system. Once in the active coastal system, longshore currents generally transport the available sediment to southern regions (Barnhardt, 2009). While there are seasonal variations in the North-South direction of transport, evidence for the dominant longshore transport direction can be seen in the prograding barrier spits that extend into Winyah Bay at the southern end of the Grand Strand, extending further than (Figure 8). Although low sediment input is generally consistent with highly eroding coastlines, the unique geologic setting of the Grand Strand has resulted in relatively low rates of erosion (<1 m/y) along the South Carolina Coast (Park et al., 2009). Yet, concerns over localized erosional hotspots; areas of coast that experience higher rates of erosion than adjacent beaches, still remain due to the large amount of development and high rates of population expansion and rapid variability of hot spot regions.

2.2 Physical Setting

The Grand Strand region experiences a mild year-round climate, with an average low 36.7°F and average highs reaching 87.7°F. Yearly precipitation averages around 100 cm, with tropical storms bringing in this majority of rainfall (Slovinsky, 2001). Additionally, the area is a microtidal environment with tidal ranges from 1.4 to 1.7 m (Slovinsky, 2001). Offshore wind direction is typically in the southwest and northeast direction, but seasonal changes occur, as seen in Figure 9. Direct wave measurements for the study area are limited, yet buoy data provides insight into wave conditions in the area and have captured the variable seasonal directions, with dominant offshore wave direction to be south, southeast, and east throughout the year.

Multiple storm events occurred during the survey periods (December 2006-January 2009) and their frequency and occurrences are shown in Figure 10. Furthermore, a large renourishment project took place in the study area from 2008 to 2009 during the survey period. The cumulative project placed over 3,500,000 cy of dredged sediment onto the shorelines of Garden City, Surfside Beach, Myrtle Beach, Arcadian Shores, and North Myrtle Beach. For the purposes of this analysis, we assume that beach renourishment projects alter any underlying framework influence on natural shoreline processes. For this reason, shoreline data occurring before the renourishment projects are focused on herein. This also facilitated examining the potential role of framework influence on beach behavior as renourishment deposits act to blanket existing surfaces and, at least for the surfzone and upper beach work to cover older outcropping strata.

In effort to evaluate the short-term spatial variability of shoreline behavior and the influence of geologic framework on its behavior this study:

1. Characterizes the behavior and variability of the mean high water contour as a measure of shoreline position on a monthly basis over a three-year period to provide a higher frequency assessment of shoreline variability than available to the previous coastal erosion study.
2. Refines the framework underlying the beach and shoreface region, integrating datasets from the coastal erosion study and contributing a new data set of multibeam imagery of the 3-D geometries along the mid-lower shoreface. Historical beach profiles show limited sediment deposition in this region and more direct erosion of underlying framework on a daily basis as part of the ravinement process of the transgressing beach system.

3. Seeks to quantify relationships between framework and shoreline variability along a broad section of coastline.

3. Methodology

This work sought to resolve, and possibly quantify, relationships between shoreline variability and geologic framework. This builds on the generalized regional geologic framework and broad characterization of shoreline change defined in the South Carolina Coastal Erosion Study (SCCES) (Barnhardt, et al., 2009). The characterization of shoreline behavior in the previous SCCES was limited to analysis of historic shorelines where individual shorelines were defined across the whole study area but were separated by several decades in time. As a result this data was most useful at considering very long term, decadal to centennial, change in the beach systems. These shorelines are sensitive to processes within the upper beachface or dune line, such as storm, seasonal changes, and interannual changes (e.g. ENSO) in addition to long-term drivers such as sea level rise and sediment supply. These limitations affect the scales at which influence of geologic framework on shoreline behavior can be considered. The SCCES also utilized the states' BERM program of long beach profiles established by the Burroughs and Chaplin Center for Marine and Wetland Studies. The network of profiles covers the entire coast of South Carolina but are widely and irregularly spaced. They were also surveyed only once or twice a year. This data set provided an important annual time series over a 15-year period but is also limited by its annual sampling, the timing of which is relative to individual storms, beach nourishment projects, and other drivers strongly influences the profiles measured. They do however, provide an important insight across the full active beach systems, dunes, surf zone, shoreface and out to the inner shelf. The detailed beach profiles are representative of the integrative processes and responses of the active beach system, though limited in alongshore continuity and limited temporal sampling.

This work focused on characterizing the behavior and variability of the shoreline, defined by the mean high water (MHW) contour (0.625 m), over a monthly to interannual timescale along a broad (100 km) section of northern South Carolina coastline. Despite being limited to a single contour, this provided a more spatially continuous characterization of shoreline behavior over a much smaller temporal scale (monthly) over a several year period.

In addition, this work contributed a new spatially continuous dataset characterizing the detailed geometry and structure of the lower shoreface using multibeam sonar along the length of the study area; significantly refining the geologic framework and character of the shoreface, building on the SCCES and to identify influence of framework features on the spatial and temporal scales of the shoreline data. Lastly, it was sought to document the character of the lower shoreface as an area where framework may be most strongly intersecting modern processes and as the area of transition between high frequency responses of the upper beach and the longer-term processes of the inner continental shelf.

3.1 Characterizing Behavior and Variability of the Mean High Water Contour: BERM Beach Contour Lines

Considerable variability is to be expected in the position of the shoreline defined by the MHW contour (0.625 m WGS_NAVD 88). This zone is frequently inundated and subject to wave and current processes on a daily basis as well as periodically aeolian processes. It is also within one of the most dynamic areas of the beach, being actively engaged in the conceptual fair-weather/foul-weather beach cycles where long period swell drives the nearshore bar and associated sand up onto the beach as a berm (Komar, 1976). Periodically, this deposition is interrupted by storm events where elevated energy of surfzone and nearshore processes often work to strip sand off the beach and becomes distributed onto the shoreface and alongshore, and potentially along the inner shelf. For these reasons, strong seasonal and episodic event influences are expected. The MHW contour is also potentially sensitive to localized changes in wave and current energy and changes in sediment availability and mobility. As such, its variability over an extended period of time across a broad section of coastline is examined to consider the potential influence of geologic framework on this indicator of beach behavior.

To quantify spatial and temporal changes in shoreline position, the mean high water contour line has been collected by Coastal Carolina University since 2006. Spatially, this data has been collected from North Myrtle Beach to Garden City (100 km). Temporally, the mean high water contour was surveyed monthly associated with planning and construction of beach nourishment and more episodically subsequent to that. All shoreline files were collected in segments based on their corresponding municipal area: North Myrtle Beach, Arcadian Shores, Myrtle Beach, Surfside Beach, and Garden City.

The ground-based method to capture MHW position utilizes a Real Time Kinematic-Differential Global Positioning System (RTK-DGPS) mounted to the roof of an all-terrain vehicle (ATV) being driven along the length of the shoreline. Elevation and position measurements from an Ashtech Z Extreme GPS receiver are acquired through Hypack surveying software. A real time kinematic correction is also acquired in Hypack through a Cellular Radio Module (CRM) that corrects for 0.010m horizontal and 0.020m vertical accuracy. Elevation and position measurements are sampled at a frequency of 5 Hz. Driven during low tide, survey lines are collected at the dune toe and the definable berm crest along the beach. To define the mean high water contour, lines were surveyed along the 0.46 and 0.76-meter elevations as defined by the real time elevation display during the survey (Figure 11). Shoreline files were then brought into Surfer visualization software and erroneous and outlier data points were edited from the dataset. All shore-parallel lines were interpolated to provide the best measurement of the MHW line, and were then exported into an ESRI geospatial vector shape file. This methodology was modified from that established by List and Farris (1999) along the Outer Banks of North Carolina and Cape Cod. The mean high water contour occurs within the very planar swash face surface and, as a result, the interpolation is considered valid and accurate to within 10 cm (List and Farris, 1999). The digitized MHW shoreline contours were geo-referenced to the WGS_NAD 1983 UTM Zone 17N datum.

For a quantitative measure of shoreline movement, rate-of-change statistics were generated with the Digital Shoreline Analysis System v.4.3, a toolbar extension in ArcGIS, employed in ArcMAP v.10.1 (Thieler et al., 2009). A user-defined baseline was digitized landward of the shorelines and transects were cast at 50-meter increments (Figure 12). Shoreline rate-of-change statistics are calculated across all shorelines at each transects intersection using linear regression analysis. This framework was used to derive three shoreline change metrics. End point rate, a measurement of the change in distance over the amount of time elapsed between earliest and latest shorelines. Shoreline change envelope is a similar measurement showing the linear change in shoreline position between the furthest and closest shorelines to the digitized baseline layer. Finally, the linear regression rate is the slope of a best-fit regression line to the shorelines intersected by each transect, were utilized as measures of shoreline variability within this study. Because the area experienced a large beach nourishment project in 2008, shoreline positions prior to the placement of the 2008 renourishment project were focused on to establish the best assessment of impact derived from framework geology (Komar, 1976; Park et al., 2009).

3.2 Defining Geologic Framework Along the Study Area: Boreholes and Chirp Seismic Data

In effort to supplement insight into geologic framework of the Grand Strand region, high-resolution CHIRP seismic profiles were collected in many locations offshore during the SC Coastal Erosion Study. The seismic reflection profiles were collected using an Edgetech 512 XSTAR CHIRP sub-bottom profiler, processed using SIOSEIS and Seismic Unix to remove heave artifacts. For more detail on data acquisition and processing, see Baldwin and others (2004). Reflection profiles discussed further in this study correspond to locations where borehole and core logs have obtained physical accounts of stratigraphic layering (Figures 13-15).

In 2002 boreholes were collected throughout the Grand Strand region by Putney and others (2002) and were incorporated as part of an USGS-South Carolina Sea Grant effort to investigate the shallow regional framework geology. The spatial distribution of cores extended across the shallow coastal plain of northern South Carolina, with 21 located adjacent to the shoreline. Further information regarding the methods used in the core and borehole extraction processes can be found in Baldwin and others (2004). The borehole logs focused herein were collected in the back dune region to provide groundtruthing of local stratigraphic framework as close to the marine CHIRP data as possible. In general, there was less than a 200-meter separation from boreholes in the back dune and the beginning of corresponding nearshore CHIRP lines. While large storm events in the past may have modified the uppermost stratigraphy above mean sea level, the overall framework defined by the boreholes is considered a good representation of the stratigraphy being transgressed and eroded into and corresponded well with the CHIRP data (Figures 13-15).

3.3 Defining Shoreface Geometry and Characterizing Framework Influences: BERM Beach Profiles

In addition to the shoreline position data, beach profiles have been collected annually as mandated by the passage of the 1988 Beachfront Management Act. Over 400 locations, irregularly spaced between 100 and 600 meters apart, have been surveyed across the state of South Carolina since 1988. Beach profiles at these locations were initially surveyed twice per year to wading depth (defined as -1.5 meters) using survey rod and transect. In 2003, beach surveys shifted to use of a total station and a survey sled supporting a tall fixed mast that was stowed across the beach out onto the inner shelf. The goal was to begin to capture the whole active beach, dune, and shoreface system to depths and distances offshore considered to include the inner shelf (defined by a distinct flattening of the profile at the base of the shoreface). Since 2006 profile data have been collected using an RTK-DGPS mounted to a backpack being carried from a benchmark location referenced to NAD 1983 UTM Zone 17N, most often starting behind the dune, into the surf zone. The subaqueous portion of the survey was collected using a single beam fathometer corrected for heave, pitch, and roll of the vessel as well as for changes in velocity of sound along the coast. Profiles were digitized into Hypack Single Beam Editor where lines are cleaned for erroneous points in the vertical as well as restricted to a narrow horizontal window away from the defined line to ensure repeatability of the survey profile. In some cases, as evident in profile 5130 in Surfside Beach, offshore errors may increase with stronger wind and wave climates leading to difficult collection (Figure 19). Profile collected prior to the 2008-2009 renourishment project are discussed within to provide the best assessment of framework influence on shoreline behavior.

Various profile metrics were calculated in the areas where beach profiles and boreholes have been jointly collected. The metrics computed involve depth of closure, slope of the shoreface, from 0 m elevation to the depth of closure, and bar volume. These were quantified using the Beach Profile Analysis Package (BMAP) of the Coastal Engineering Design and Analysis System (CEDAS) v.4.0 created by the Coastal and Hydraulics Laboratory of the US Army Corps of Engineers. These profile metrics provided quantitative measures of profile geometry and character to consider against the potential influence of framework geology, or seismic reflectors, and shoreline behavior. The mean high water (MHW) line serves as the relative position on all beach profiles and is represented as the 0.625 m isobath. Slope of the shoreface was quantified between zero meter elevation and to the offshore limit of profile change, or depth of closure (DoC), manually determined by the decrease in standard deviation to near 0 relative to shore profile variability. Profiles were then draped into Fledermaus v.7.5.1 alongside CHIRP reflective profiles, borehole logs, and multibeam sonar data for further assessment of interplay between framework geology and shoreline morphology.

3.4 Multibeam Sonar Data

While alongshore contours and cross-shore profiles provide detailed insight into beach morphology and position, data are constrained both temporally and spatially. In effort to characterize the nearshore framework influence on shoreline variability, the lower shoreface and transition from shoreface to the inner shelf was characterized using high-resolution multibeam sonar. These data were collected on October 16, 2015, February 22, 2016, and March 15, 2016.

The initial survey line, from October 16, 2015, was obtained in effort to provide improved insight into physical shoreface characteristics. Subsequent surveys were obtained using the Oct15 survey as a reference, navigating nearshore in areas where previously collected data veered further seaward, and offshore where the survey line previously captured above the 6-meter contour in effort acquire a continuous longshore contour swath of bathymetry and backscatter. A Kongsberg 3002D multibeam echo sounder (300 kHz) was mounted to the bottom of the Coastal Carolina University research vessel R/V Coastal Explorer. To avoid cross-communication between sounding heads, one is set to 293 kHz, while the other is set to 307 kHz. The dual-head system has a maximum ping rate of 40 Hz, creating 508 beams. Precision measurements are obtained simultaneously through usage of a Kongsberg Motion Reference Unit 5 for a roll and pitch accuracy of 0.001° with a heave accuracy of 0.02 m. Multibeam measurements were supplemented with a high-resolution Seapath 200 RTK-DGPS to acquire navigational information, with 0.01 m horizontal and 0.02 m vertical positional accuracy. Multibeam data provides the ability to map the seafloor and characterize backscatter data by emitting sound waves in a fan shape (Figure 20) below the vessels' hull and recording the time of return and the strength of the returned signal. Depth of the multibeam swaths collected for this study range between -4.89 to -10.22 meters, and widths range from 24-36 meters. All multibeam lines presented were edited using CARIS HIPS and SIPS 9.0 software at 1-meter resolution. Backscatter mosaics were created using FMGT v.7.5.1 software and imported into Fledermaus alongside beach profiles, CHIRP, and borehole data for enhanced visualization.

In effort to establish comparable statistics between multibeam and shoreline metrics, floating point backscatter bathymetry data were digitized in ArcGIS and a similar workflow was employed to extract backscatter values. The contour tool within the Spatial Analyst toolbox in

ArcMAP was used to construct contours at every meter depth. The 6-meter contour was the most continuous contour along the length of the data and was used in the assessment of backscatter variability along the shoreface. This is presumed to be a measure of framework character in that the backscatter value can be related to the nature of the sea floor. For many areas along the Grand Strand, seaward of the nearshore bar there is very little if any modern sediment overlying the geologic framework. To utilize the backscatter as an indicator of framework, a point is created at the intersection between the 6-meter contour and the shoreline transects cast digitized from the Digital Shoreline Analysis System. Further, a 1-meter buffer around each point is created to avoid selection of a non-representative backscatter value (Figure 21). Backscatter values within the buffer are extracted and averaged using the Zonal Statistics as Table tool within the ArcMAP Spatial Statistics toolbox.

3.5 Statistical Analysis

DSAS-generated shoreline change and backscatter data files were brought into Matlab v.10.2 and SCE, LRR, and backscatter intensity were plotted. Currently at the end of its renourishment cycle, the recently collected multibeam data are to be representative of the condition before the 2008-2009 renourishment project along the Grand Strand. All shoreline change measurements and backscatter intensities are multiplied by 50 meters to account for the transect spacing considered in DSAS. Pearson's correlation coefficients between the shoreline change rate, linear regression rate, and the backscatter intensity values were determined in various sections, divided by geologic metrics discussed further in the results. Metrics were analyzed and correlated against various other metrics as seen in Table 1 and their spatial distribution can be examined in Figure 23. For physical metrics distributed alongshore, each transect was classified as having the feature present or absent. The standard score was calculated for measurements of shoreface slope, shoreline change, and backscatter intensity. When correlated, the average of each standard score was determined and each measurement was classified as either higher or lower than average. The subsequent 2-tailed significance value for each correlation was evaluated in effort to determine statistically significant relationships between shoreline and backscatter variability.

Power spectral density of both the DSAS-generated rates of shoreline change and multibeam backscatter intensities were treated as spatial signals and analysis of longshore wavelengths in variability is computed. The spatial frequencies identify energy contained at various frequencies, defining demonstrable spatial wavelengths in alongshore shoreline features. Shoreline datasets within this study contained undefined values where data has not been collected, specifically the northern portion of Surfside Beach into southern Myrtle Beach. Undefined values were removed from the data set and were linearly interpolated to generate a continuous signal. Power spectral density is computed using Welch's overlapped segment averaging estimator in Matlab. Welch's method divides the signal into overlapping segments, computes the power spectral density for each segment, and averages all the segments. During processing, a Hamming window is used to more accurately assign power to correct frequencies, in addition to noise reduction. A 50% overlap was utilized to eliminate signal reduction near the end of each windowed segment.

Chi-square test analyses were used to determine whether or not a relationship between the various metrics listed in Table 1, backscatter variability, and shoreline change values exist. In effort to construct a 2×2 contingency table, each transect was classified according to whether the metric was or was not present. Where relationships involved quantitative values, the standard score was calculated and each point was classified as having either higher or lower values than the average. The standard table of distribution with one degree of freedom was used to determine relationships based on chi-square values.

Cross-correlation analysis of the shoreline change and backscatter variability datasets quantified the strength of the linear regression between the two. Cross-correlation analysis allows for an investigation of relationships that may be offset to the south or north, either lagging or leading of the backscatter dataset. This allows for an investigation into the possibility of a spatial-shift in response given an interconnected relationship. The lags investigated herein are in terms of transects, either offset by a positive or negative lag up to 3 transects, or 150 meters. A negative lag between backscatter intensity and shoreline change response indicates a response in the shoreline occurred to the north of the bathymetric backscatter. Further, positive correlation coefficients indicate that both variables are either increasing or decreasing together; while negative correlations indicates one variable decreases while the other is increasing. Results, however, did not show any significant correlations given lags and have been regarded as having negligible affect on shoreline, shoreface relationships.

In effort to further constrain longshore differences in physical or geologic forcings that may be influencing shoreline response and backscatter variability, shorelines were divided based on the presence or absence of paleochannels along each transect casted in ArcMAP, and shoreline change and backscatter variability were analyzed based on the divisions. Locations containing paleochannels were further divided into deep and shallow paleochannels based on average depth recorded by Baldwin and others (2005) (Figure 5). Shoreline change envelope and backscatter variability were cross-correlated within each segment of shoreline and backscatter divided by paleochannel absence or presence. A chi-square test was then used to identify relationships between shoreline change and backscatter when paleochannel presence was considered.

4. Results

4.1 Short-term Shoreline Variability

The baseline and grid of transects used for the Digital Shoreline Analysis System short-term variability is shown in Figure 12. Transect spacing was 50 meters and the geologic and physical metrics used in assessing relationships are shown in Table 1 (Morton et al., 2005; Schwab et al., 2013). Shoreline change rates computed across 1008 transects were computed for all shorelines, years 2006-2009 (Table 3). In effort to avoid nourishment sediments from obscuring possible framework influence, a focus on the 2006-2009 prerenourishment shorelines was ideal (Park, et al., 2009). Surfside Beach and Garden City renourishment projects took place the earliest of the cities, from January 2008-March 2008, resulting in the least amount of prior shoreline data. Conversely, the largest quantity of data for shoreline change rates encompasses Myrtle Beach due to the late renourishment, taking place in November 2008-February 2009 (Table 4). Figure 23 showcases the variation of shoreline position alongshore, quantified by the linear regression rate and shoreline change envelope. Mean calculations for the net shoreline movement (NSM), end point rate (EPR), shoreline change envelope (SCE), and linear regression rate (LRR) are shown in Table 5. In South Carolina inlet zones are managed differently reflecting the dominance of inlet processes on shoreline movement (South Carolina Guide to Beachfront Property, South Carolina Ocean and Coastal Resource Management). Due to the analogously higher mobility, shoreline change rates displaying significant influence from inlet processes were negated in regional quantifications of beach erosion patterns. Short-term shoreline change rates are relatively high- -7.5 m/yr in Myrtle Beach when compared to a regional -0.2 m/yr retreat average- when compared with the 2005 USGS National Assessment of Shoreline Change (Morton and Miller, 2005). Higher rates of erosion, specifically along Myrtle Beach (-7.5 m yr^{-1}), are presumably due to a combination of the inclusion of renourishment projects in the National Assessment, contrasts in methodology and frequency of data collection, and the inherent variability of the mean high water line during data collection. The highest average rate of erosion was recorded in Myrtle Beach with a linear regression rate of -7.5 m yr^{-1}. North Myrtle Beach exhibits the lowest percentage of shoreline change rates at 16.8% erosion at an average -2.52 m yr^{-1}.

Spectral density of shoreline sections was analyzed in effort to identify any quantifiable spatial scales of shoreline change behavior. Along all shorelines energy generally increases towards longer wavelengths (Table 6), as expected along a shoreline dominated by larger-scale shoreline patterns. The dominant spectra for each shoreline section are seen in Table 6. Notable are numerous consistencies in spatial wavelengths of 160 m throughout Garden City, Myrtle Beach, and Arcadian Shores. Dominant energy spectra in Surfside Beach and North Myrtle Beach are 400 m and 256 m, respectively. Figures 24-28 and Table 6 exhibits the corresponding dominant spectral densities plotting on a log-log scale to provide an enhanced view of dominant powers contained within component frequencies.

4.2 Spatial Correlation Using Mapped Bathymetry and Backscatter

Recognizing the dynamic nature of the mean high water contour line as a shoreline indicator, multibeam sonar imagery of the lower shoreface was acquired where previous work demonstrated much less frequent sediment cover and movement of fair-weather foul weather nearshore bar/ beach sediment processes (Barnhardt et al., 2009). The lower shoreface is also an area where the shallow geologic framework observed in borings and CHIRP profiles from the USGS Coastal Erosion Study (Barnhardt et al., 2009) locally should intersect the modern active surface within the shore face.

Offshore cusp features imaged in nearshore multibeam are apparent just below the 6-meter contour in many locations along the Grand Strand (Figure 29). The widths of the offshore cusps along the Grand Strand vary, ranging from 8-40 meters across, with typically less than 0.5 m relief. Backscatter extracted from multibeam data reveals distinct contrasts in intensity in between the cusps, from the crests to the troughs. As seen in Figure 29, the cusps appear to be cutting into lower backscatter material. The series of boreholes were further used to consider the variation in geologic framework along the coast (Barnhardt et al., 2007 and Putney, et al., 2004). The boreholes were collected just adjacent to the shoreline and provide greater detail into the contrasting compositions between the Cretaceous and Pleistocene units. The Cretaceous Peedee Formation composed mainly of calcareous mud and siltstones with minor shell fragments (Putney et al., 2002). The Pleistocene units contain nearshore marine, fluvial, and shelly calcareous sandstone deposits. Where these units extend to the shoreface, the exposure of this boundary likely leads to varying erosion rates and boundary flow patterns (Murray and Thieler, 2004). While it is not possible to discern the exact nature of this relationship, the data presented suggest an apparent spatial relation. While very specific in describing the geologic character and elevations of contacts between different lithologies, these boreholes are widely spaced along the coast. The nearshore multibeam lines were considered alongside the 2004 borehole logs, aligning in 3 locations along the Grand Strand. Figure 30 shows an example of the strong association of a lithologic boundary and the elevation of the top of the cusps, suggesting relict outcropping of antecedent geology.

Side scan sonar data, collected as part of the USGS Coastal Erosion Study, was utilized as a spatially coherent indication of inner shelf bathymetry and framework. These data produced 100% side scan coverage in most places from the seaward side of the nearshore bar out to 6 kilometers from the coast (Figure 31). This provides a consistent, if not highly specific, parameter of the geologic character of the sea floor along the coast. Further, inner shelf side scan sonar imagery collected in 2003 provides a means for analyzing connectivity of the inner shelf cusp features and offshore structure. Figure 32 reveals a strong relationship between the offshore sidescan backscatter imagery and the persistence of the nearshore cusps. Visible in the sidescan sonar imaging are the presence of alternating low and high intensity linear scour depressions. A chi-square test, based on visual correlations, confirmed a significant relationship (chi-square value 226.006; 1 degree of freedom) between the persistence of offshore cusps and linear scour depressions extending offshore (Table 10). In the vast majority (88.9%) of cases offshore cusps align with the presence of inner shelf scour depressions. The presence of the inner shelf scour depressions, however, are often present where nearshore cusps are not. Further, Figure 31 indicates the extension of the linear scour depressions into larger inner shelf sand linear scour depressions.

4.3 Geostatistics and Quantified Correlations

Visual correlations between cusps imaged in multibeam, sidescan sonar, and borehole logs reveal an apparent relationship between framework geology and nearshore subaqueous features (Figures 13-15, 33). Quantifying the strength and magnitude of these relationships further confirms their connectivity and connects their presence to the paleochannels networks. Correlation coefficients between ±0.40 - ±0.60 are considered to be representative of moderate strength relationships, while weak relationships are below ±0.40 and strong relationships above ±0.60. Table 8 shows the 2 × 2 contingency table reveling a strong relationship between the presence of offshore cusps and the absence of paleochannels. For 1 degree of freedom, 10.83 is the critical chi-square value at the 99.9% confidence level. There is only a 0.001 probability that a chi-square value will exceed this critical value. However our value critical value is 193.145, suggesting a highly significant relationship between the presence of offshore cusps and paleochannel location. While 88.9% of cases where cusps are present there is also an absence of paleochannels, not all locations where paleochannels are absent corresponds to cusp presence. Cross-correlation results suggest a moderate-strength (-0.419; p-value 0.000) inverse relationship between cusp and paleochannel presence and are listed in Table 11.

Further cross-correlation analyses were executed to quantify spatial relationships between nearshore features, framework geology, and shoreline variability. Offshore cusps also had correlations with the shoreline change envelope standard value (-0.375; p-value 0.000) and the backscatter intensity standard value (-0.350; p-value 0.000). Visible alongshore are also the presence of rhythmic cusps, characteristic of many dissipative and intermediate shorelines, and are further correlated to offshore metrics. Strong correlations result between degree of shoreface slope, onshore cusps, and paleochannel presence. Table 11 lists the results of cross-correlation analyses between multiple metrics and will be further discussed in the following section.

The relationship between the 6-meter contour multibeam backscatter and the shoreline change envelope was further investigated to evaluate the moderate correlation between both metrics and the presence of offshore cusps. Sections of shoreline were categorized by an absence of a paleochannel, shallow paleochannels (<-12.55 meter depth), and deep paleochannels (>-12.55 meter depth). Significant correlations (p-values <0.05) were categorized by having no correlation, positive correlation, or negative correlation and a chi-square test was used to analyze the strength of relationships between backscatter and shoreline change, given each characterization of paleochannel at that location. The chi-square test shows that there is a strong relationship, with a p-value < 0.001, between backscatter and shoreline change where deep paleochannels are present (Table 9). It is worth noting, however, that while the majority of the correlations are positive, nearly 25% of the correlations were negative. A critical value of 929.595 and an effect size of 46.5% reveal a strong relationship, but the correlation dissipates in areas lacking paleochannels.

5. Discussion

5.1 Physical Descriptions of Bathymetric Features

When overlain with multibeam, the sidescan sonar imagery shows a compelling relationship between the offshore cusps and the offshore linear scour depressions extending into larger linear scour depressions along the inner shelf. As the resolution of the sidescan imagery is 2 m/pixel (compared to 1m/pixel resolution of the multibeam imaging), it is not abundantly apparent if all offshore cusps line up exactly with the sidescan scour depressions. Nearly all regions that contained offshore cusps, however, were in regions where linear scour depressions are present (Table 10). Earlier work has analyzed the offshore nature of the inner shelf; specifically the linear scour depressions of high and low backscatter in the side scan sonar imagery (Barnhardt, 2009). In these cases, the offshore linear scour depressions followed the same low backscatter at the crest and high backscatter in the trough pattern as seen in the offshore cusps. The linear scour depressions were found to contain fine sands at the crests with coarse sand and gravel in the troughs, a result of sediment partitioning through winnowing of finer sands. Assuming offshore cusp extension into the linear scour depressions, and eventually offshore linear scour depressions, it is reasonable to infer that the ground truthing attained from the South Carolina Coastal Erosion Study can apply to the offshore cusps that experience similar backscatter patterns. Where offshore cusps have been imaged, the linear scour depressions appear to connect to the cusps.

Evidence found in the alignment of borehole logs and CHIRP seismic profiles indicate the influence of framework units on the formation of the nearshore cusps. Alignment of the crest of the offshore linear scour depressions to the cretaceous boundary layer is seen in multiple locations where logs extend to similar depths (Figure 13-15). Further, seismic profiles reveal a distinct reflector located along the shoreface that aligns with the Cretaceous boundary (Figures 13-15). Borehole logs detail the differences in composition between the two units (Figure 16-18). The base of the cusps consistently reveals higher backscatter material, possibly representing a course erosional lag or physical outcrop extending offshore recorded within the logs.

The relationship between the presence of nearshore cusps and the underlying Cretaceous strata is apparent where exposed, but the cusp geometry indicates influence from longshore current flows and bottom hydrodynamics (Figure 34). Previous studies have confirmed the net southerly flow of sediments and currents along the Grand Strand, and Barnhardt (2009) confirmed its influence on the asymmetric shape of the offshore linear scour depressions captured in sidescan sonar imagery (Gayes et al., 2003; Barnhardt, 2007; Gutierrez et al., 2006) (Figure 33). A similar geometry is exhibited in the nearshore cusps, further supporting their connection to the offshore linear scour depressions and influence from current flows (Figure 34). A change in geometry of the cusps is seen in parts of northern North Myrtle Beach, where recorded longshore transport rates reverse towards the north (Kana et al., 2013). In these locations, the slope angles of the cusps shift towards supporting net northern current movements. Future studies would need to address process-oriented impacts on cusp formation and presence, deepening the understanding of sediment transport pathways along the coast. Doing so will contribute to enhancing variable storm impact predictions and behavior of beach nourishment projects. The data presented herein, however, provide the necessary means to deepen the understanding of relationship between the framework, shoreline, and nearshore environments.

5.2 Shoreline Change

Shoreline change rates along the Grand Strand have been monitored since the 1980's. Traditionally, erosive potential of the shoreline has been assessed through seasonal topography changes in BERM beach profiles. The average rate of coastal change at the central Grand Strand, within Myrtle Beach, was measured to be 0.2 m yr^{-1} (Barnhardt, 2009). This rate is considered to be quite stable, however the shoreface has appeared to be receding at a much quicker pace (0.8 m yr^{-1}) (Barnhardt, 2009). The result is an apparent shoreface steepening of the Myrtle Beach profile, likely a result of distribution and settlement of renourishment fill (Figure 35). The shoreline data used for this study focused on GPS-recorded pre-nourishment MHW shoreline positions only. Calculated rates highly exceeded those previously recorded, as expected with the inherent variability of the mean high water line. Both Garden City and North Myrtle Beach contain the lowest shoreline change rates, and is likely due to sediment availability from nearby river input from Winyah Bay and Hog Inlet. The southern reaches of the Grand Strand reflect accumulation of sediment from the northern areas, mobilized from longshore transport.

While the shoreline rates of change are exceedingly high, a few unique characteristics are noticeable. Namely short, consistent spatial wavelengths recorded throughout locations in some of Garden City, Myrtle Beach and portions of North Myrtle Beach. Spectral analysis identified typical wavelengths of these undulations in shoreline change correspond with similar wavelengths seen in multibeam imaging. Also present along sections of coastline are significant wavelengths on the order of 400-600 meters, similar in both shoreline change rates and multibeam backscatter variability. As there is no consistent visible feature onshore or offshore within the 400-600 meter spatial frequency, the similar wavelengths may be providing insight into a combination of hydrodynamic processes and variable framework influences. Further, spectral analysis was not capable of identifying wavelengths on the order of beach cusps (typically between 11-16 meters in width), limited by the 50 meter transect sampling rate. However, the width of the offshore and beach cusps are strikingly similar (Figure 36). Their relationship was examined amongst the spatial correlations and is discussed in the following section.

5.3 Spatial Correlation of Geologic Framework and Shoreline Erosion Variability

Previous studies have begun quantifying connections between nearshore morphology and framework influence (Browder & McNinch, 2006; Riggs et al., 1995; Anima et al., 2002; McNinch, 2004; Schwab et al., 2000; Riggs et al., 1996; Schupp et al., 2006; Miselis and McNinch, 2006). While research has continued to enhance the understanding that framework-influenced nearshore morphology has on shoreline behavior, quantitatively linking framework and shoreline behavior along the Grand Strand has remained difficult. Much effort has been placed on mapping of the Grand Strand beaches and framework geology, but this study has begun to enhance the connections between framework and shoreline that have similarly been examined in other regions. Most notably, this study has revealed encouraging associations between nearshore cuspate features persisting in locations of outcropping framework and longshore shoreline morphology. While correlation coefficients in this study can reach high values (-0.744), a few considerations need to be taken when addressing correlations that are generally considered to be small or moderate. Firstly, there are few studies that examine correlation values with respect to shoreline behavior and effect size, and it is necessary to note correlations that typically represent moderate correlations. Secondly, it is possible that not all offshore areas containing cusp features have been imaged. Without full imaging of the nearshore, it is possible that correlations involving cusp presence have been skewed.

Still, with these considerations, nearshore cusp features appear to have a moderate correlation with areas of coastline lacking a paleochannel network. Collectively considered with the correlation between presence of offshore cusps to the absence of paleochannels and alignment with the moderate correlation to shoreline change, these features appear to be reflective of geologic framework and longshore transport of sediment. The inverse correlation to the shoreline change envelope values, implying nearshore cusp presence where the shoreline change envelope is low, may be the reflection of a combination of physical and geologic influences. The correspondence between the presence of offshore cusps and smaller, or absent, nearshore bars suggests the possibility of cross-shore sediment flows moving sediment offshore (Figure 37). Additionally, visual inspection of cusp presence compared to shoreline change values suggests a relationship to more variable coastlines. Research conducted by Hapke and others (2010) found similar results in that linear scour depressions present at the 10-meter contour off Fire Island, New York corresponded to shoreline accretion. This study found a similar relationship between offshore linear scour depressions and absence of nearshore bars, even though the study compared linear scour depression presence to 75-year shoreline change rates. Inherently, shoreline variability on a 75-year temporal scale distinctly varies from that of a 2-year scale. Continually changing physical and geologic forcings, both natural and anthropogenic, may be more apparent on shorter, seasonal scales. Hapke and others (2010) additionally created a spatiotemporal regression plot of Fire Island, finding a consistent influence from framework on shoreline change. Additional bathymetric surveys and hydrographic testing would be needed to provide a more statistically significant characterization of the spatial relationship along the Grand Strand. However, the results of the study presented herein add to the promising evidence of framework influences along to shoreline change, apparent on shorter time scales.

Additional results found that nearshore cusps also have moderate correlations with both the shoreline change envelope (-0.375) and the degree of shoreface slope (0.307) (Figure presented in Results section). While the cusps do not have as strong of a correlation with the steepness of the shoreface, the absence of paleochannels highly correlates with steeper shoreface profiles. If cusps extend throughout numerous other locations along the shoreline where the Cretaceous boundary is extended to the shoreface, these correlation values could be expected to increase. The morphodynamic classification of sandy shorelines additionally provides insight into sediment transport pathways along the Grand Strand. Steeper beach profiles typically correspond to rip cell set-up (Wright and Short, 1984). In areas where steeper profiles are present and cusps are present rip heads may be contributing to sediment deposition onto the cusp features. To further assess the relationship of sediment and shoreline change, considering framework composition, additional statistics were run on backscatter and shoreline change.

A chi-square test was used to assess the effect of sediment cover over regions of paleochannels, and their impact on shoreline change. Multibeam backscatter intensity and shoreline change envelope were correlated both on a regional and paleochannel-defined scale. Across the length of the Grand Strand a correlation is not apparent, whereas significant correlations (p value <0.05; $R^2 > 0.350$) were more distinguishable when the considerations of paleochannel presence were taken. Given the results from the power spectral density analysis, revealing most significant longshore wavelengths of shoreline change on the largest scales (>3.2 km) the low (0.135) correlation across the study area is not remarkably surprising. The chi-square test of the correlations between backscatter and shoreline change was able to further assess their relationship given paleochannel presence. The large effect size and high chi-square value signify significant relationships. In areas lacking paleochannels there are no cases of correlation between the backscatter intensity and shoreline change. It is likely that factors other than sediment distribution have a large contribution to shoreline change, i.e. shoreface slope, framework influence, and linear scour depression/cusp morphology. Previous research done by Barnhardt (2009) investigated the sedimentology of the Grand Strand region and found that areas containing deep paleochannels generally coincide with larger gravel-fill units. It is likely that these deposits have a greater influence on bottom flows and wave propagation than areas dominated by cusp and bar influence to wave incidence given consistent wave climate.

5.4 Conceptual Model of Shoreface Slope System

Enhancing models and of shoreface evolution and connection to remains an imperative process to developing a deeper understanding of beach variability. The data presented herein reveal interesting connections between beach geometries, shoreface characteristics, inner shelf bathymetry, and framework influence. Offshore cusps have a moderate correlation to where paleochannels are absent, suggesting that they are found in regions that have not been repeatedly incised by river drainage. Further, both the spatial relationship between the Cretaceous and Pleistocene boundary to the top of the offshore crests and CHIRP seismic reflectors indicate the boundary influence on locations where offshore cusps are present (Figures 30 and 32). In all locations where the outcropping Cretaceous boundary is present along the shoreface (Figure 32) the offshore cusps are established. As apparent by visual inspection, and reflected in the chi-square test (Table 10), these offshore cusps appear to extend into the linear scour depressions along the inner shelf. The mechanisms and processes by which the offshore cusps reveal connection between framework geology and inner shelf bathymetry are discussed here.

Where the Cretaceous boundary is exposed, the contrasting compositions are revealed, affecting bottom flow and sediment mobility in the region (Murray and Thieler, 2004). As the Pleistocene unit is more susceptible to erosion than the underlying Cretaceous, the underlying composition has the potential to introduce bottom turbulence and sediment partitioning and accumulation (Barnhardt, 2009; Murray and Thieler, 2004). Where finer grains begin to accumulate across the exposed Cretaceous unit, the low-relief offshore cusps form. As wave and tidal currents further interact with the cusps the small features self-perpetuate into larger scale linear scour depressions along the inner shelf, eventually sustaining themselves into the large-scale ridges seen in Figure 33. As the offshore cusps start as very low relief (typically ~0.5m) and occur just below the depth of closure across the region, it is not likely that the cusps create large impacts to incident wave angles affecting the shoreline (Figure 38). However, it is conceivable that the cusps impact sediment mobilization at this location and may be transported to about the depth of closure during larger-energy events and storms (Figure 38). An example of this pattern is seen in the Figure 39 CHIRP profile. Where seismic reflectors reach the shoreface, previous incisions are apparent. The incisions appear to reflect storm impact on the bottom layers of sediment, mobilizing sediment to be transported further alongshore or into the active beach region.

5.5 Implications for management applications

The Grand Strand is in a unique setting along the Atlantic coast. The expansive shore-attached beaches and low sediment input have in part contributed to the lower than national average long-term erosion rates. Still, alongshore variability in erosion rates requires further understanding, as it is particularly important to understand the processes and mechanisms controlling larger variability on shorter time scales. This study has revealed a strong spatial relationship between offshore backscatter intensity and the shoreline change envelope, or shoreline variability, where paleochannels are present. This relationship is further supported by correlation between offshore cusp presence and the absence of paleochannels, suggesting the possibility of interaction between offshore cusps, nearshore morphology, and shoreline change. Where paleochannels are present, backscatter intensity (sediment size) has a stronger correlation to higher shoreline variability. While the cause and effect nature of the relationships, and their influencing processes, are not discernable from this data, connecting the offshore regions are valuable for shoreline management.

The Grand Strand is a region highly reliant on renourishment projects to replenish subaerial beach widths. Alterations to the nearshore morphology have the potential to alter incident wave activity and sediment transport pathways. Addition of material to the shoreface has the potential to mask the nearshore linear scour depressions and change potential refraction around cusps and nearshore sediments. As cusps tend to persist in regions of higher shoreface slopes, sediments appear to be transported to 6-meter contour aligned with the Cretaceous unit boundary. Further, there remains a substantial relationship between shoreline change and multibeam backscatter at the 6-meter contour where deep paleochannels are present. These apparent interactions between the shoreface profile and nearshore region challenges the conventional consideration of the depth of closure as the extent of seaward sediment exchange. Considerations in renourishment budgets and temporal extent would need to be adjusted to incorporate these findings.

Studies investigating the framework geology along the Grand Strand have provided great insight into a regional characterization of South Carolina's northern coast. Further studies along this shoreline are needed to confirm the mechanisms for the interaction between offshore bathymetry and shoreface and beach behavior. Grab samples should be taken at the locations of offshore cusps to provide further ground truthing, in addition to coring taken in similar locations. Hydrodynamic studies, including current flow meters and particle cameras can assist in discerning bottom flow influence. Finally, further multibeam imaging should be collected alongshore to fully characterize the lower shoreface transition into inner shelf. However, if these regions are directly connected, future renourishment efforts will need to take into consideration the pathways for sediment dispersal throughout the whole region, extending further offshore than the depth of closure reference. Adding to the subaerial beach may provide protection to homes during storms, but increasing the understanding of shoreline behavior could prevent large losses of sediment given regional controls on distribution behavior. It remains critical to further the understanding of coastal systems, both on long and short-term scales, to adjust to future negative effects from storm impacts and rising sea levels.

6. Conclusions

A growing amount of research has highlighted the possible influence of geologic framework on shoreline erosion variability, especially in regions devoid of recent renourishment projects. Studies analyzing the shoreline variability during these times result in the most accurate assessments of future shoreline change predictions. Along the 62-km Grand Strand shoreline rates of change from the years 2006-2009 are high and largely variable, indicating the influence of short-term monthly data collection and the result of measurement of a highly variable mean high water position. Multibeam sonar imaging taken at the base of the shoreface allowed for the quantification of backscatter intensities, which contained similar spatial wavelengths with the shoreline change envelope values. Where deep offshore paleochannel presence were considered, there were significant correlations between higher offshore backscatter and increased shoreline change. This relationship supports research indicating the influence of framework variability and shoreline behavior. Multibeam imagery further revealed irregularly spaced offshore cusp features just below the depth of closure. Previous borehole and seismic data suggest that these offshore cusps are the result of erosion of the Cretaceous framework boundary. Visual correlation to previously collected inner shelf sidescan sonar data suggests an extension of the nearshore cusps to offshore networks of linear scour depression features, seemingly influenced by longshore currents. Numerous other correlations between physical and geologic metrics indicate a relationship between offshore cusps and paleochannel presence, shoreface slope and paleochannel presence, and onshore cusps and shoreface slope. If the connection can be verified by further grab samples, coring, and bottom flow studies, the sediment transport dynamics between the inner shelf, base of the shoreface, shoreface geometry, and shoreline behavior could provide great assistance to coastal managers and researchers in effort to mitigating and protecting against future storm impacts and erosion deficits.

Figures

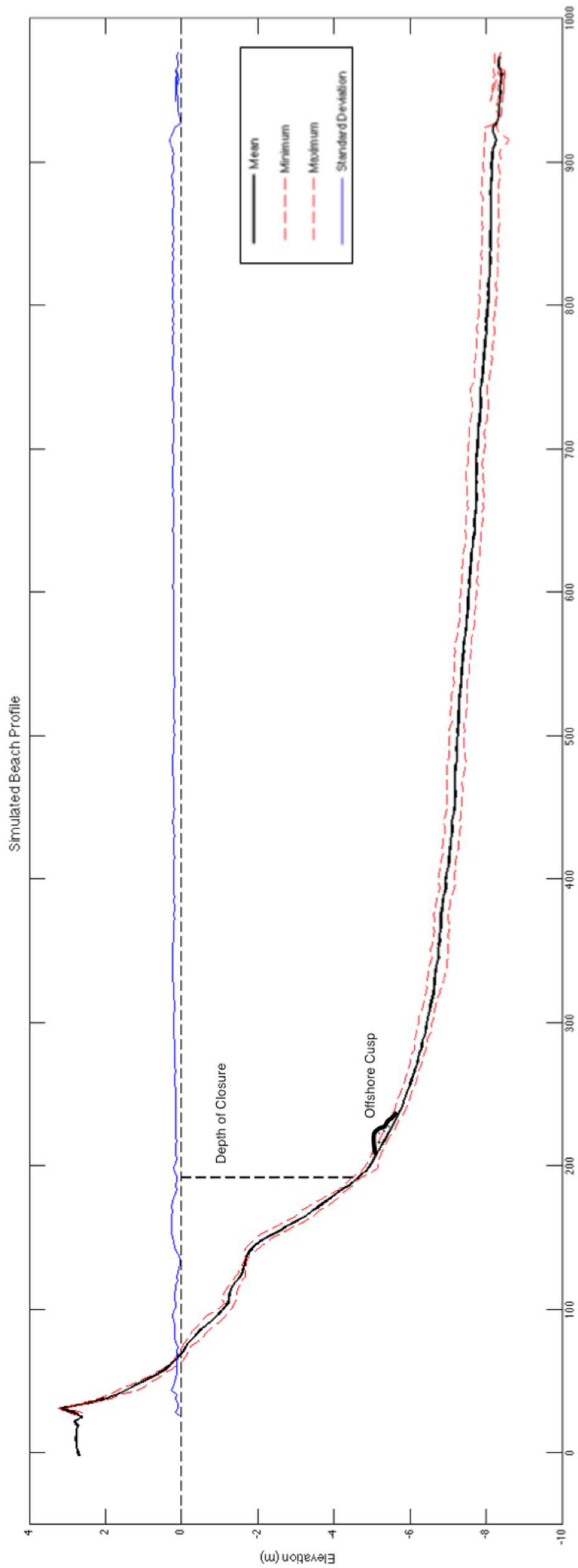

Figure 1: An illustration of the location and description of the depth of closure. Regions seaward of the depth of closure are defined by having no onshore sediment exchange, whereas shoreward of the depth, sediment is exchanged within the active beach and is available for transport alongshore.

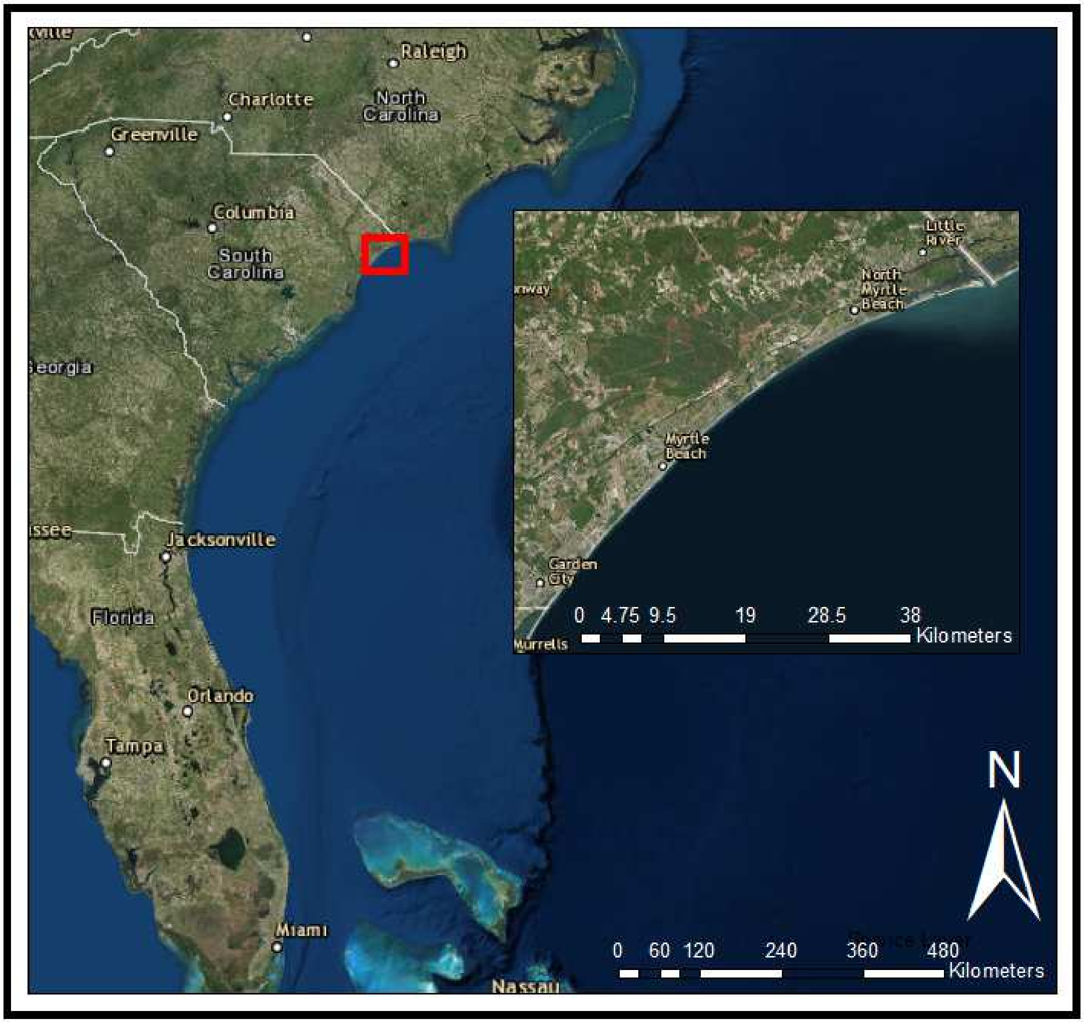

Figure 2: The 62 kilometer shoreline of the Grand Strand, situated in northern South Carolina, just along the border of North Carolina.

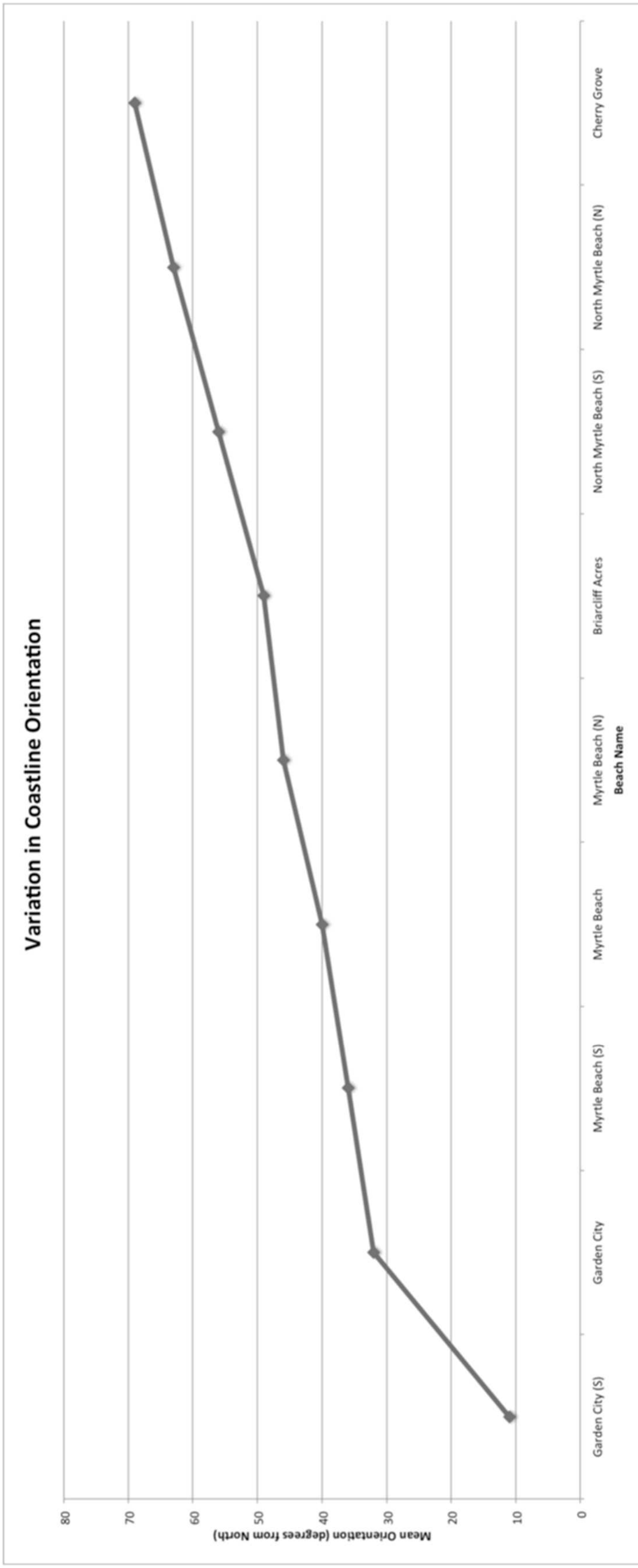

Figure 3: The mean degree of shoreface orientation alongshore from southern Garden City through northern North Myrtle Beach, as adapted from Slovinsky (2001). Shoreline orientation is recorded in degrees from North and were determined by calculating degrees of change between BERM profile lines throughout South Carolina.

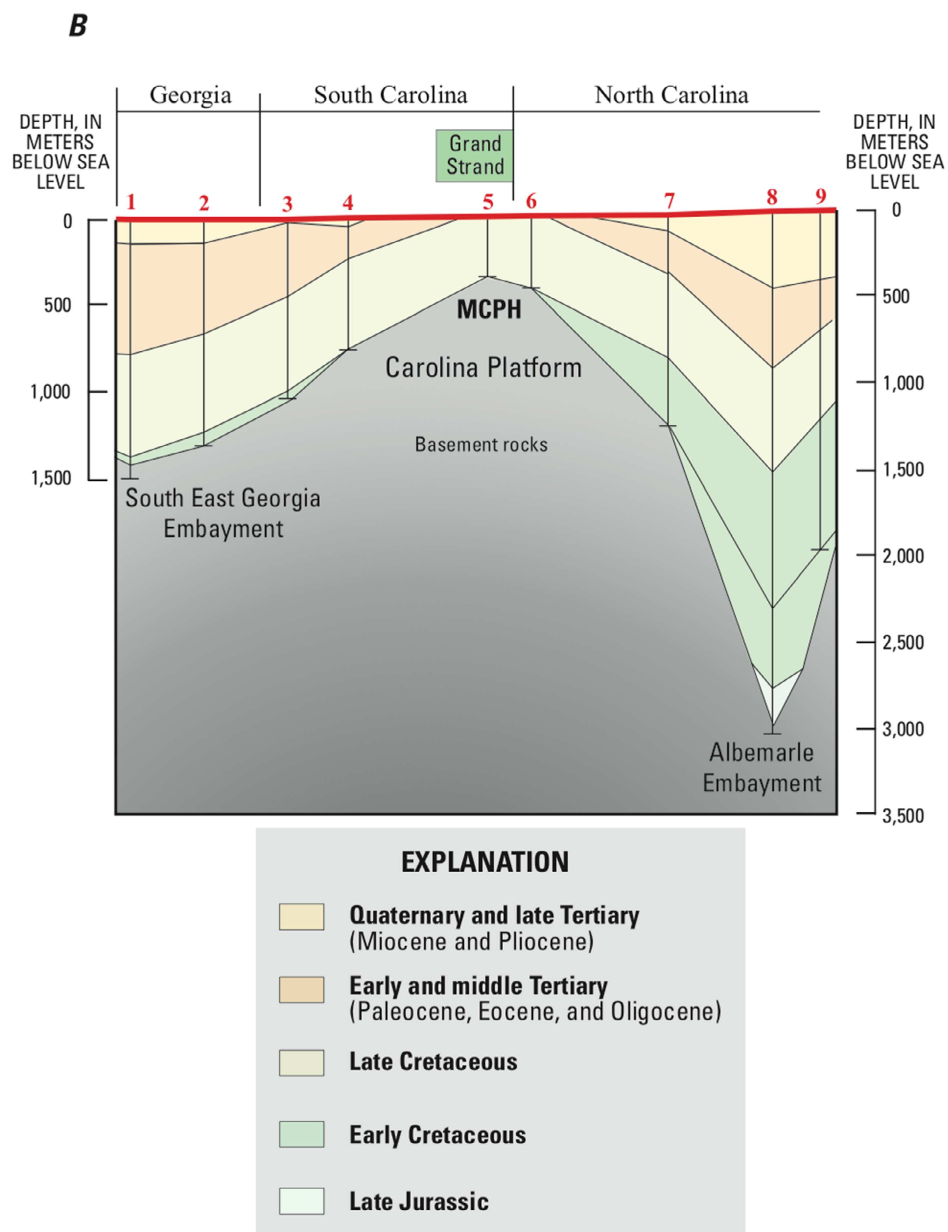

Figure 4: A cross-section illustration of the Carolina Platform, indicating the position of the Grand Strand a top of the Mid-Carolina Platform High, constructed by Gohn (1988) from deep-borehole data.

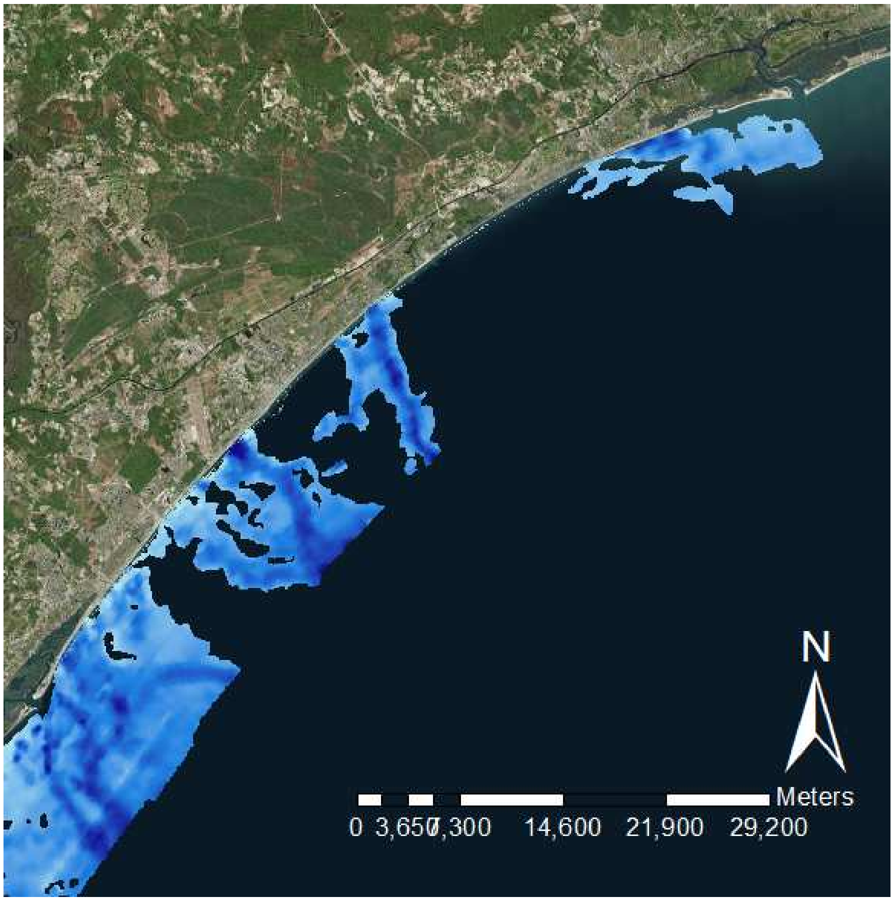

Figure 5: Paleochannel records along the Grand Strand as recorded by Baldwin and other (2009). Deeper blues reference deep paleochannels, with lighter blues representing shallower channels.

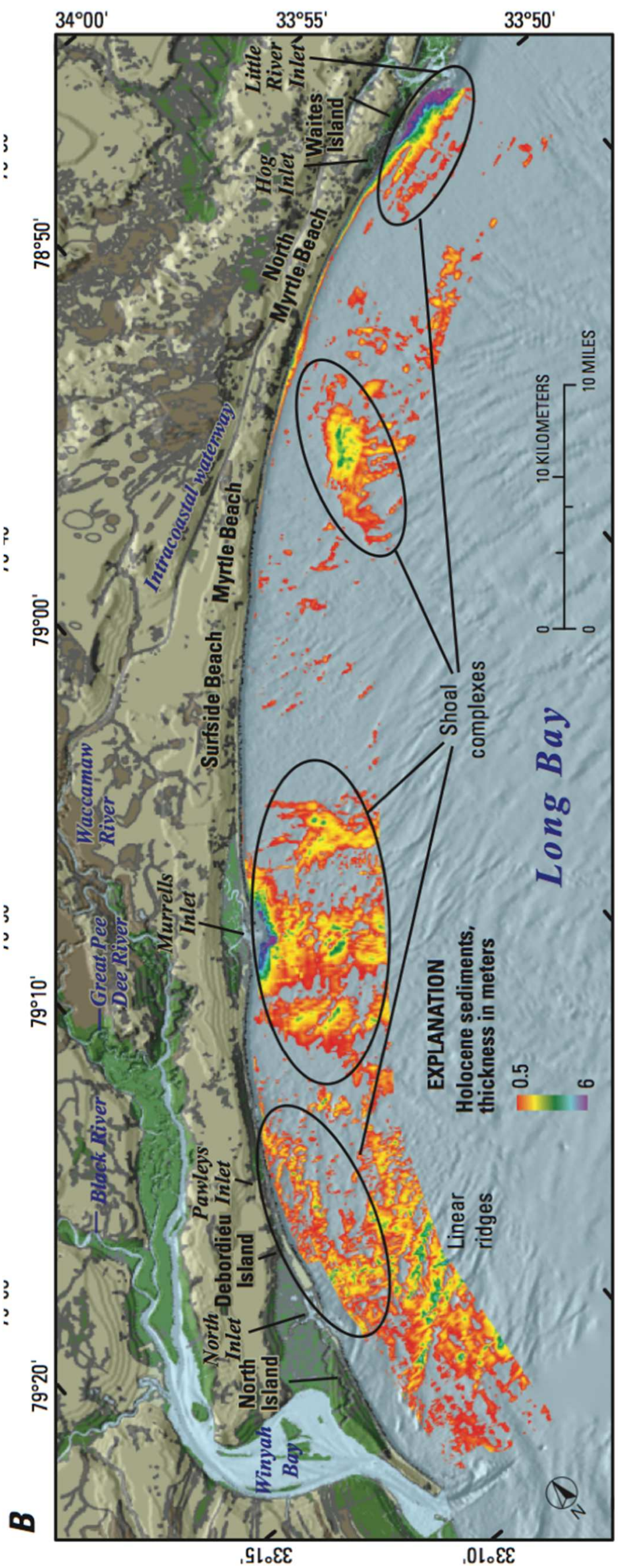

Figure 6: Distribution of Holocene sediments (in thickness, m) across northern South Carolina, including the Grand Strand north of Murrells Inlet. Sediment thickness generally increases from north to south. Adapted from Baldwin and others (2007).

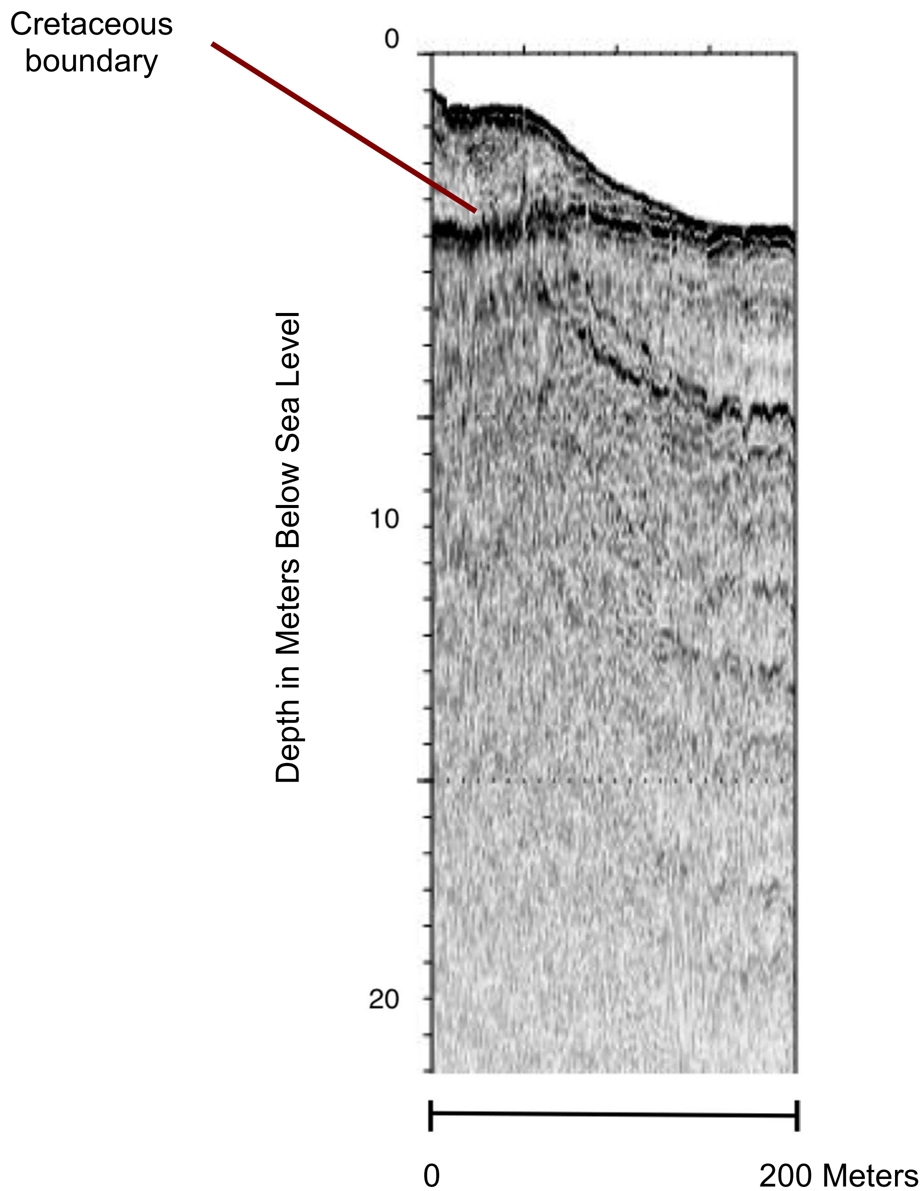

Figure 7: Subbottom CHIRP profile taken in central Myrtle Beach, showing the inner shoreface and underlying geologic framework represented by the high reflector ravinement surface.

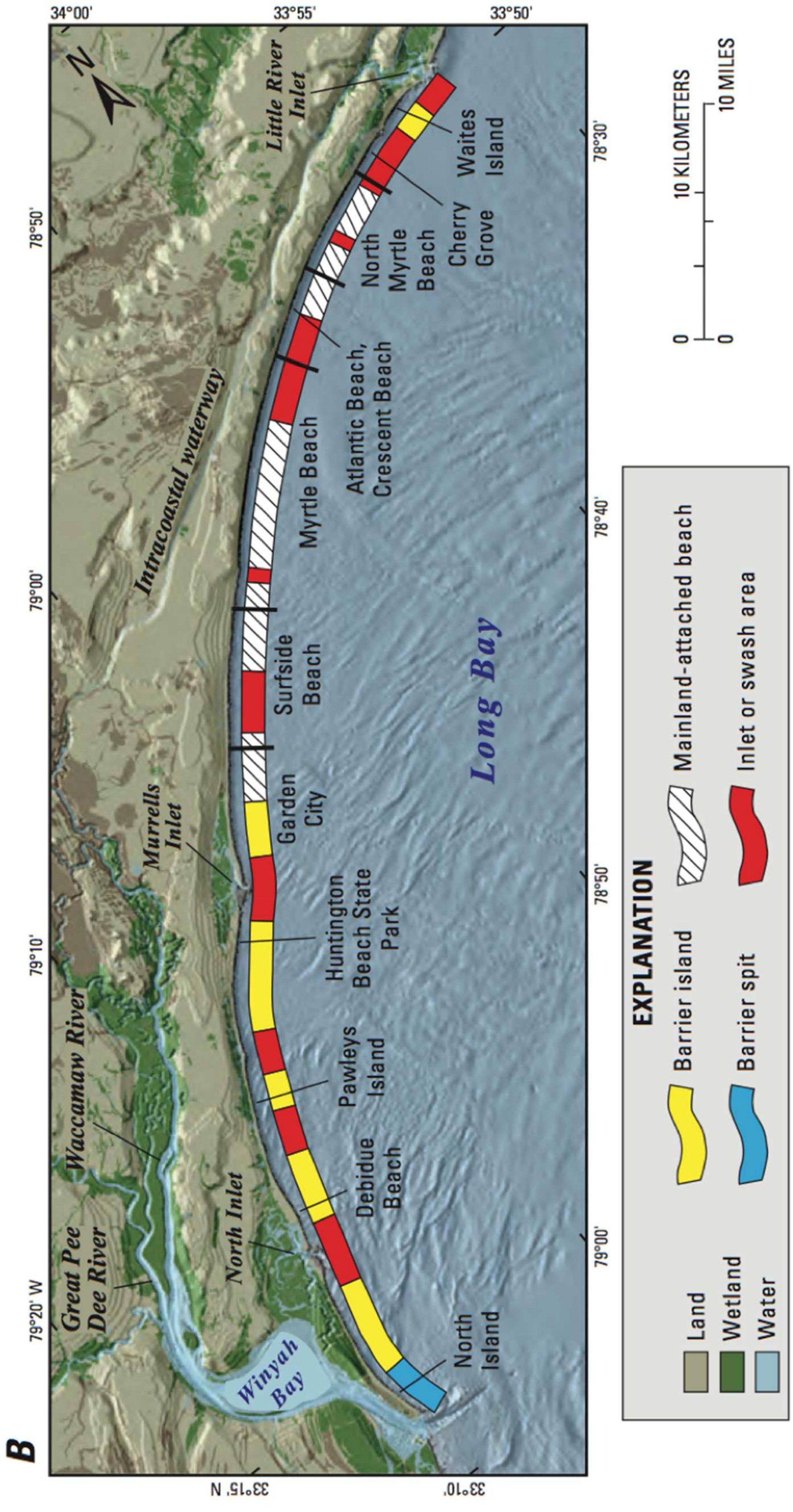

Figure 8: Physical types of coastal landforms indicated by the parallel bands as adapted by Barnhardt and others (2007).

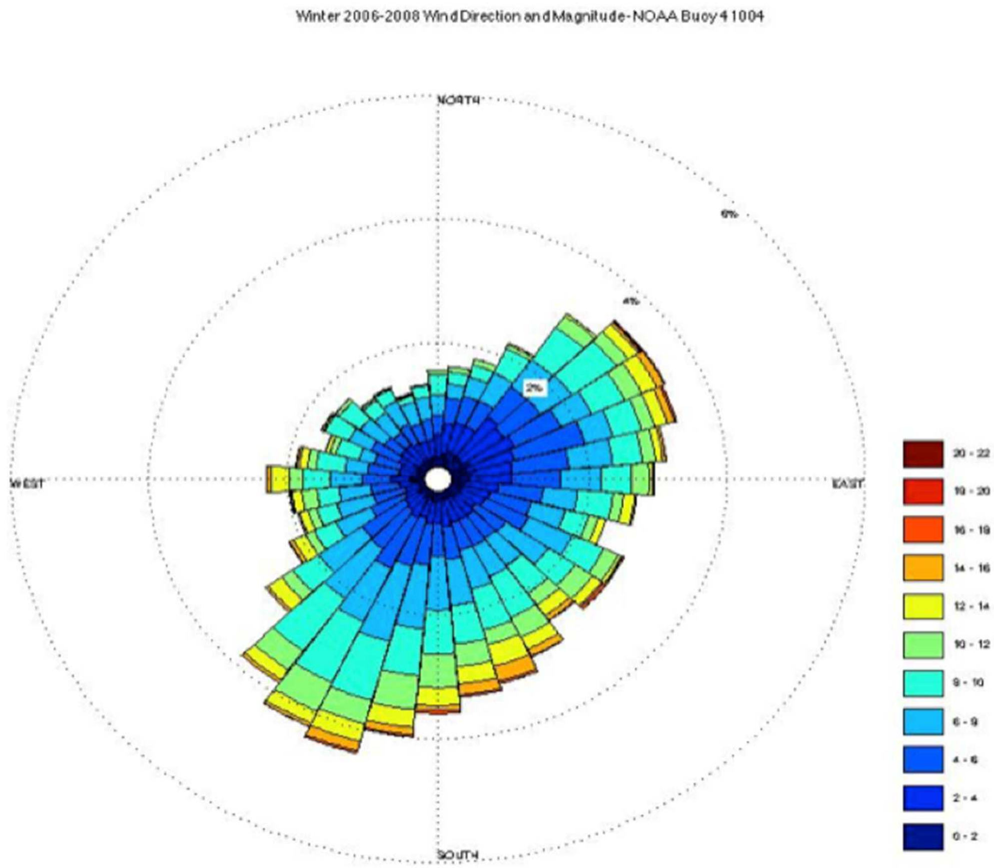

(Winter wind rose; Figure cont. below)

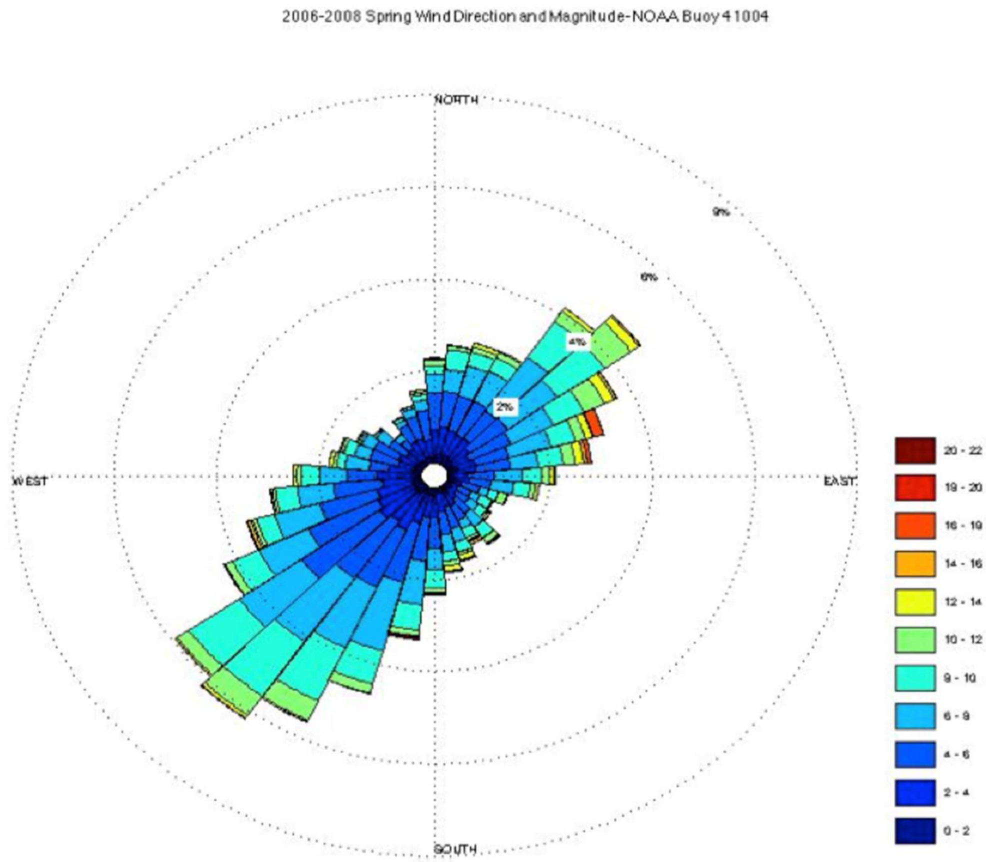

(Spring wind rose; Figure cont. below)

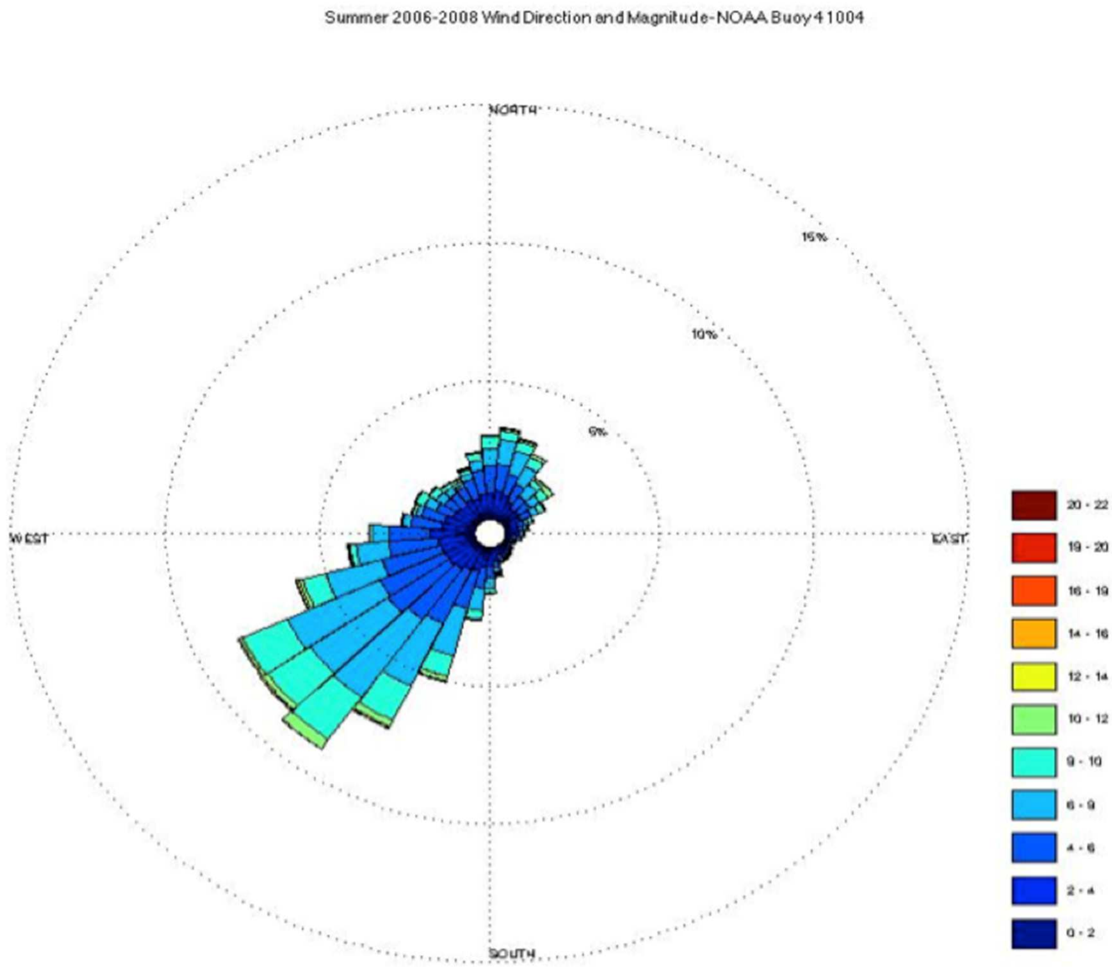

(Summer wind rose; Figure cont. below)

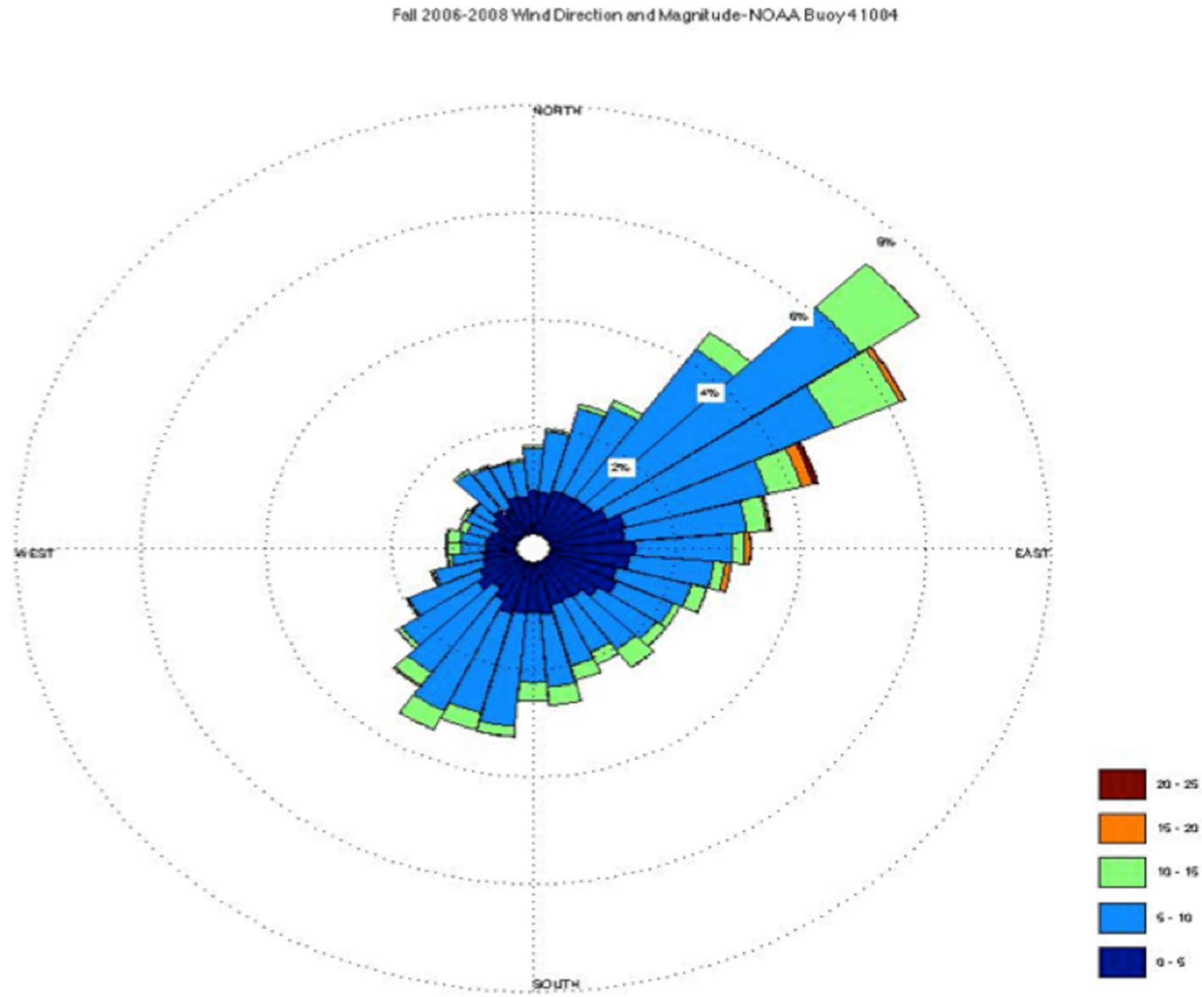

(Fall wind rose)

Figure 9: Seasonal wind direction and magnitudes as measured from Buoy 41004 offshore of Charleston, SC. Measured wind speeds are from 2007-2009, showing predominantly N-S directions.

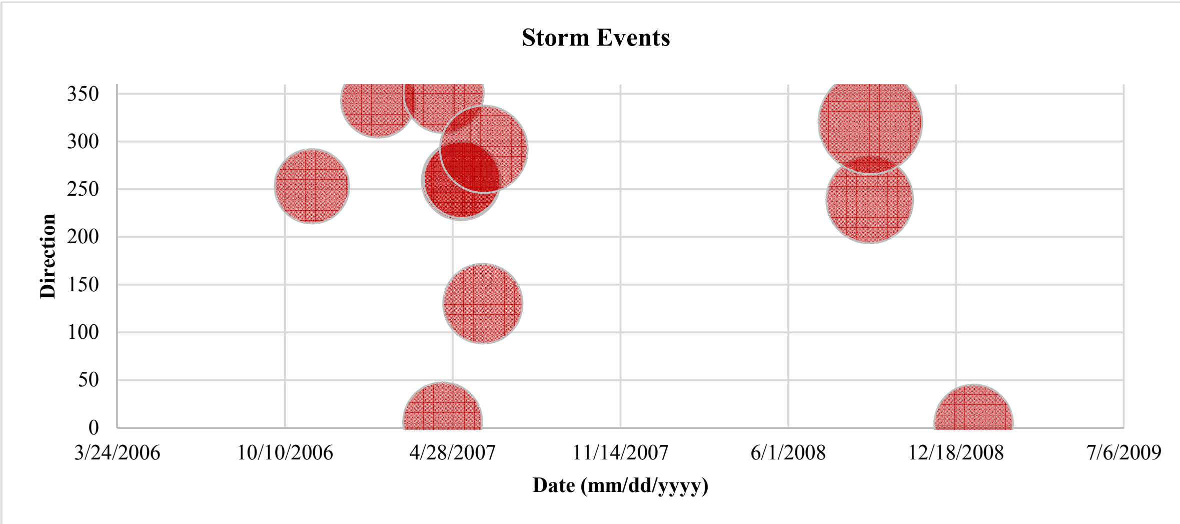

Figure 10: Recorded storm events, graphed in prevailing wind direction in degrees from North, along the Grand Strand from October 2006 through January 2009, encompassing the period before the renourishment projects. Recorded wind speed is depicted in the size of the icons.

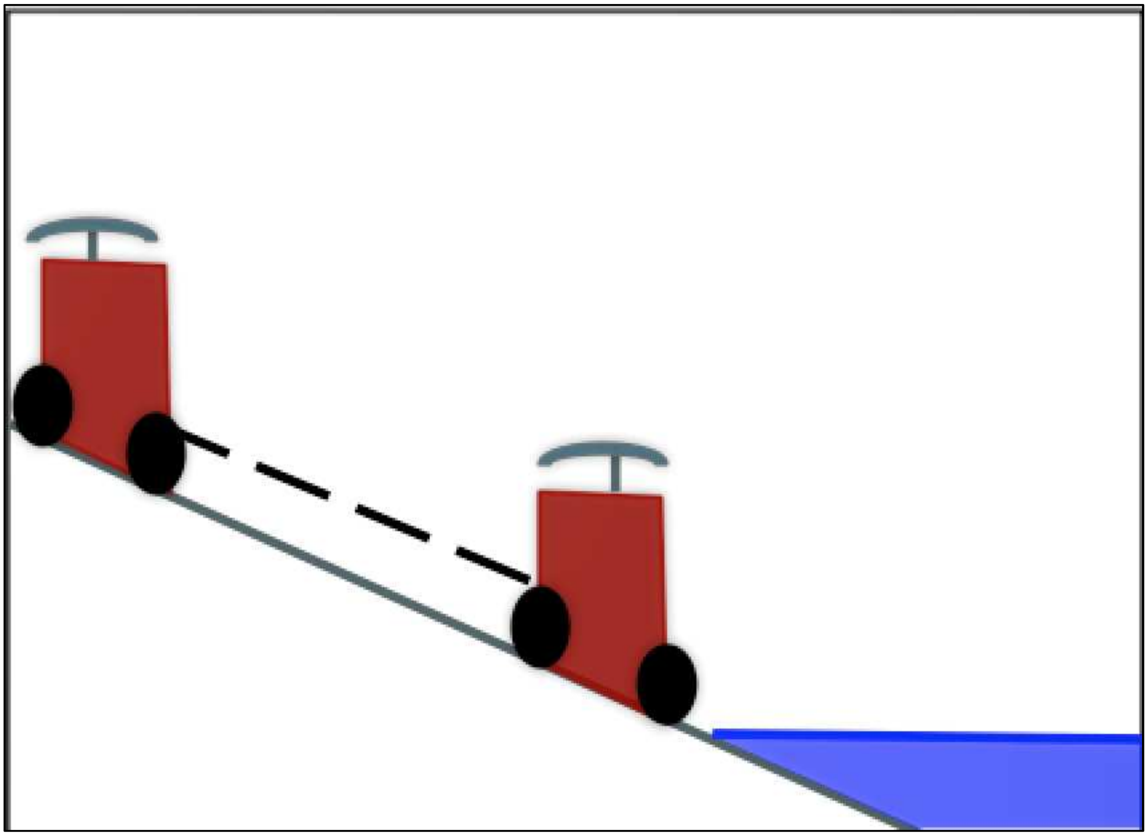

Figure 11: Schematic image of ATV-mounted GPS measurement of the mean high water line based on positional surveys. An accurate MHW line is interpolated from the 0.46 and 0.76-meter elevations, just above and below the mean high water contour. When shorelines are collected along the length of the shoreline a 10cm accuracy reading is determined.

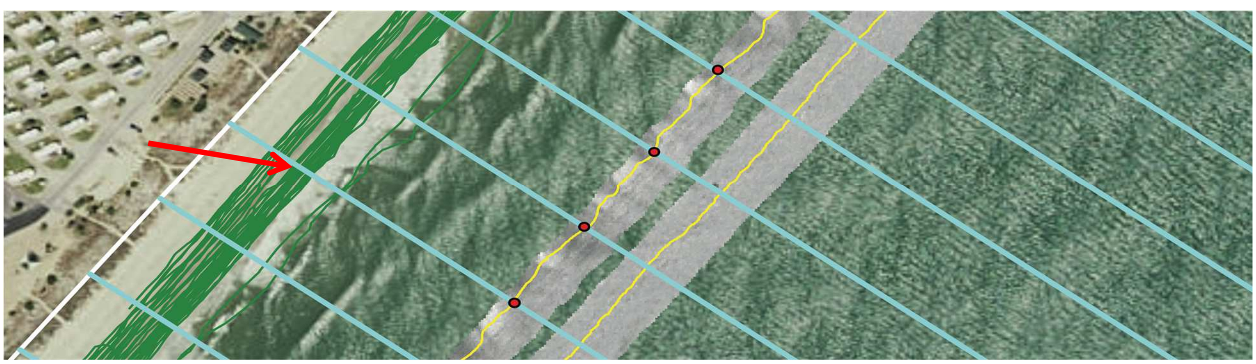

Figure 12: Mean high water shoreline positions from 2006-2009 are seen in green. A user-defined baseline is seen in white; DSAS transects are cast at 50m increments. The intersection of the transects and shorelines (indicated by the red arrow) are the point at which shoreline rate of change statistics are calculated. Multibeam backscatter is imaged offshore, with meter contours in yellow. Backscatter values are extracted at the intersection of the 6m contour and DSAS transects.

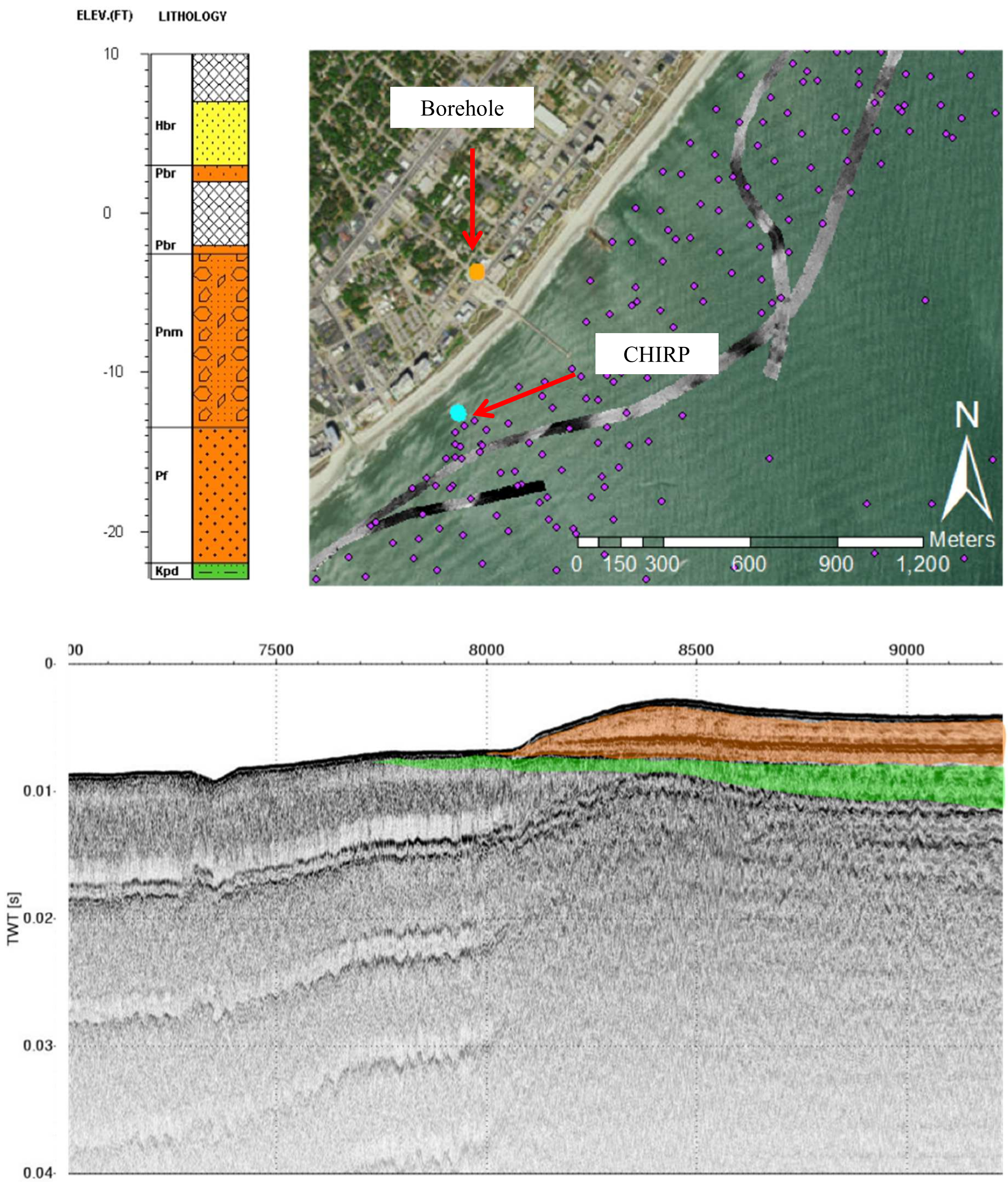

Figure 13: Borehole 'Hor-05' in Central Myrtle Beach. The orange point represents the location of the borehole, the cyan the location of the CHIRP, while the remaining purple points represent various other CHIRP shotpoints. The distinct reflector indicating the boundary between the Cretaceous and Pleistocene is indicated at the break of the green and orange layers, respectively. For a description of the borehole log, see Figure 16.

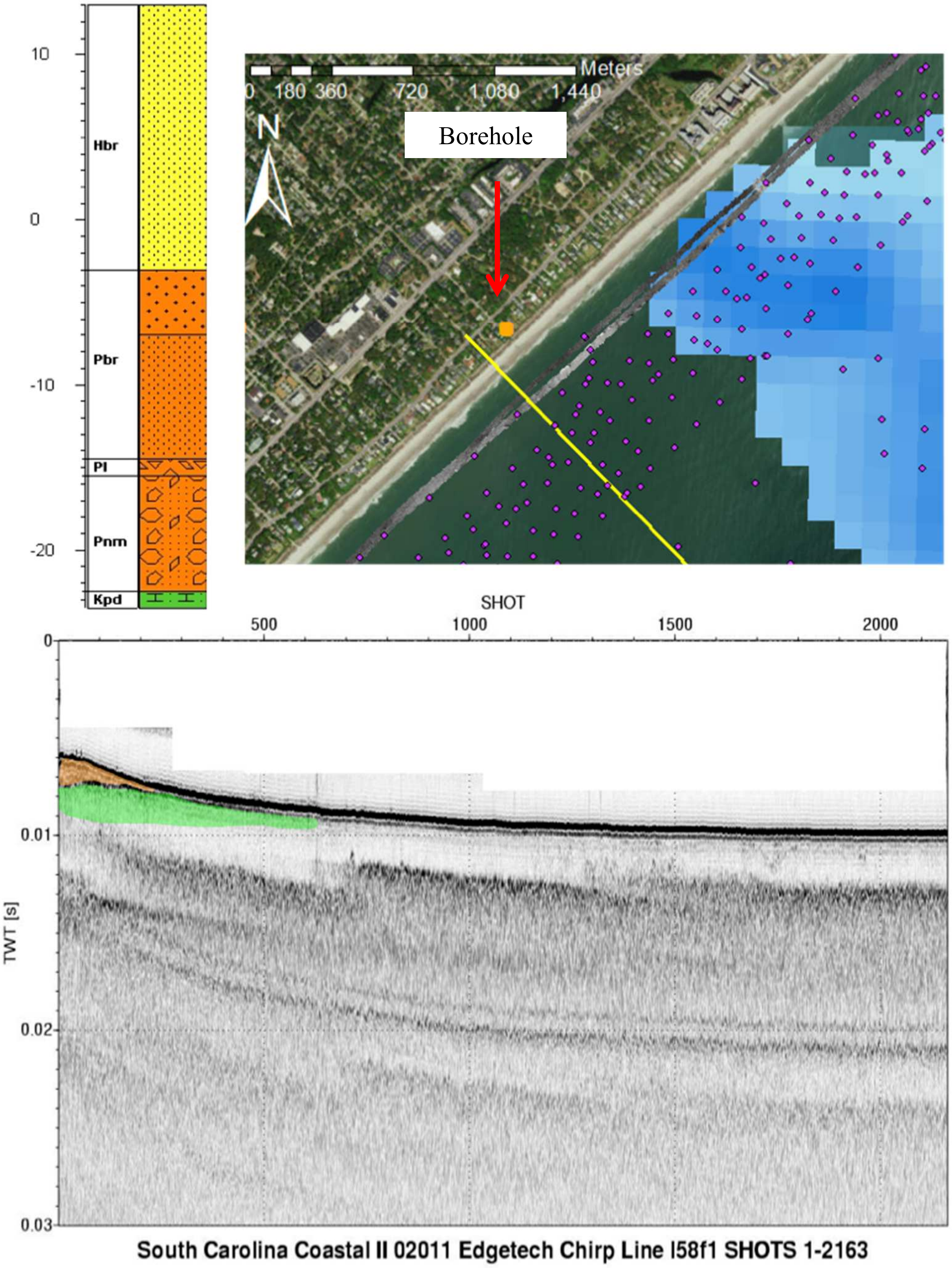

Figure 14: Borehole 'Hor-07' located in Myrtle Beach. The orange point represents the location of the borehole, the yellow represents the nearshore profile, while the remaining purple points represent various other CHIRP shotpoints. For a description of the borehole log, see Figure 17.

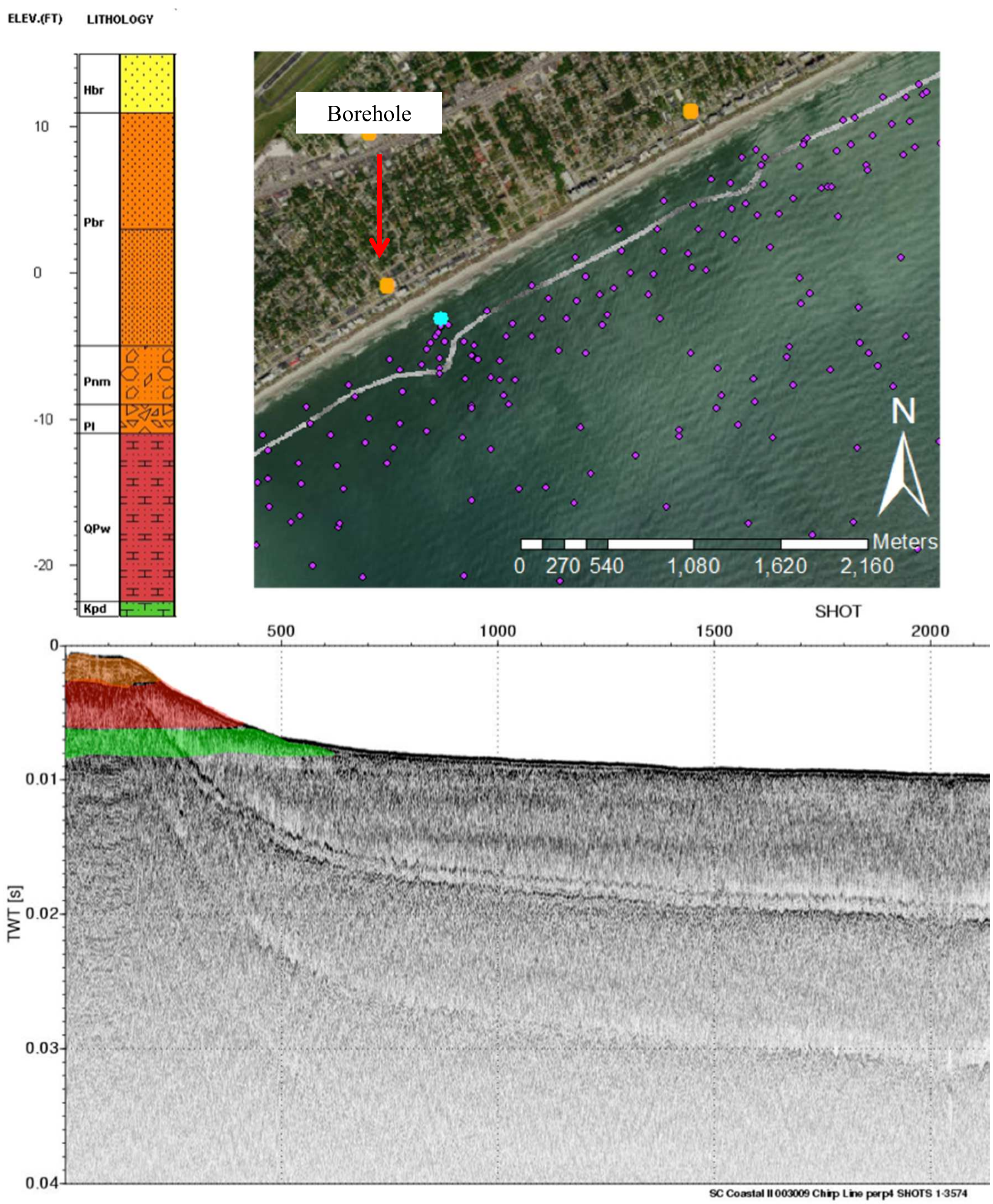

Figure 15: Borehole 'Hor-12' loacted in North Myrtle Beach. The orange point represents the location of the borehole, the cyan the location of the CHIRP, while the remaining purple points represent various other CHIRP shotpoints. For a description of the borehole log, see Figure 18.

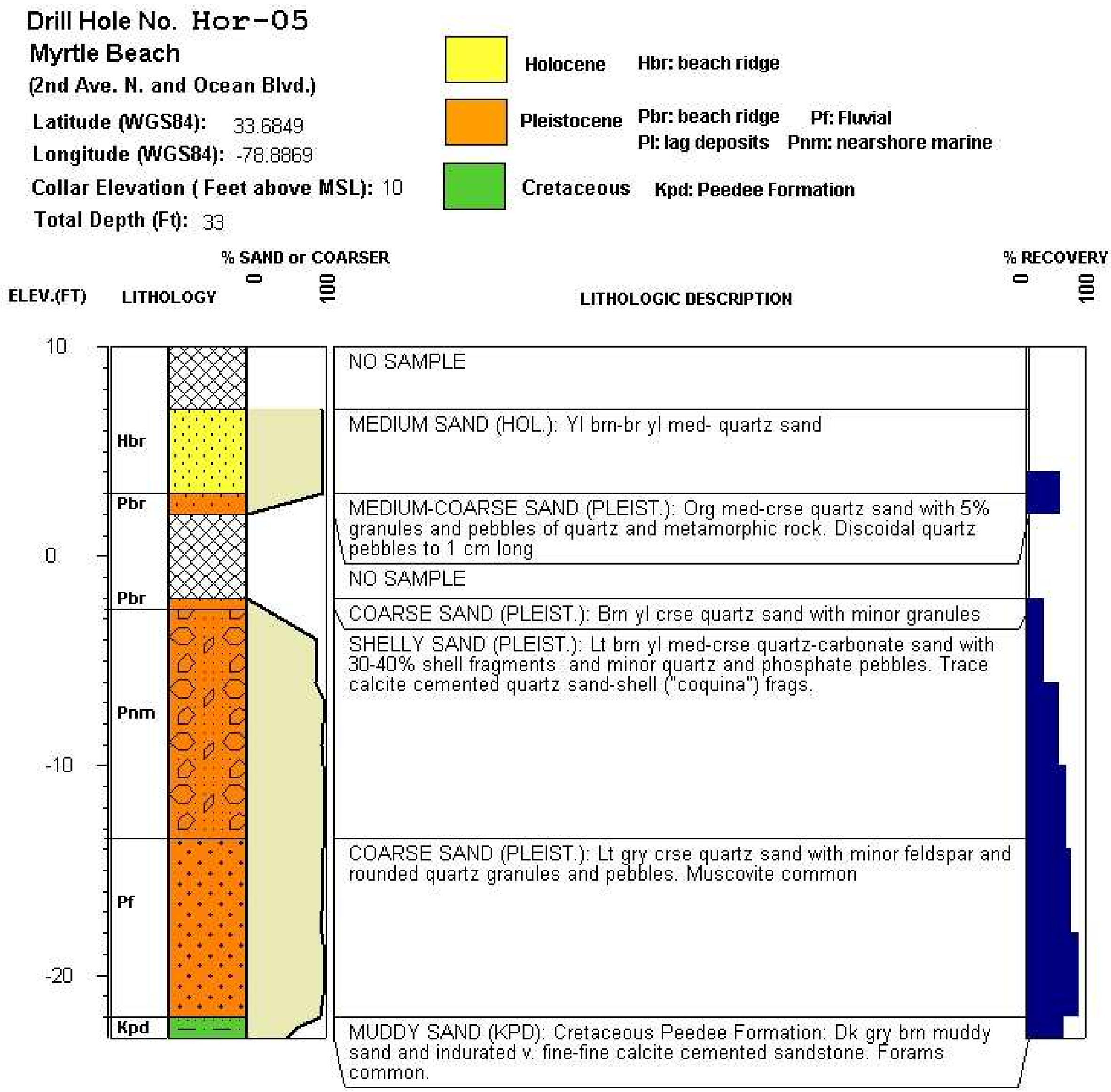

Figure 16: Borehole log for Hor-05 as accounted by Putney et al. (2002).

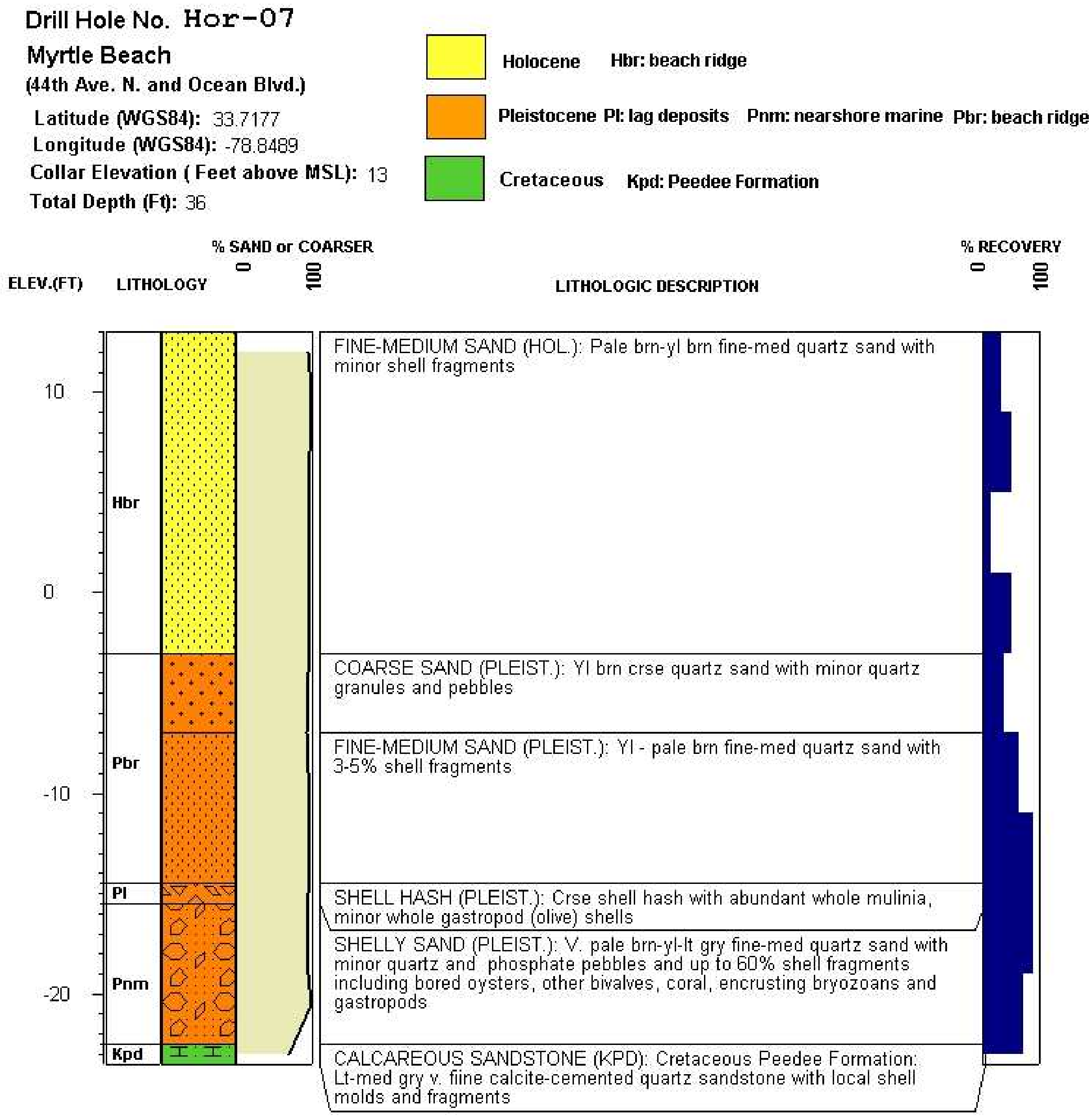

Figure 17: Borehole log for Hor-07 as accounted by Putney et al. (2002).

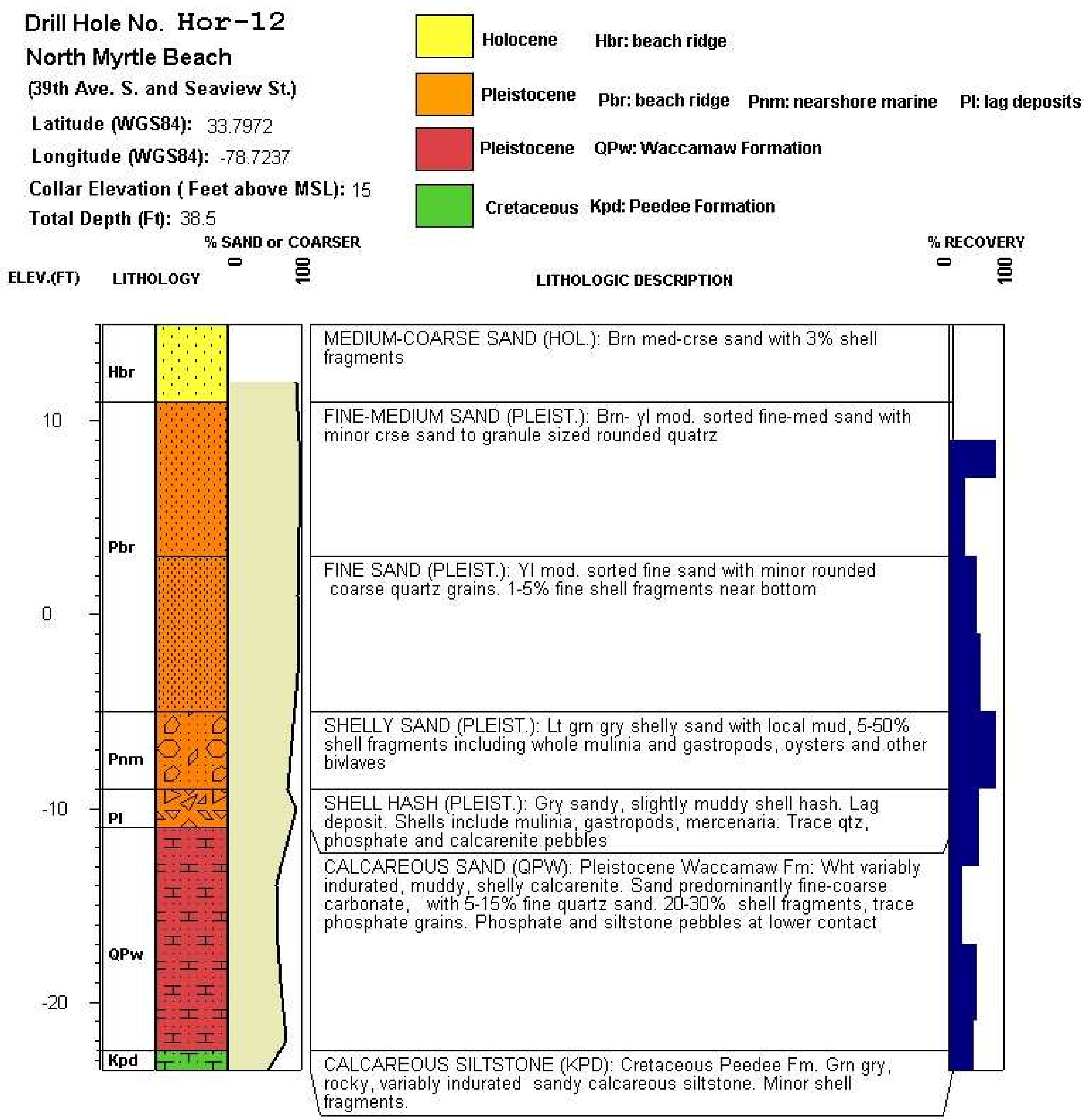

Figure 18: Borehole log for Hor-09 as accounted by Putney et al. (2002).

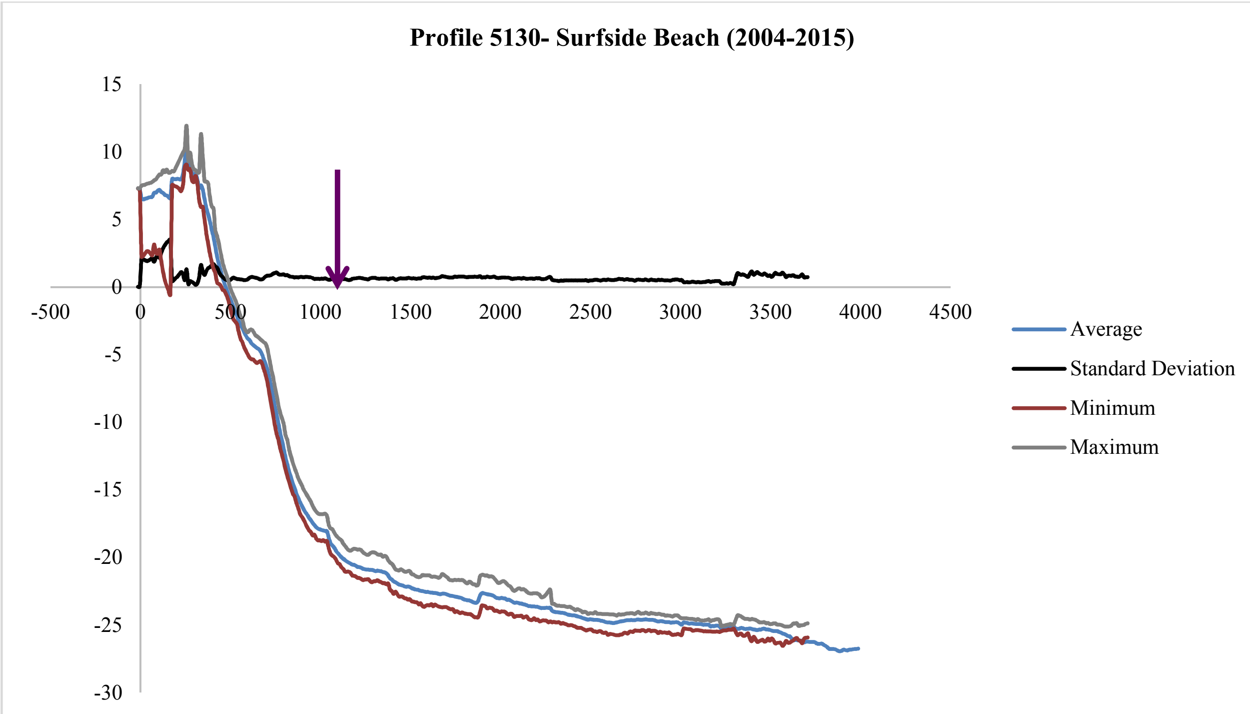

Figure 19: A typical BERM beach profile, located in Surfside Beach, used to define characteristics of the shoreface. The decrease in standard deviation is used to identify 'closure' (identified by purple arrow), while the change in slope into a relatively flat rise is used to define the depth of the shoreface.

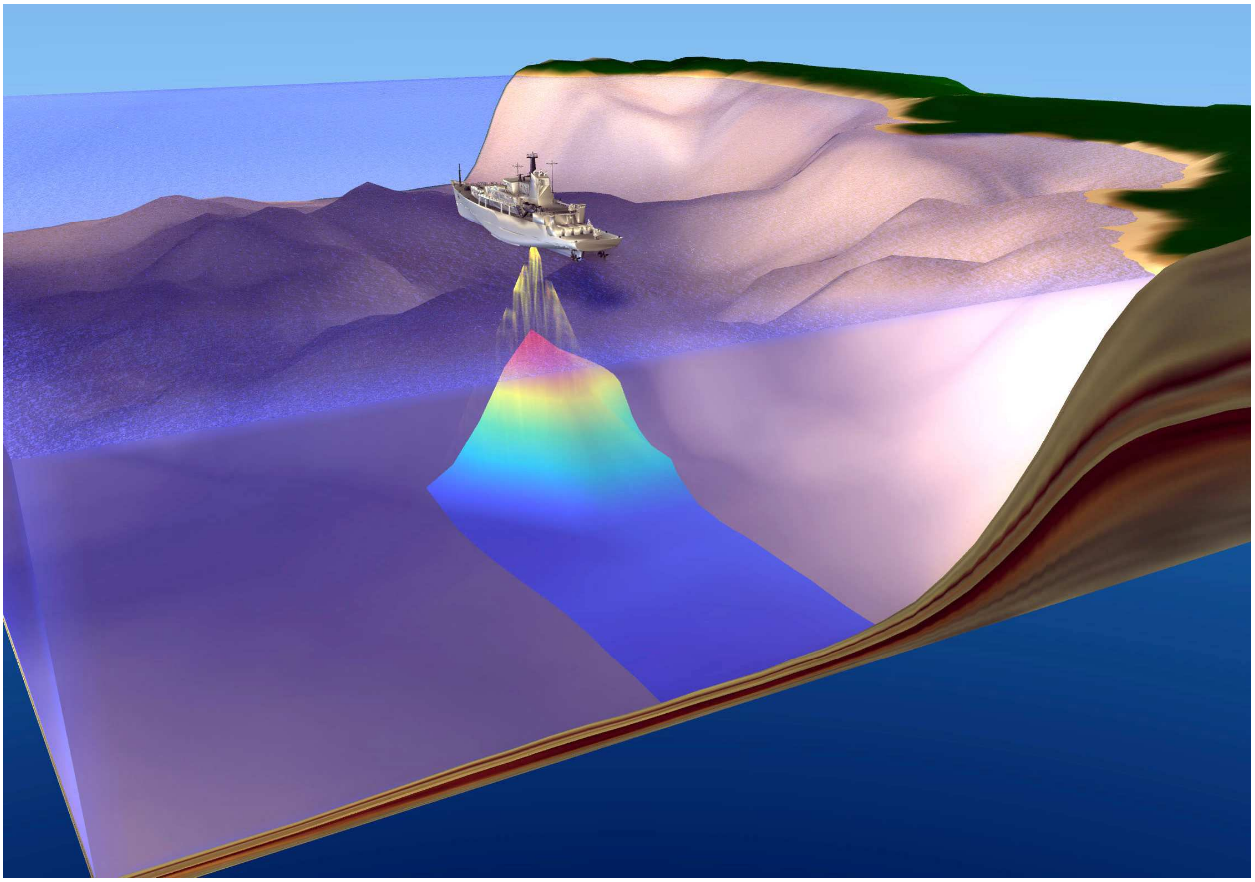

Figure 20: A schematic of multibeam sonar seen as adapted from The United States Navy.

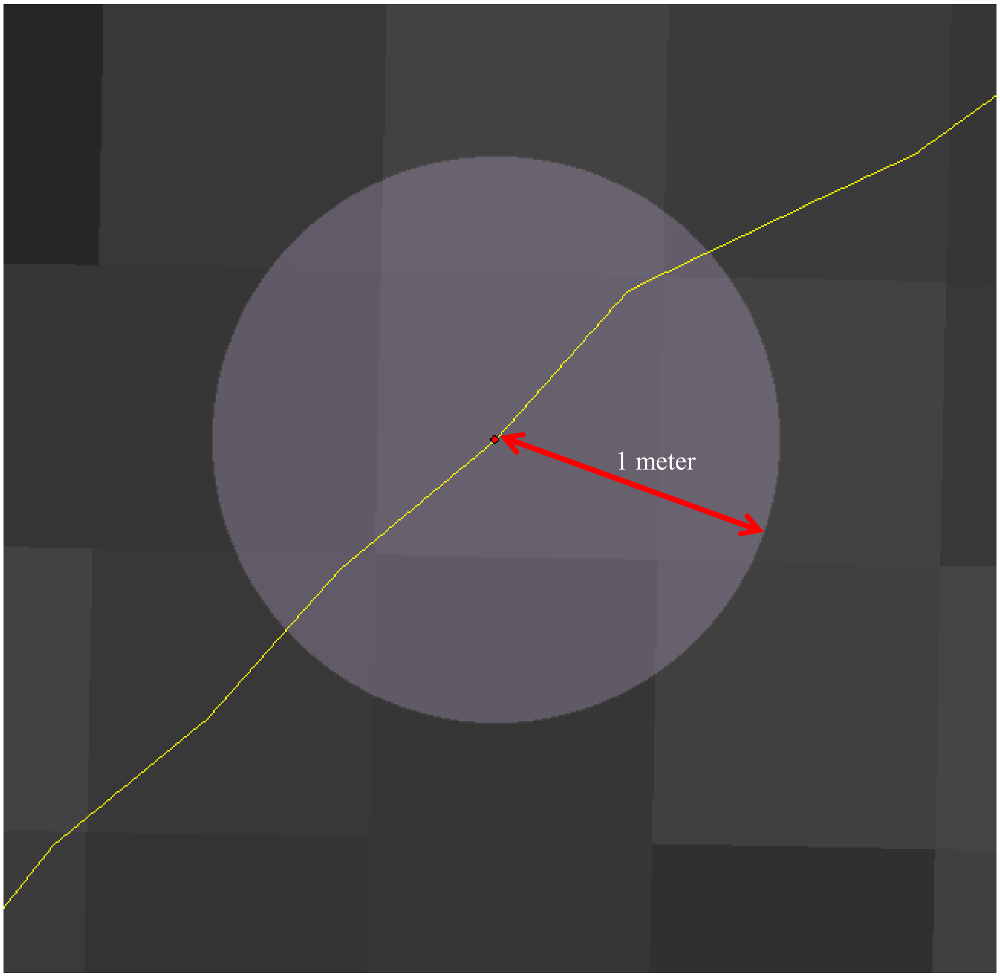

Figure 21: One-meter backscatter pixels are seen in the varied grey scale squares. The intersection of DSAS transects and the 6m contour is represented by the red dot. A one-meter contour is created on all sides of the point of intersection (2 meter diameter) and the average of the extracted backscatter values is calculated to assess variability.

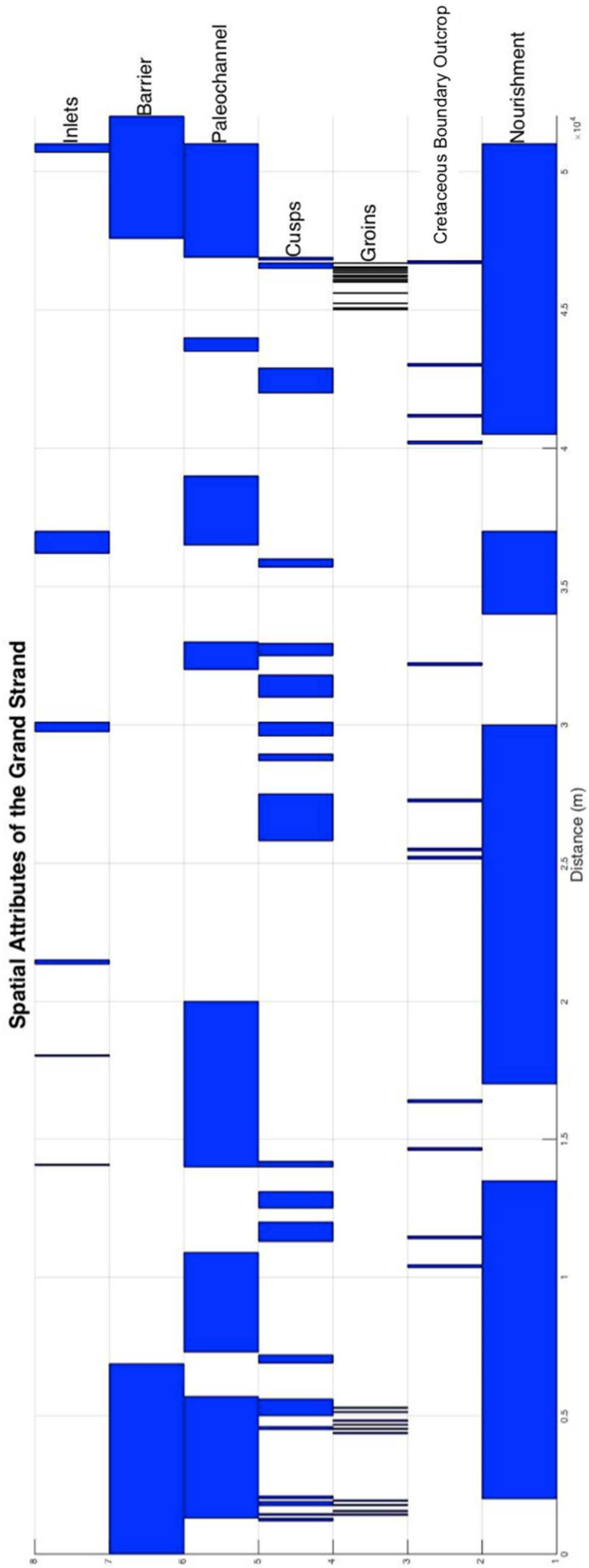

Figure 22: Spatial features along the Grand Strand, including inlets, barrier islands and spits, paleochannels, groins, offshore cusps, and nourishment projects.

Geologic Metrics
Offshore Cusp Presence
Paleochannel Presence Shoreline Change Envelope Degree of Shoreface Slope Backscatter Intensity
Paleochannel Presence
Degree of Shoreface Slope Backscatter Intensity
Shoreline Change Envelope
Backscatter Intensity Degree of Shoreface Slope
Onshore Cusp Presence
Degree of Shoreface Slope Paleochannel Presence

Table 1: Geologic and physical metrics used in cross correlation chi-square analyses.

Metric	Offshore Cusp Presence
Paleochannel Presence	-0.419
Shoreline Change Envelope	-0.375
Degree of Shoreface Slope	0.307
Backscatter Intensity	-0.35
Metric	Paleochannel Presence
Degree of Shoreface Slope	-0.744
Backscatter Intensity	0.228
Metric	Shoreline Change Envelope (Z)
Backscatter Intensity	0.135
Shoreface Slope	-0.136
Metric	Onshore Cusp Presence
Degree of Shoreface Slope	0.739
Paleochannel Presence	-0.597

Table 2: Physical and geologic metric correlations utilized to characterize spatial relationships along the Grand Strand.

SHORELINE	DATE	SHORELINE	DATE
GARDEN CITY/SURFSIDE BEACH	January-07	**North Myrtle Beach**	January-07
	February-16		February-07
	March-07		April-07
	April-07		May-07
	May-07		July-07
	June-07		August-07
	July-07		September-07
	August-07		October-07
	September-07		December-07
	October-07		January-08
	December-07		February-08
MYRTLE BEACH	March-07		March-08
	October-07		April-08
	December-07		May-08
	February-08		June-08
	May-08		July-08
ARCADIAN SHORES	January-07		
	February-07		
	May-07		
	June-07		
	July-07		
	August-07		
	October-07		
	December-07		
	February-08		
	March-08		
	May-08		

Table 3: Survey dates of shoreline position throughout the study area prior to the 2008-2009 renourishment project.

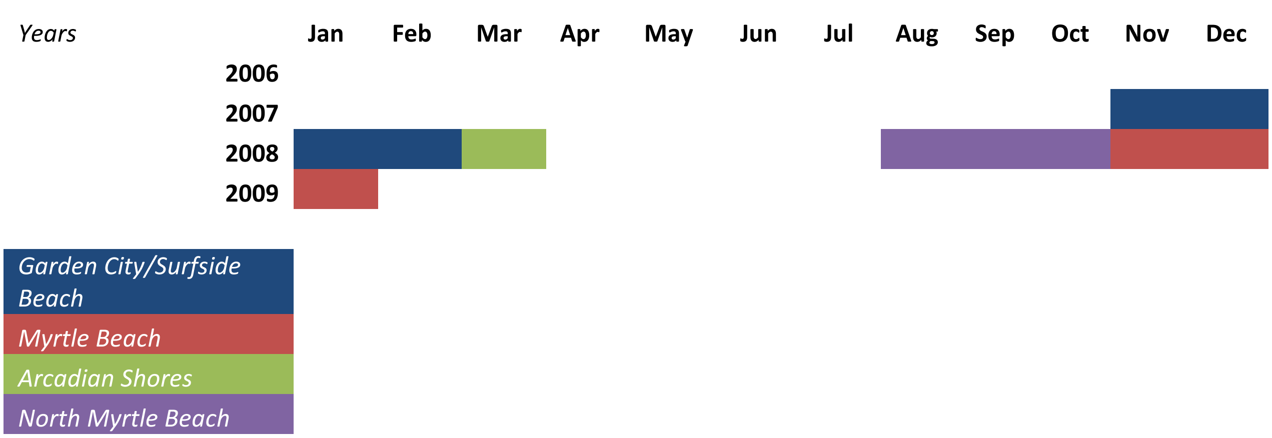

Table 4: Temporal distribution of renourishment projects throughout the Grand Strand.

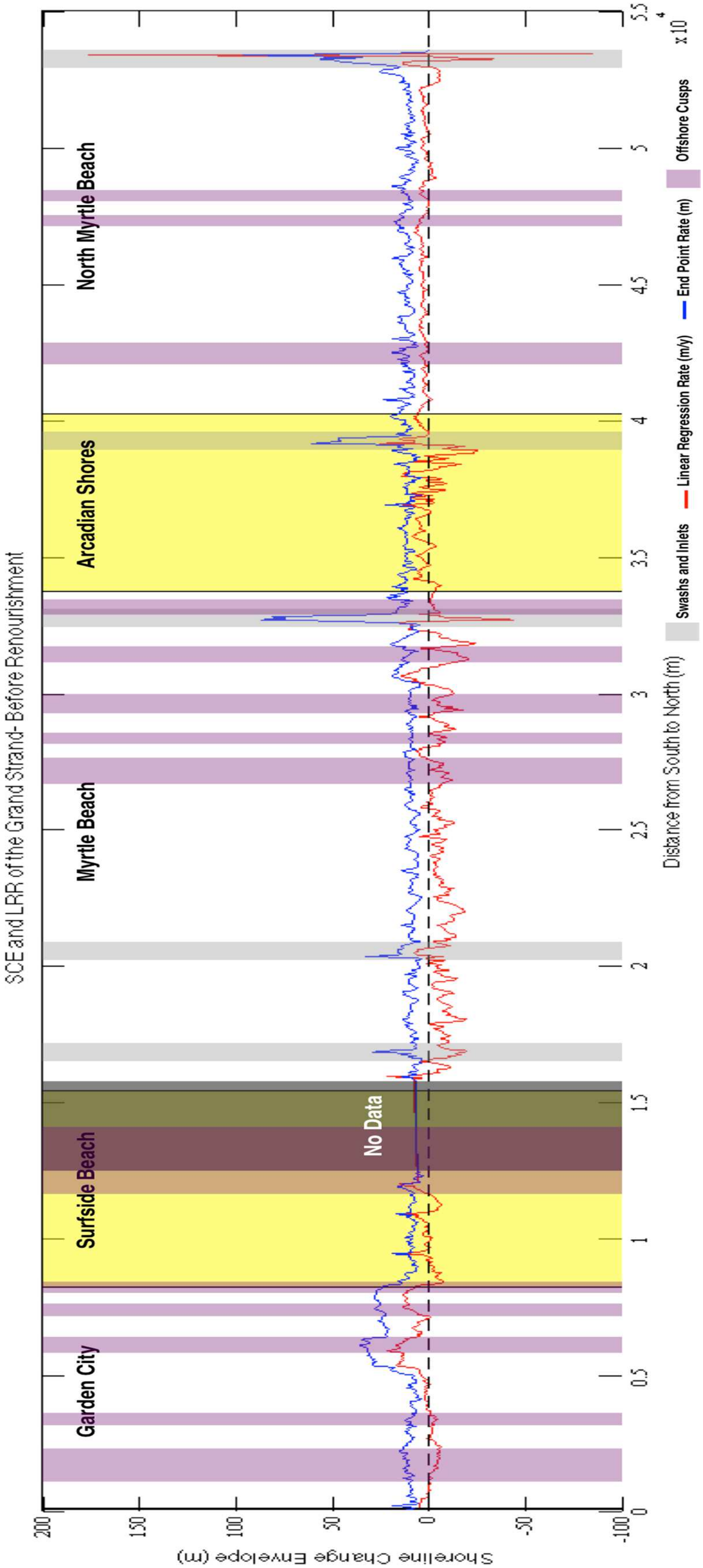

Figure 23: Shoreline change envelope (m; blue) and linear regression rate (m/y; red) for the Grand Strand, south to north. Inlets are highlighted in gray and characteristically experience higher levels of shoreline change and variability than the rest of the shoreline. A gap in data collection occurred in northern Surfside Beach, into southern Myrtle Beach around the Myrtle Beach State Park shoreline. Recorded offshore cusps and highlighted alongshore in the purple.

WITHOUT INLET INFLUENCE							Erosion Rates	(m/y)	Accretion Rates	(m/y)
City	No. of Transects	Mean NSM	Mean EPR	Mean SCE	Mean Shoreline Change Rate (m/yr)	% Erosion	Maximum	Mean	Maximum	Mean
Garden City	164	7.87	8.61	14.35	2.24	44.1	-6.65	-2.62	21.24	6.02
Surfside Beach	144	6.31	7.1	12.99	2.38	34.8	-8.03	-3.27	17.68	6.35
Myrtle Beach	366	-4.88	-8.81	8.97	-5.89	84.5	-20.03	-7.5	20.98	4.87
Arcadian Shores	130	3.17	2.69	12.93	0.32	82.1	-19.05	-4.47	14.22	4.82
North Myrtle Beach	204	3.9	2.62	12.04	2	16.8	-12.68	-2.52	14.65	2.89

Table 5: Shoreline change accretion and erosional rates along the Grand Strand, excluding inlet regions. Percent erosion quantified the percent of shoreline experiencing negative linear regression rates, whereas erosion and accretion rates solely include values of either negative or positive linear regression rates, respectively.

City	Significant Spatial Frequencies SCE (m; PSD)	Significant Spatial Frequencies LRR (m; PSD)	Significant Spatial Frequencies Backscatter Intensity (m; PSD)
Garden City	1600	1600	2133
	800	533	711
	533	290	426
	290	188	320
	168		128
Surfside Beach	1600	1600	1066
	1066	639	457
	1000	400	266
	400	290	200
	200	168	103
	168		
	145		
Myrtle Beach	6397	4266	4266
	3200	1066	2133
	1279	800	1066
	1066	512	556
	800	355	492
	412	297	297
	209	172	193
	164		121
Arcadian Shores	3200	1279	533
	1600	914	400
	1066	639	133
	533	533	106
	376	400	
	320	266	
	228	142	
	152		
North Myrtle Beach	1279	1600	1279
	581	639	914
	376	457	581
	246	320	457
	125	160	200
			148

Table 6: Significant spatial frequencies identified in power spectral density analysis for the shoreline change envelope, linear regression rates, and backscatter intensities along the Grand Strand.

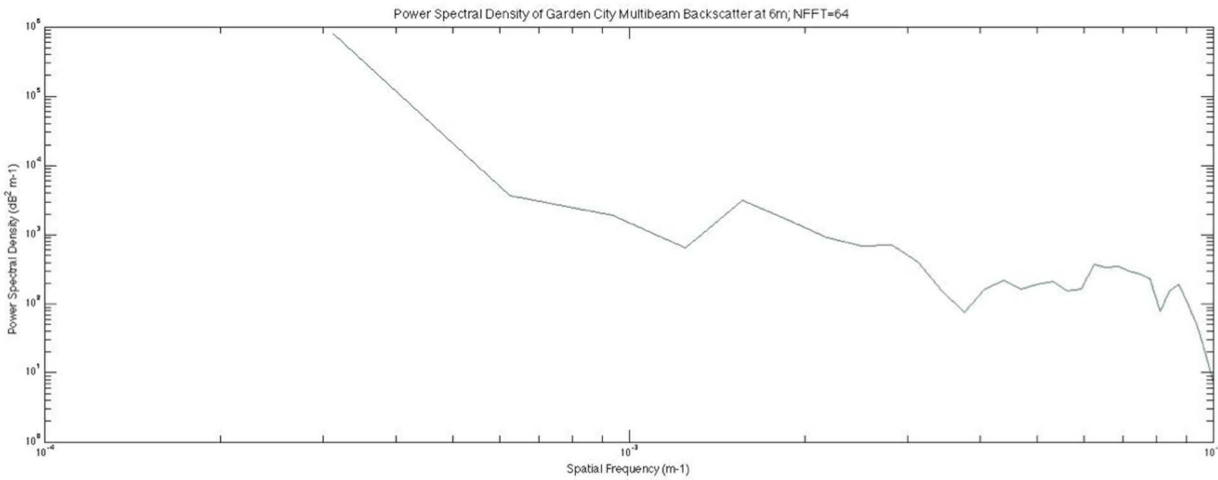

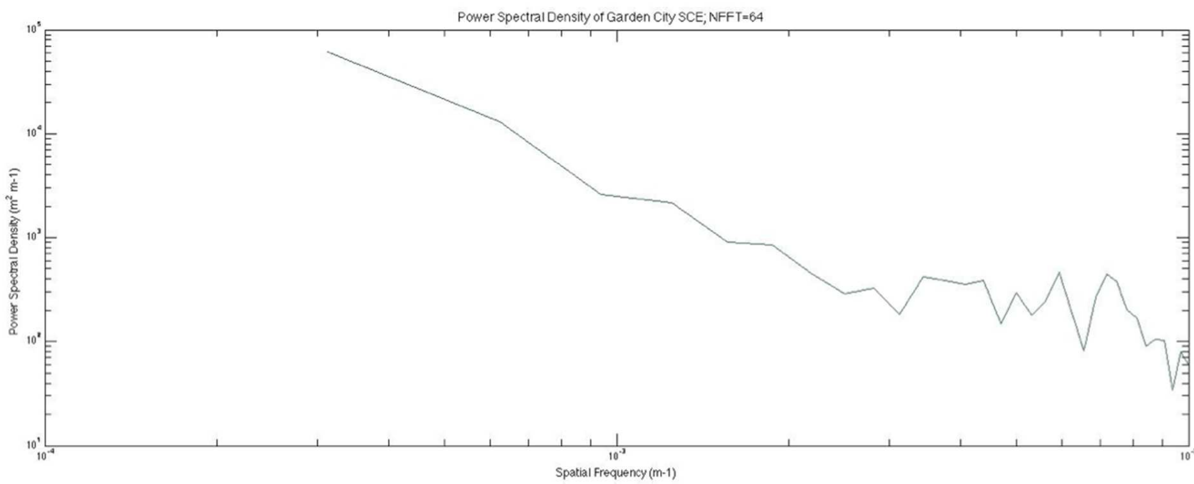

Figure 24: Power spectral density graphs on a log-log scale for Garden City. Significant frequencies are reported in Table 5.

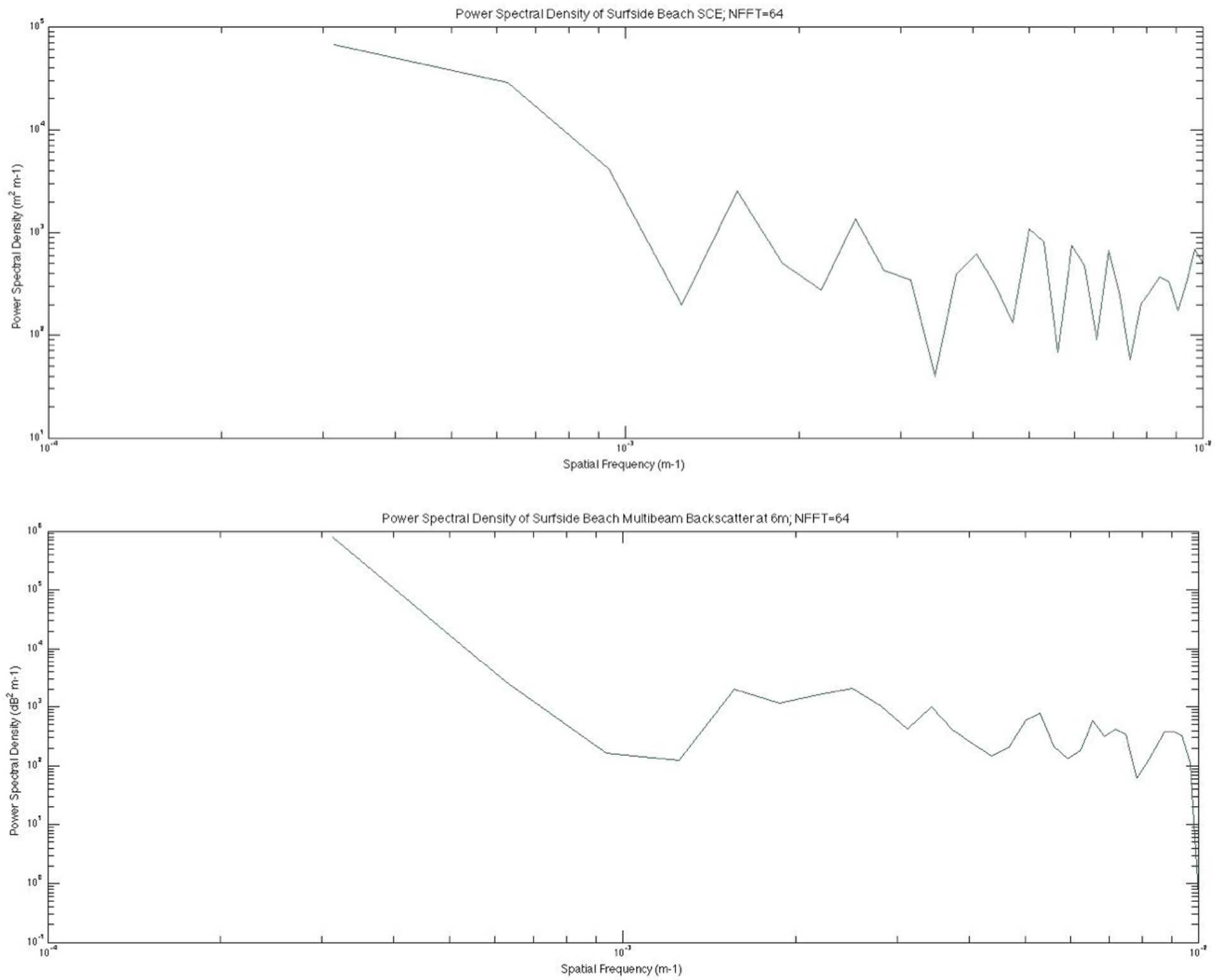

Figure 25: Power spectral density graphs on a log-log scale for Surfside Beach. Significant frequencies are reported in Table 5.

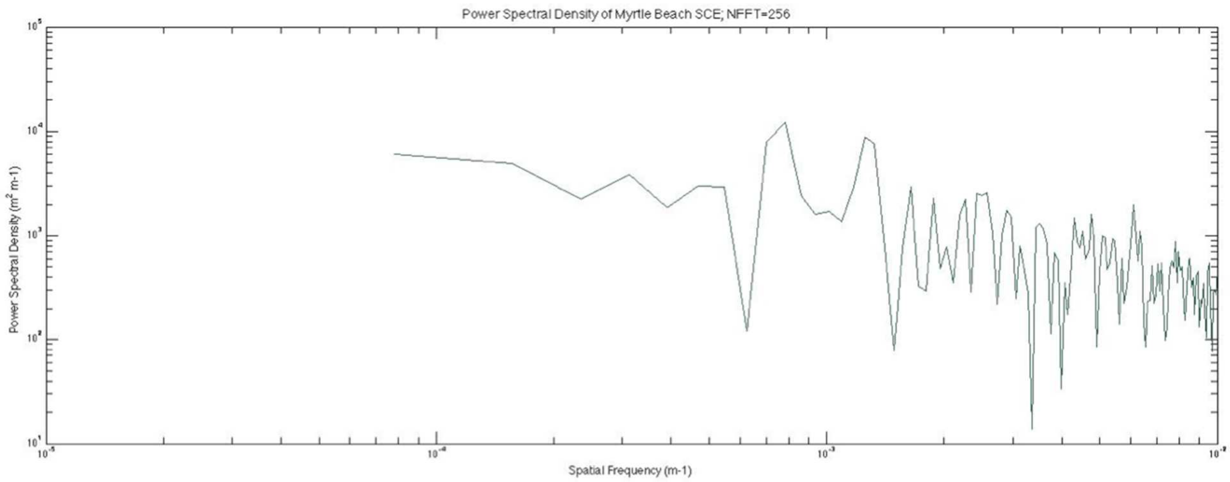

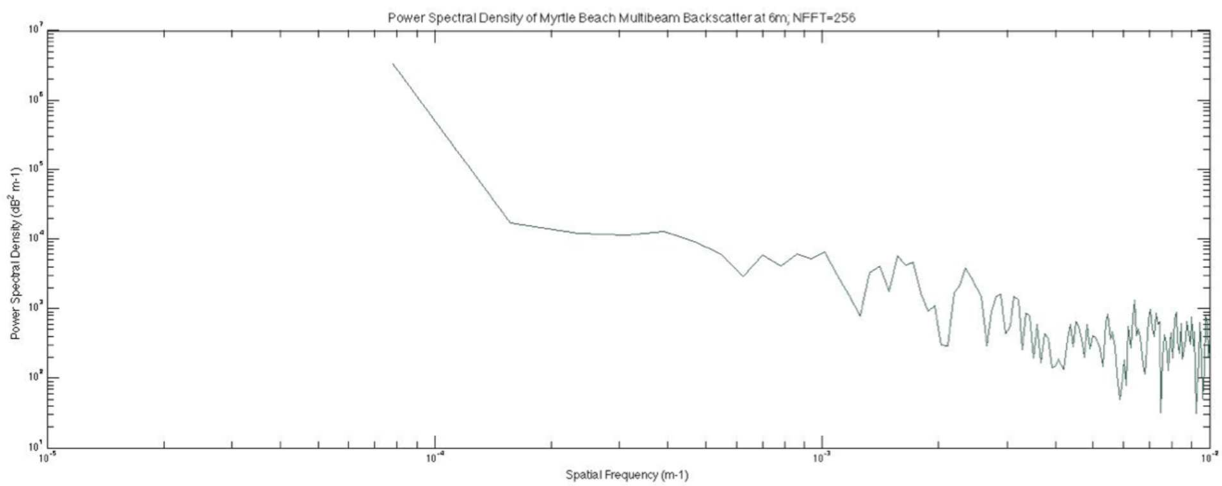

Figure 26: Power spectral density graphs on a log-log scale for Myrtle Beach. Significant frequencies are reported in Table 5.

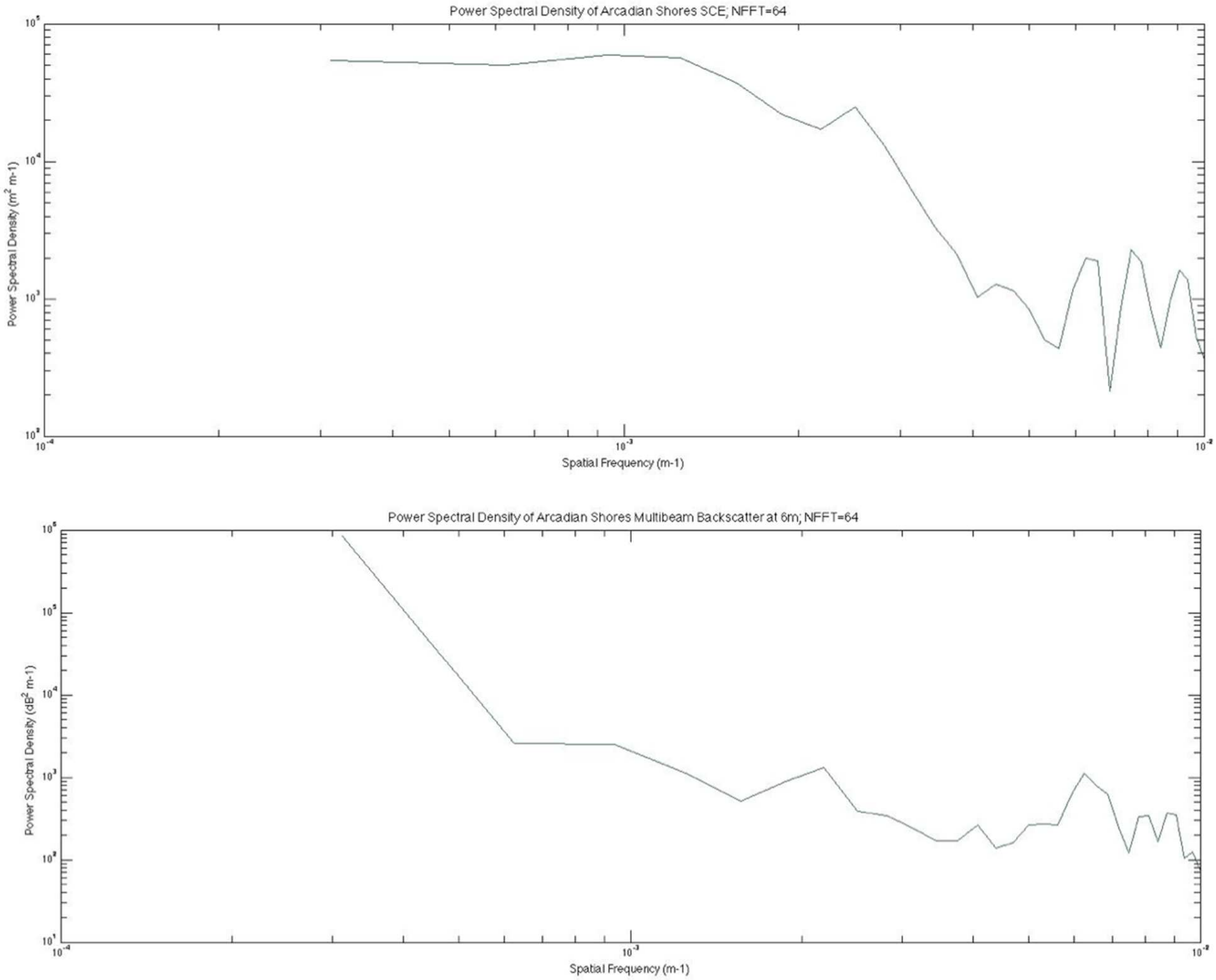

Figure 27: Power spectral density graphs on a log-log scale for Arcadian Shores. Significant frequencies are reported in Table 5.

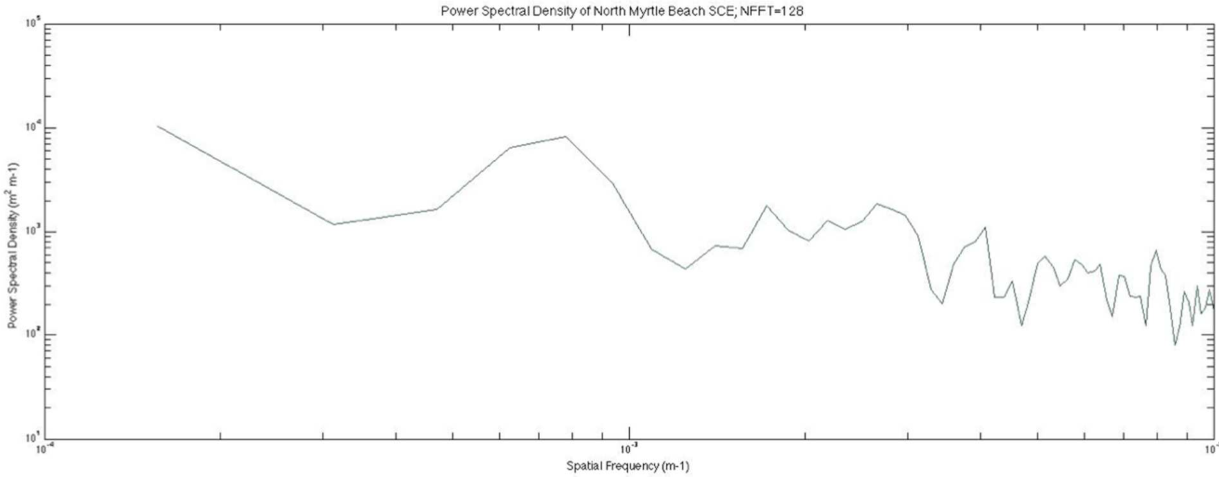

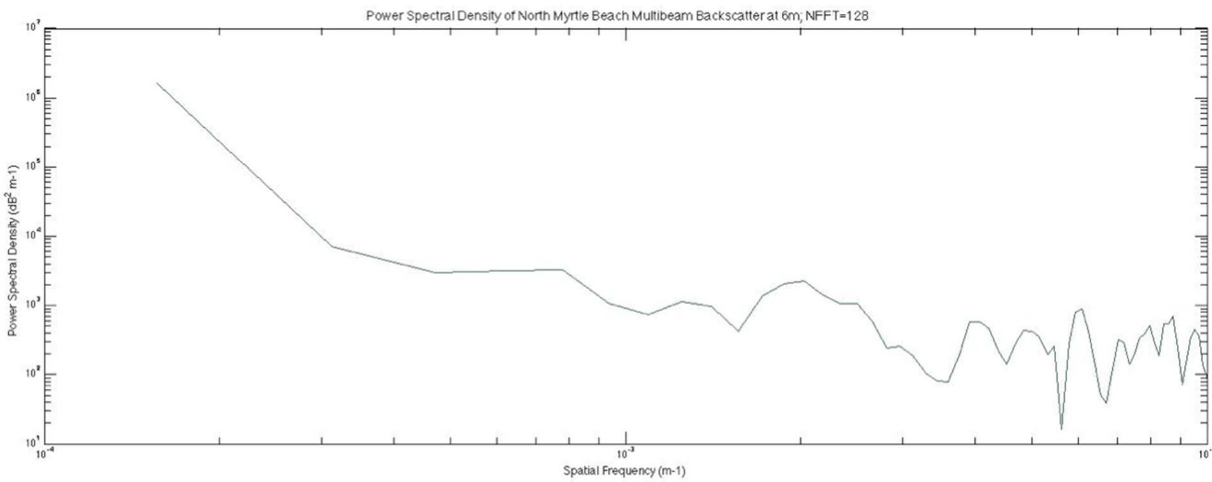

Figure 28: Power spectral density graphs on a log-log scale for North Myrtle Beach. Significant frequencies are reported in Table 5.

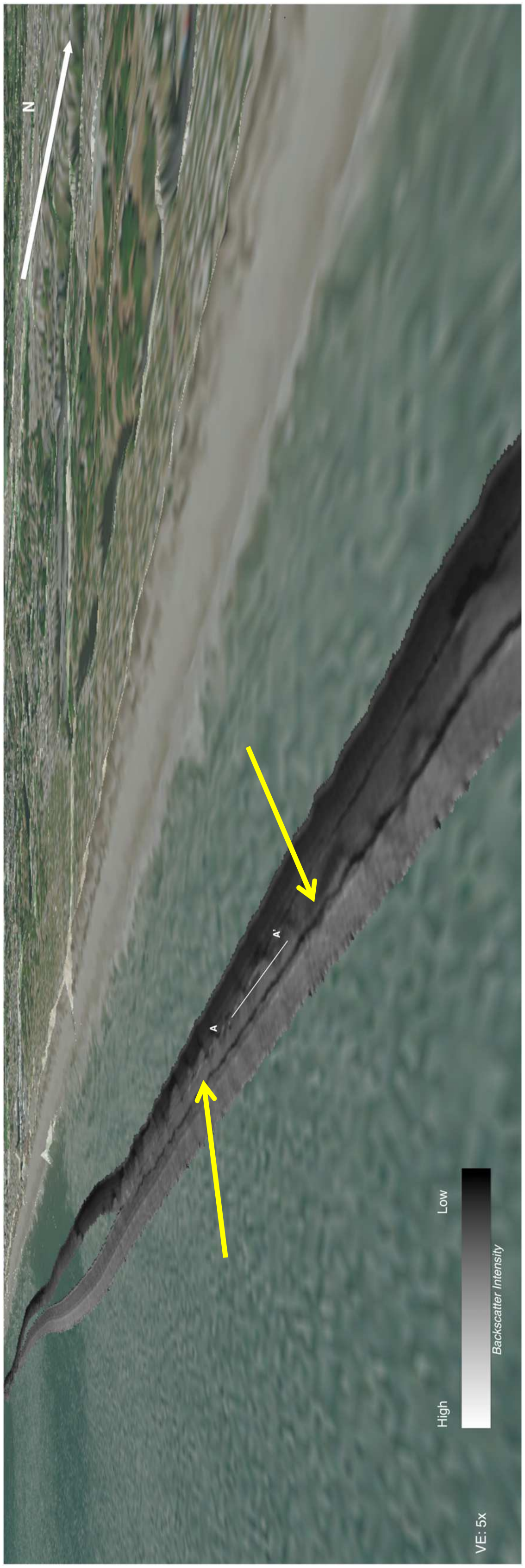

Figure 29: An example of offshore cusps (indicated by yellow arrows) imaged in multibeam bathymetry with draped backscatter, located in Surfside Beach. Locations consisting of offshore cusps have similar geometries, although length and depth of cusps vary.

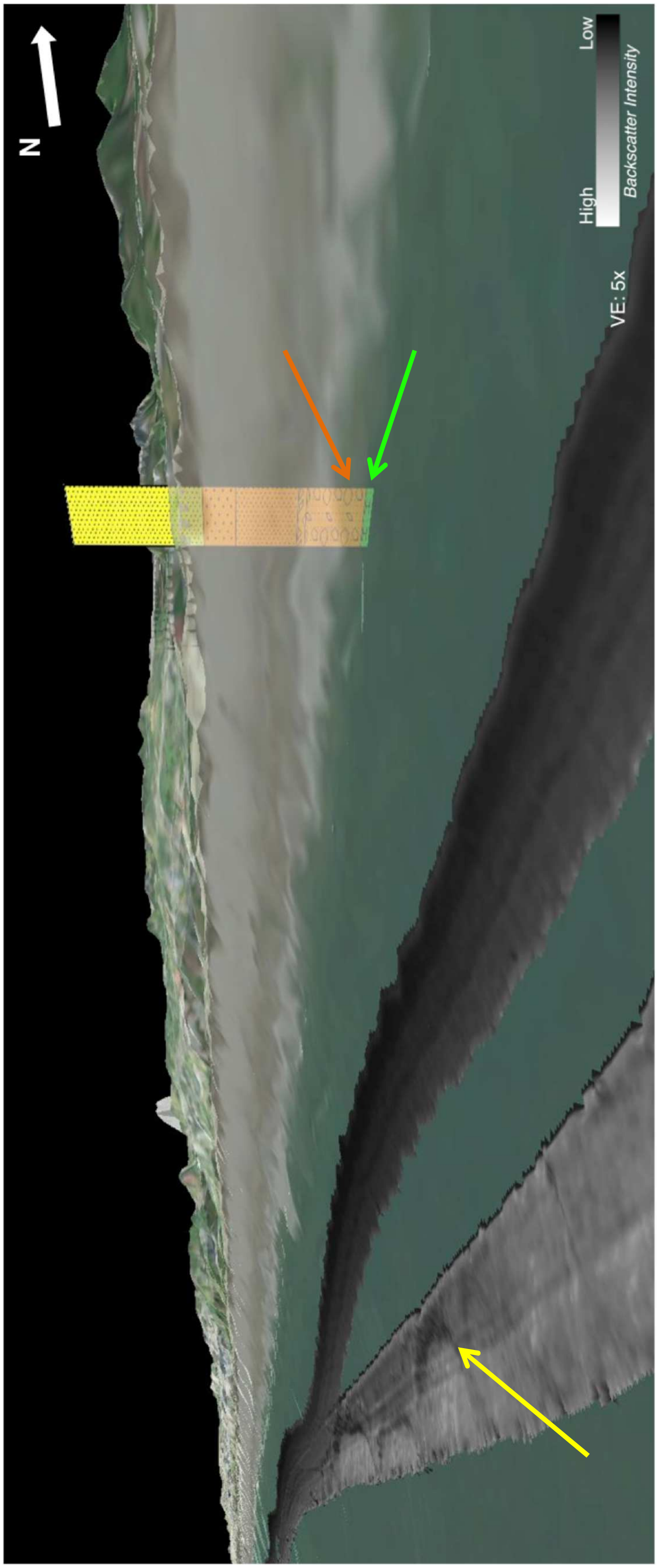

Figure 30: Offshore cusps imaged alongside a shoreline borehole log. The yellow arrow indicates cusp location, green indicating the Cretaceous unit, while the orange arrow indicates the Pleistocene unit. The crest of the cusps aligns with the top of the Cretaceous boundary documented in the log (green unit). The Cretaceous unit consists of calcareous sandstone overlain by the shelly sand Pleistocene deposits.

Figure 31: Nearshore multibeam imagining in Arcadian Shores overlain onto sidescan sonar imagery taken in 2003. Visual inspection reveals a strong relationship between the offshore cusps and linear scour depressions seen in backscatter extending offshore.

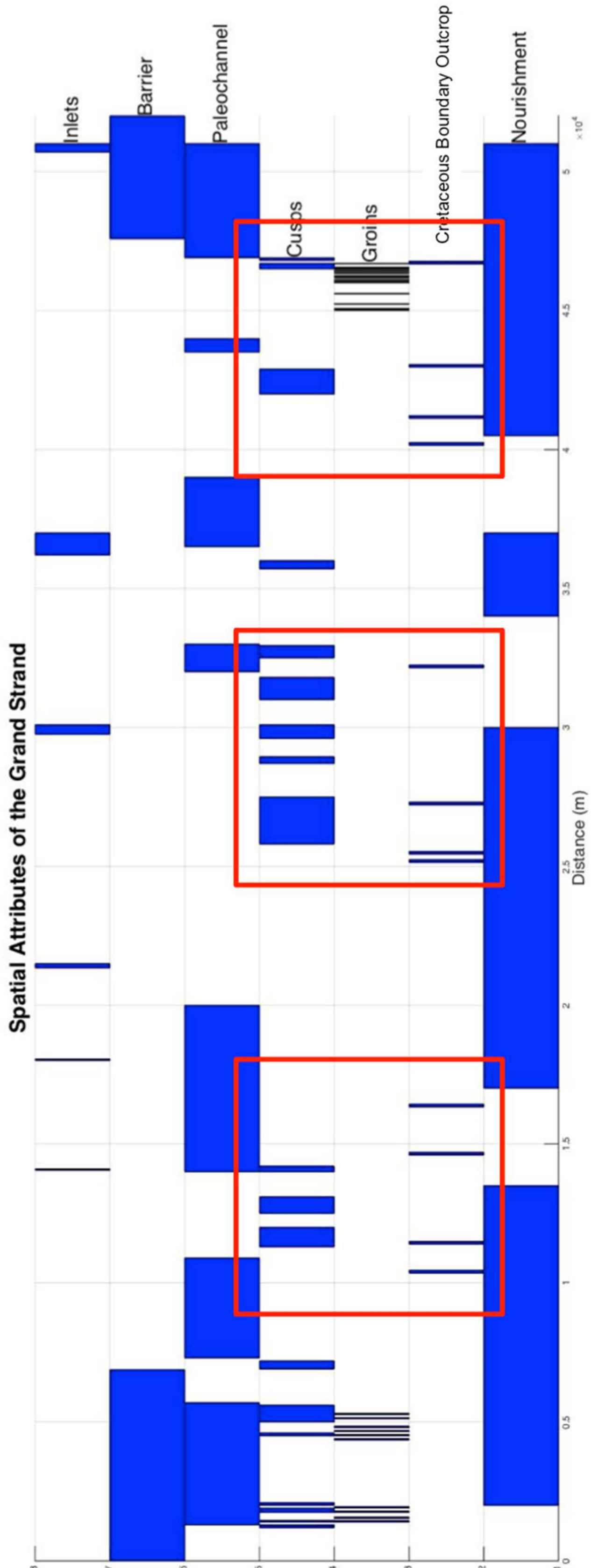

Figure 32: Spatial relationship between where the Cretaceous boundary is outcopping on the shoreface along the Grand Strand- limited by locations where CHIRP seismic profiles have been imaged along the inner shoreface. Where outcropping, offshore cusps reflect similar distributions.

Metric	Linear scour depressions Present	No Linear scour depressions Present	Total
Offshore Cusps	285	22	307
No Offshore Cusps	323	437	760
Total	608	459	1067
Chi-Square 226.006			
Effect Size 17.5%			

Table 7: Chi-square table analyzing the relationship between visual correlations between the presence of offshore cusps in multibeam and offshore linear scour depressions in side scan sonar.

Metric	No Paleochannel	Paleochannel	Total
No Offshore Cusps	321	439	760
Offshore Cusps	273	34	307
Total	594	473	1067
Chi-Square 193.145			
Effect Size 15.3%			

Table 8: Chi-square table analyzing the relationship between the presence of offshore cusps and the presence of paleochannels.

Metric	No Correlation	Correlation-Positive	Correlation-Negative	Total
No Paleochannel	501	0	0	501
Shallow Paleochannel	87	89	0	176
Deep Paleochannel	0	297	97	394
Total	588	386	97	1071
Chi-Square 929.595				
Effect Size 46.5%				

Table 9: Correlations were computed between shoreline change envelope and backscatter alongshore, then divided based on the presence of shallow or deep paleochannels and significant positive or negative correlations. Presented is a chi-square table analyzing the relationship between correlations and paleochannel type and presence.

Metric	Linear scour depressions Present	No Linear scour depressions Present	Total
Offshore Cusps	285	22	307
No Offshore Cusps	323	437	760
Total	608	459	1067
Chi-Square 226.006			
Effect Size 17.5%			

Table 10: Chi-square table analyzing the relationship between the presence or absence of offshore linear scour depressions, imaged in side scan sonar, and the presence or absence of offshore cusps.

Metric	Offshore Cusp Presence
Paleochannel Presence	-0.419
Shoreline Change Envelope	-0.375
Degree of Shoreface Slope	0.307
Backscatter Intensity	-0.35
Metric	Paleochannel Presence
Degree of Shoreface Slope	-0.744
Backscatter Intensity	0.228
Metric	Shoreline Change Envelope (Z)
Backscatter Intensity	0.135
Shoreface Slope	-0.136
Metric	Onshore Cusp Presence
Degree of Shoreface Slope	0.739
Paleochannel Presence	-0.597

Table 11: Correlations between physical and geologic metrics mentioned in Table 1.

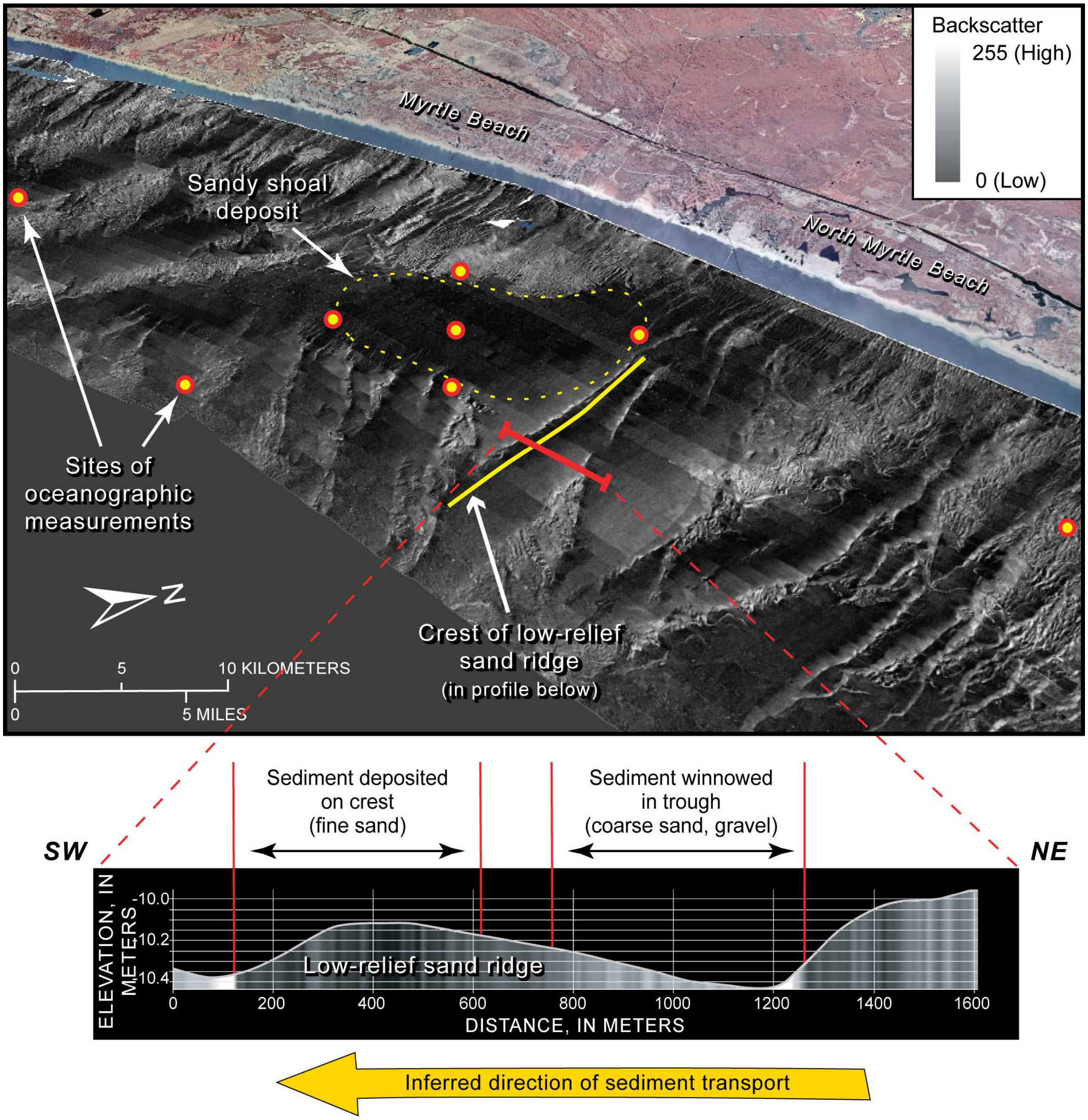

Figure 33: A side scan sonar image of backscatter draped on bathymetric data showing offshore shoal and linear scour depression systems in Myrtle Beach and North Myrtle Beach. Yellow and red points in the top image represent where instruments were deployed to collect bottom samples. These were used to ground truth backscatter, and analysis confirmed low backscatter regions contain fine sands and troughs contain coarse sands and gravel. The bottom image implies the direction of flow across the sediment beds, from north to south. Adapted from Barnhardt, 2009.

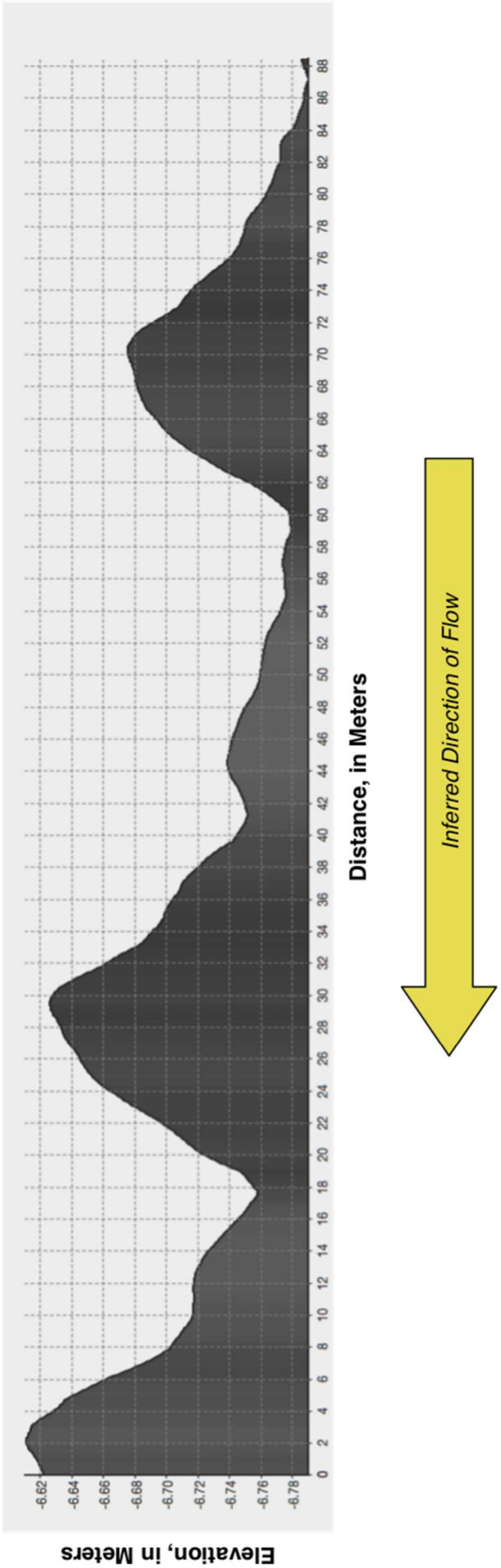

Figure 34. A cross section, taken from the Surfside Beach cross section seen in *Figure 29,* indicating the inferred direction of flow from north to south, as similar to research documented in Barnhardt (2009) and seen in *Figure 32*.

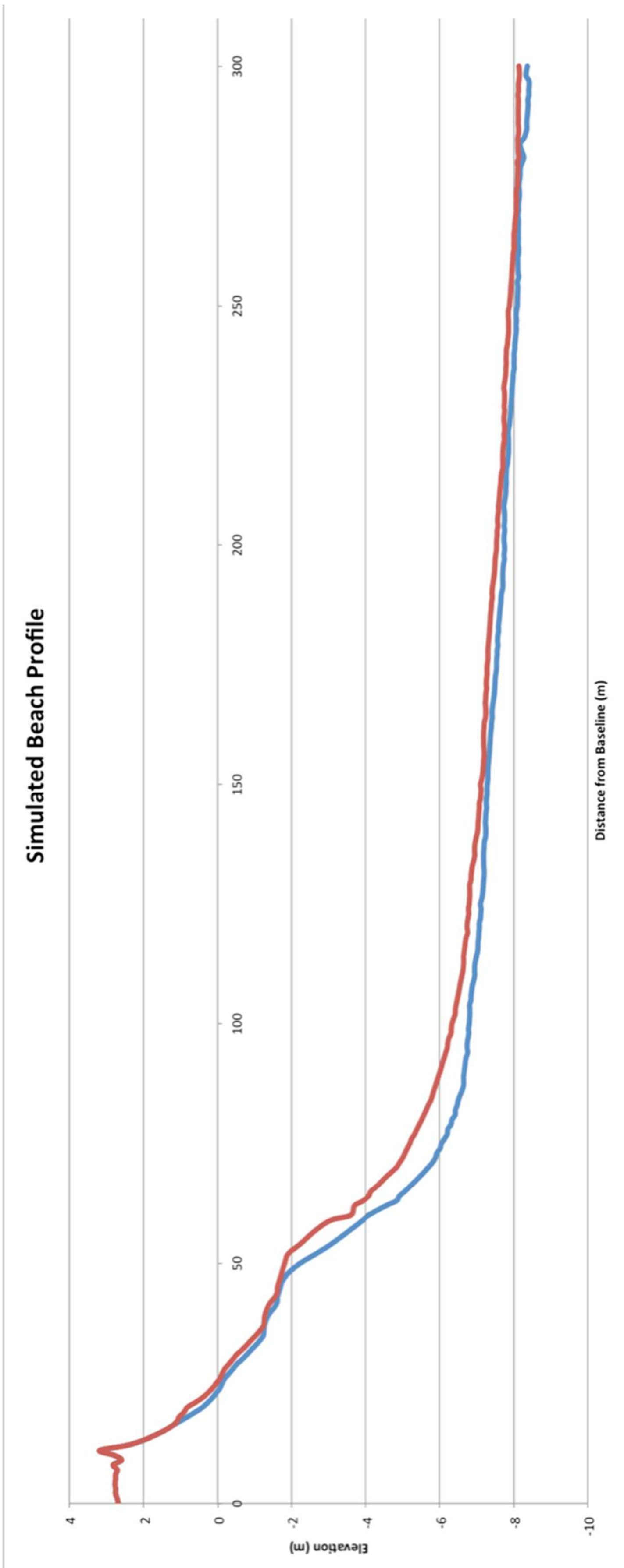

Figure 35: A simulated beach profile showcasing shoreface steepening. The red profile indicates the shoreface before base erosion, and the blue profile showcases the effect of bottom shoreface erosion without upper shoreface erosion.

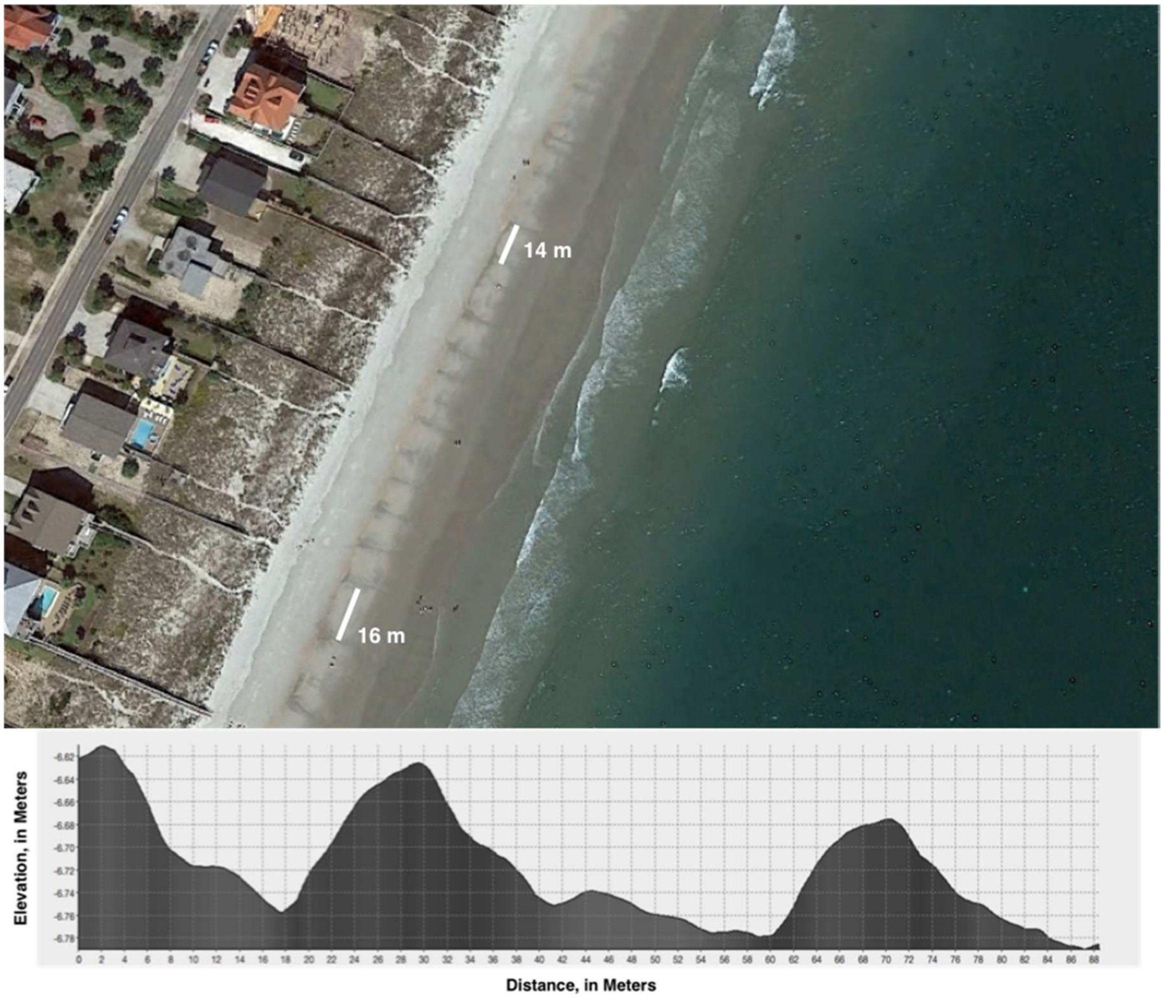

Figure 36. A cross section of multibeam backscatter and bathymetry over the offshore cusp features, just offshore of the onshore cusps seen in the above image. The similar length in wavelengths of offshore and onshore cusps indicate a possible connection.

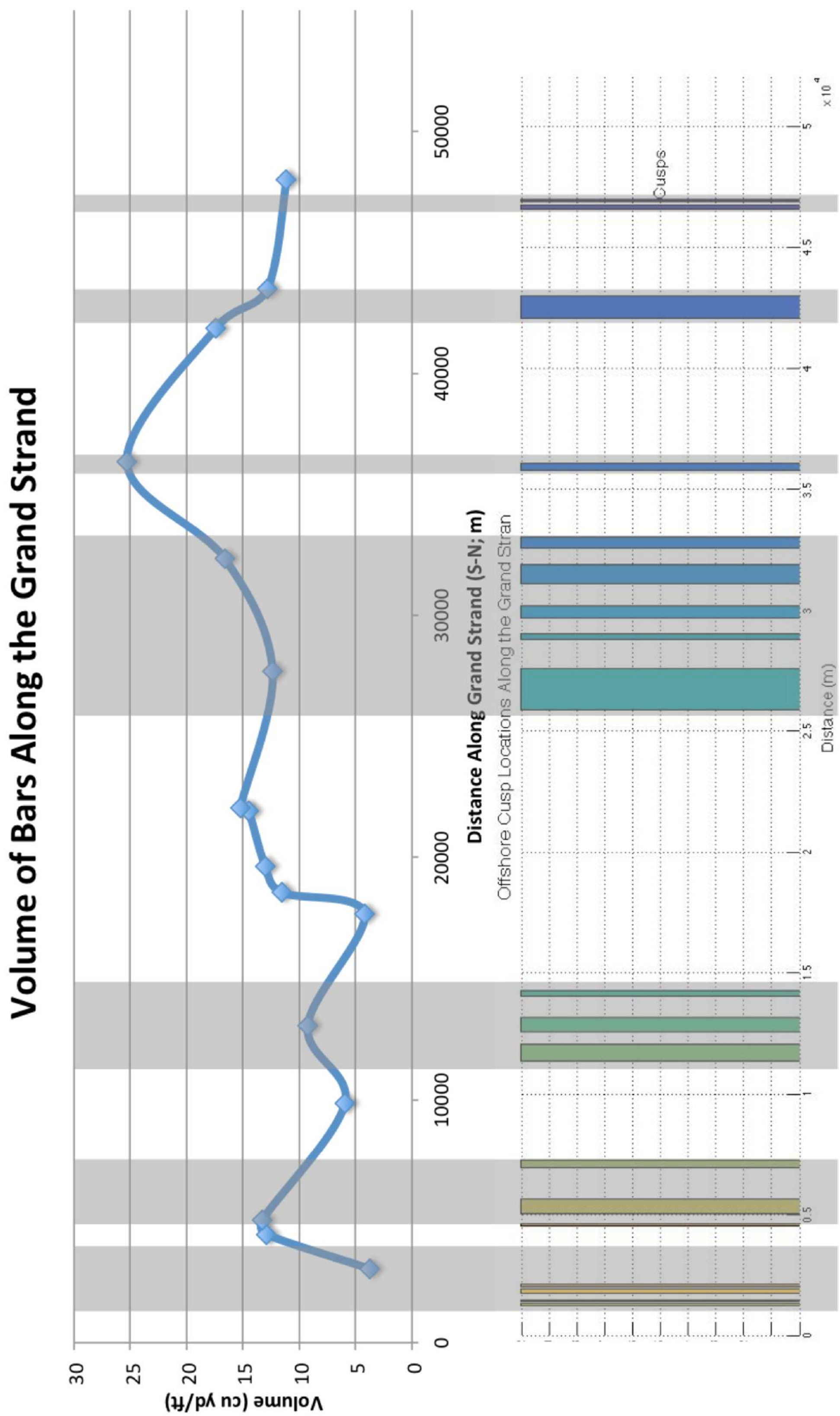

Figure 37: The presence of offshore cusps corresponding to the volume of nearshore bars alongshore. The presence of offshore cusps appear to be spatially related to areas of relatively higher bar volume.

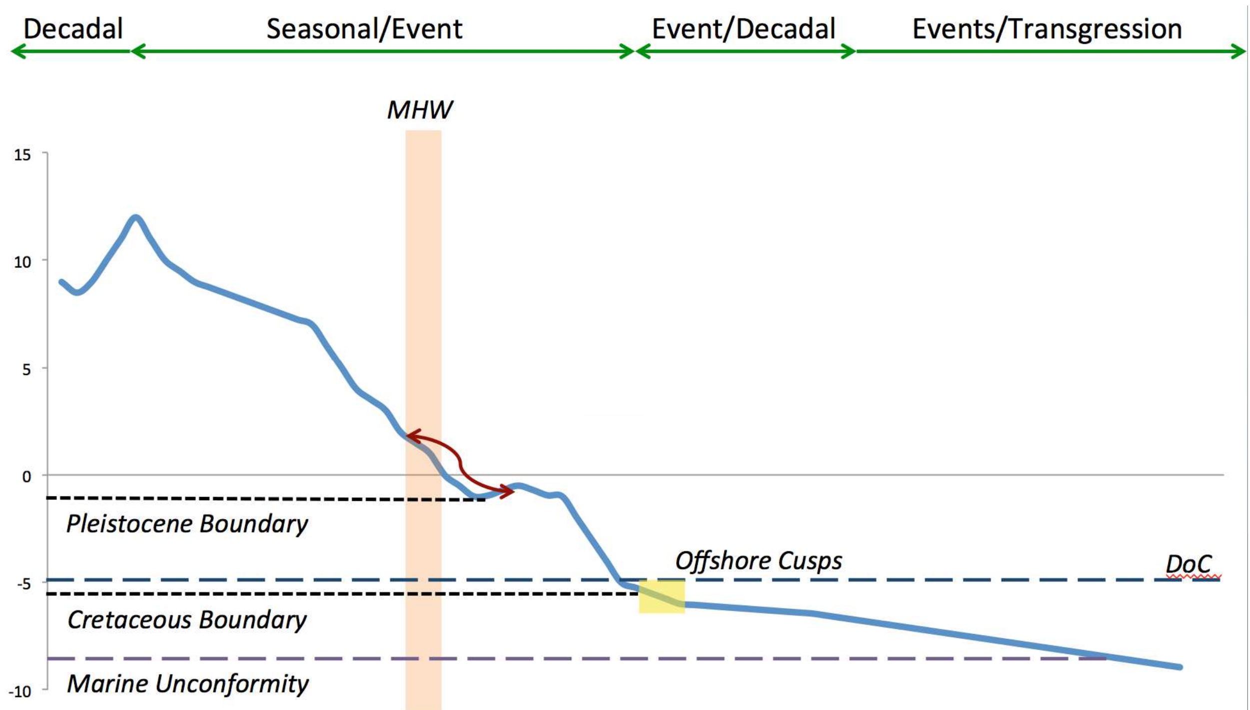

Figure 38. Schematic identifying the location of the offshore cusps in relation to stratigraphic boundaries along a typical Grand Strand beach profile. Temporal scales of change along each beach region are indicated at the top portion of the image. The offshore cusps are most often located below the depth of closure, however larger scale events may transport some of cusp sediments into the active beach.

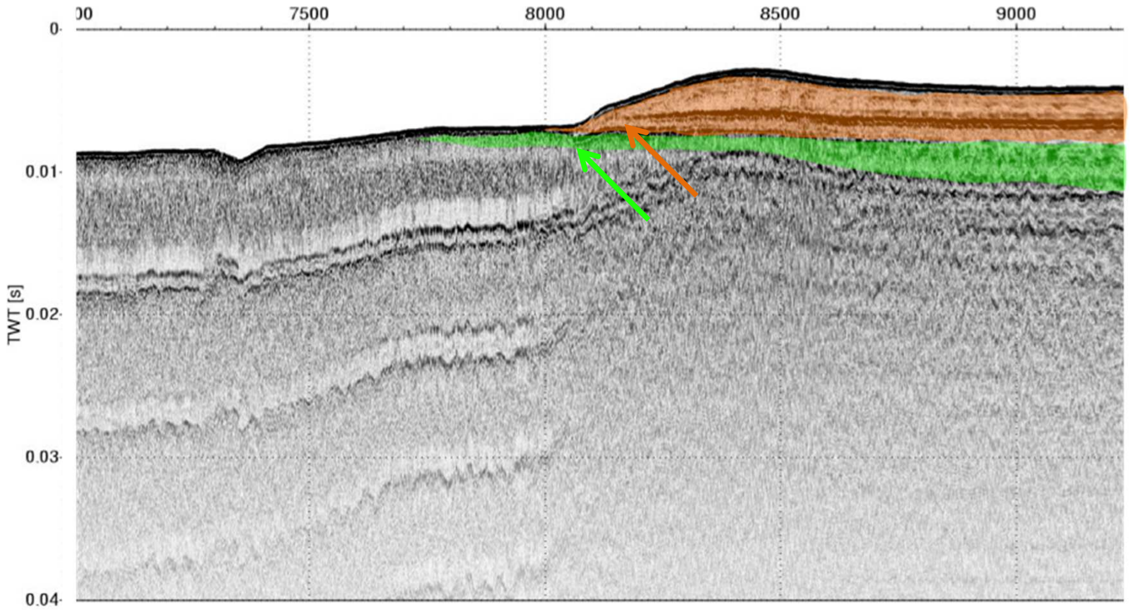

Figure 39. CHIRP seismic profile located in Myrtle Beach. The orange arrow is indicating the effect the Pleistocene boundary has on the shoreface evolution and geometry, similarly seen by the Cretaceous boundary (as indicated by the green arrow)- where offshore cusps are located.

Works Cited

Anima, R.J.; Eittreim, S.L.; Edwards, B.D.; Stevenson, A.J. 2002. Nearshore morphology and late Quaternary geologic framework of the northern Monterey Bay Marine Sanctuary, California. *Marine Geology,* 181(1-3): 35-54.

Army Corps of Engineers Field Research Facility. (n.d.). Retrieved from http://www.frf.usace.army.mil

Barnhardt, W., 2009. Coastal Change Along the Shore of Northeastern South Carolina: The South Carolina Coastal Erosion Study. *United States Geological Survey,* (Circular 1339), 77.

Belknap, D.F., and Kraft, J.C., 1985. Influence of antecedent geology on stratigraphic preservation potential and evolution of Delaware's barrier systems. *Marine Geology,* 63(1-4), 235-262.

Dean, R.G., 2002. Beach Nourishment: Theory and Practice. World Scientific.

Douglas, B.C. and Crowell, M, 2000. Long-term shoreline position prediction and error propagation. *Journal of Coastal Research,* 16(1), 145-152.

Everts, 1987. Continental shelf evolution in response to a rise in sea level. In: Nummedal, D.; Pilkey, O.H., and Howard, J.D. (eds.), Sea Level Fluctuation and Coastal Evolutión. Society of Economic Pale- ontologists and Mineralogists Special Publication No. 41, pp. 49-57.

Gayes, P.T.; Donovan-Ealy, P.; Harris, M.S., and Baldwin, W., Assessment of Beach Renourishment Resources on the Inner Shelf Off Folly Beach and Edisto Island, South Carolina. Draft Report, Coastal Carolina University, Conway, SC, 59pp.

Gutierrez, B. T., G. Voulgaris, and P. A. Work (2006), Cross-shore variation of wind-driven flows on the inner shelf in Long Bay, South California, United States, J. Geophys. Res., 111, C03015, doi:10.1029/2005JC003121.

Hapke, C.J.; Lentz, E.E.; Gayes, P.T.; McCoy, C.A.; Hehre, R.; Schwab, W.C.; Williams, S.J., 2010. A Review of Sediment Budget Imbalances along Fire Island, New York: Can Nearshore Geologic Framework and Patterns of Shoreline Change Explain the Deficit? *Journal of Coastal Research,* 263: 510-522.

Harris, M.S.; Gayes, P.T.; Kindinger, J.L; Flocks, J.G.; Krantz, D.E.; Donovan, P., 2005. Quaternary Geomorphology and Modern Coastal Development in Response to an Inherent Geologic Framework: An Example from Charleston, South Carolina. *Journal of Coastal Research,* 21(1): 49-64.

Kana, T.W.; Traynum, S.B.; Gaudiano, D.; Kackowski, H.L.; Hair, T., 2013. The physical condition of South Carolina beaches 1980-2010. *Journal of Coastal Research,* Sp.69: 61-82.

Komar, P.D., 1976. Beach Processes and Sedimentation. New Jersey: Prentice Hall, 429p.

Kriebel, D.L., and Dean, R.G., 1985. Estimates of erosion and mitigation requirements under various scenarios of sea level rise and storm frequency for Ocean City, Maryland.

Leatherman, S. P.; Zhang, K., and Douglas, B.C., 2000. Sea level rise shown to drive coastal erosion. *Eos,* 81 (6), 1-3.

List, J.H. and Farris, A.S., 1999. Large-scale shoreline response to storms and fair weather. Coastal Sediments '99 (Long Island, New York, ASCE), pp. 1324-1338.

List, J.H.; Farris, A.S.; Sullivan, C., 2006. Reversing storm hotspots on sandy beaches: Spatial and temporal characteristics. *Marine Geology,* 226(3), 261-279.

Miselis J.L., and McNinch J.E., 2006. Calculating shoreline erosion potential using nearshore stratigraphy and sediment volume: Outer Banks, North Carolina. *Journal of Geophysical Research,* 111, F02019.

Morton, R.A. and Miller, T., 2005. National Assessment Of Shoreline Change: Part 2, Historical Shoreline Changes And Associated Coastal Land Loss Along The U.S. Southeast Atlantic Coast. *USGS Open File Report 2005-1401.*

Nelson, T.R. and Hapke, C.J., 2015. Shoreface response and recovery to Hurricane Sandy: Fire Island, NY. *U.S. Geological Survey.*

Park, J.Y.; Gayes, P.T., and Wells, J.T., 2009. Monitoring Beach Renourishment along the Sediment-Starved Shoreline of Grand Strand, South Carolina. *Journal of Coastal Research,* 25(2), 336-349.

Patchineelam, S.M.; Kjerfve, B., and Gardner, L.R., 1999. A preliminary sediment budget for the Winyah Bay estuary, South Carolina, USA. *Marine Geology,* 162(1), 133-144.

Pilkey, O. H.; Young, R.S.; Riggs, S.R.; Smith, A.W.S.; Wu, H., and Pilkey, 1993. The concept of shoreface profile equilibrium: A critical review. *Journal of Coastal Research,* 9, 255-278.

Putney, T.R., Katuna, M.P., and Harris, M.S., 2004, Sub- surface stratigraphy and geomorphology of the Grand Strand, Georgetown and Horry Counties, South Caro- lina: Southeastern Geology, v. 42, no. 4, p. 217–236.

Riggs, S.R.; Cleary, W.J., and Snyder, S.W., 1995. Influence of inherited geologic framework on barrier shoreface morphology and dynamics. *Marine Geology,* 126, 213-234.

Schupp, C.A.; McNinch J.E., and List, J.H., 2006. Nearshore shore-oblique bars, gravel outcrops, and their correlation to shoreline change. *Marine Geology,* 233, 63-79.

Schwab, W.C.; Thieler, E.R.; Allen, J.R.; Foster, D.S.; Swift, B.A., and Denny, J.F., 2000. Influence of inner-continental shelf geologic framework on the evolution and behavior of the barrier-island system between Fire Island Inlet and Shinnecock Inlet, Long Island, New York. *Journal of Coastal Research,* 16, 408-422.

Schwab, W.C.; Baldwin, W.E.; Hapke, C.J.; Lentz, E.E.; Gayes, P.T.; Denny, J.F.; List, J.H.; Warner, J.C., 2013. Geologic evidence for onshore sediment transport from the inner continental shelf: Fire Island, New York. *Journal of Coastal Research,* 29(3): 526-544.

Short, A.D., and Wright, L.D., 1983. Physical Variability of Sandy Beaches. *Developments in Hydrobiology* (pp. 133-144). Springer Netherlands.

Slovinsky, P., 2001. Spatial Variation of Beach Morphology Along Coastal South Carolina. Columbia, South Carolina: Department of Geology, University of South Carolina, Master's thesis, 166pp.

South Carolina Guide to Beachfront Property. (n.d.). Retrieved from http://www.scdhec.gov/library/CR-003559.pdf

Thieler, E.R.; Pilkey, O.H.; Young, R.S.; Bush, D.M., and Chai, F., 2000. The use of mathematical models to predict beach behavior for U.S. coastal engineering: A critical review. *Journal of Coastal Research,* 16(1), 48-70.

Thieler, R.; Himmelstoss, E.A.; Zichichi, J.L.; Ergul, A., 2009. The Digital Shoreline Analysis System (DSAS) Version 4.0 – An ArcGIS Extension for Calculating Shoreline Change. *USGS Open File Report 2008-1278.*

Thieler, E.R. and Danforth, W.W., 1994. Historical shoreline mapping (I): Improving techniques and reducing positioning errors. *Journal of Coastal Research,* 10(3): 549-563.

Washington DC: United States Environmental Protection Agency, 179p.